

**Lunar and Planetary Laboratory
Department of Planetary Sciences**

**K/T Boundary Impact Ejecta in the Raton
Basin (Colorado and New Mexico)**

**Planetary Field Geology Practicum
PTYS 594a
14-18 May, 2000**

QE40
.P63
K7
2000

University of Arizona

Arizona

LIBRARY
LUNAR & PLANETARY LAB

17038

Editor's Note

I don't know why the hell I volunteered to put this thing together, much less research and write two talks. Perhaps it's to make up for such past O'Brien field trip classics as "Lunar Mythology" and "Petroglyphs of Newspaper Rock." Maybe I just had a burst of motivation. It's probably a combination of both. Regardless, it's been interesting to see what everyone's put together, and I guess it beats sitting on my couch and doing nothing.

This will definitely be an interesting trip, both academically and logistically. Since we're still not exactly sure what areas will be off-limits due to forest fires in the area, there will most likely be some last minute changes made along the way. I'd hate to see an LPL field trip go exactly according to plan, as that could set a dangerous precedent.

So, for the next 5 days we'll be sitting in vehicles with one another and dealing without campfires, surviving solely on cold Spam, beef jerky, and Southern Comfort (maybe that's just my food group), possibly sleeping in the rain, and entertaining ourselves with pointless obscene CB chatter. By the end, we'll all be exhausted and smell pretty bad, but will have learned a lot more than we would in almost any class we've ever taken and we'll have a damn good time in the process. Thank God for field trips!

A handwritten signature in black ink, appearing to be the name 'Dane' or similar, written in a cursive style.

Contents

Semi-Useful Stuff:

Itinerary	3
Road map	5
Map of Jemez Mountains region	6
Map of Valles Caldera	7
Geologic timescale	8
Stratigraphy of the Jemez Volcanic Field	9
Mineral names	10
Igneous rock classification	12

Enroute:

The Rio Grande Rift	13
Josh Emery	
East-west magnetic trends across southwestern US/northern Mexico	15
Erich Karkoschka	

Valles Caldera:

Eruption and disruption of ash flows	17
Pete "Where the Hell Did My Hair Go?" Lanagan	
Cooling units of the Bandelier tuff	21
Jani Radebaugh	
Resurgent domes	26
Joe "No-Text" Spitale	
Moat rhyolites: Rhyolite domes & flows around Valles Caldera	32
Ingrid Daubar	
Hydrothermal activity and travertine deposits in Valles Caldera	34
Paul Withers	
Life in hot water: Astrobiology and hydrothermal environments	38
®	
Erosion and deposition on the Pajarito Plateau, New Mexico	42
Gwen Bart	

Raton Basin:

The Late Cretaceous global environment	46
Dave "The Editor" O'Brien	
K/T boundary layers in the Raton Basin: A shocking tale	49
B	

Chemical and mineralogical diagenesis of impact ejecta Jen "Hostess With Neuroses" Grier	53
Impact ejecta and volcanic ash layers: What's the difference? Ross Beyer	58
Other K/T boundary sites in North America Fred Ciesla	60
How are marine K/T sequences different? Jason Barnes	62
The Chixilub crater Adina Alpert	64
Impact ejecta mechanisms: How do we know that Chixilub is the source of the K/T boundary debris? Andreas Ekholm	69
The K/T impactor: Asteroid or comet? Dave O'Brien	75
Global wildfires resulting from the K/T impactor Jonathan Fortney	78
Tertiary Volcanism in the Raton Basin Celinda Kelsey	82

History:

History of the Raton Pass and the Cimarron Trail Terry "Country Boy" Hurford	84
The civil war in New Mexico (and Arizona!) Andy Rivkin	86

PtyS 594a Itinerary

Valles Caldera and the K/T Boundary Sequence in the Raton Basin

14-18 May 2000

*Modified to avoid fire situation in the Bandelier National Monument and Los Alamos areas
Additional changes are possible*

Day 1: Sunday, 14 May

Leave LPL at 8 am

Campbell to I-10 east to Deming (216 miles)

At Deming, take state road 26 to Hatch (46 miles)

Stop for lunch along the Deming-Hatch cutoff

At Hatch, take I-25 north to Albuquerque (191 miles)

Continue on I-25 to Bernalillo (17 miles)

Take state road 44 to state road 4 (26 miles)

Take state road 4 north, stopping at Soda Dam if time allows (16? miles)

(1.7 mi beyond Jemez Springs post office and 0.4 mi beyond Jemez Ranger Stat.)

Rather than camping near Rabbit Mountain (~22 miles from Soda Dam), we will look for a suitable site closer Soda Dam, perhaps in the vicinity of the Jemez River crossing or Valle Grande.

Day 2: Monday, 15 May

Break camp so trucks are moving at 8 am.

Return to state road 4

Go to Soda Dam if we were unable to stop on Day 1

Go to Valle Grand Overlook into Valles Caldera along SR4

Go west on SR4 to one of two outcrops of El Cajete pumice (moat rhyolite sequence)

Rather than going to Bandelier National Monument and hiking through a volcano and lava lake sequence along the Falls Trail, we will work our way along the west side of Valles Caldera along state route 126 and forest roads 106, 376, and 380.

We will stop for lunch somewhere along the west side of the Valles Caldera.

We will not be able to see the surge deposits in Los Alamos, exit the Caldera area along state road 502, or drive to Raton via Taos. Rather, we will need to return to state road 4 and retrace our path to I-25 at Bernalillo.

Take I-25 to Trinidad (220 miles)

Take state route 12 west to the Trinidad State Recreation Area (<10 miles)

Set up camp at a reserved group camp site; water, tent pads, a fire pit, a barbecue, a group shelter, volleyball, and horseshoes are available.

Day 3: Tuesday, 16 May

Break camp so trucks are moving at 8 am

Take state route 12 east, returning to Trinidad (<10 miles)

Stop for view of Spanish Peaks and discuss magmatic components in Raton area
Starkville South K/T boundary site (collect samples)

Clear Creek North K/T boundary site

If time allows, go to the Raton or Berwind Canyon K/T boundary site; otherwise camp early
Return to the group camp site at the Trinidad State Recreation Area

Day 4: Wednesday, 17 May

Break camp so trucks are moving at 8 am

Take state route 12 west

Madrid K/T boundary site

Long Canyon K/T boundary site

Pause for lunch in the Long Canyon area

Return to I-25 at Trinidad

Take I-25 south past to the Glorieta and Pecos area (~160 miles)

Camp in the Sante Fe National Forest

Day 5: Thursday, 18 May

Break camp so trucks are moving at 8 am

Take I-25 to Albuquerque (~80 miles)

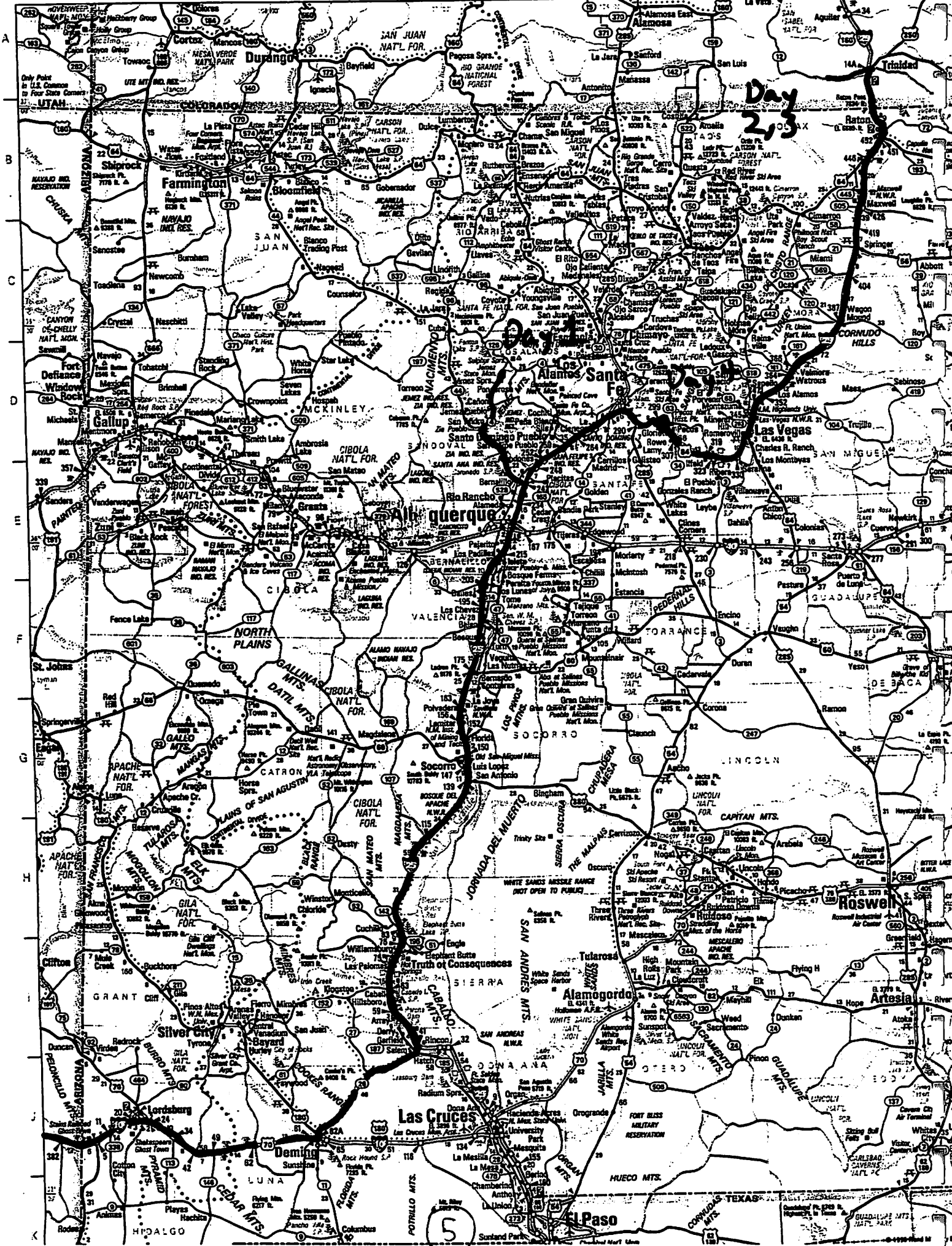
Continue on I-25 to Hatch (191 miles)

At Hatch, take state road 26 to Deming (46 miles)

Stop for lunch along the Deming-Hatch cutoff

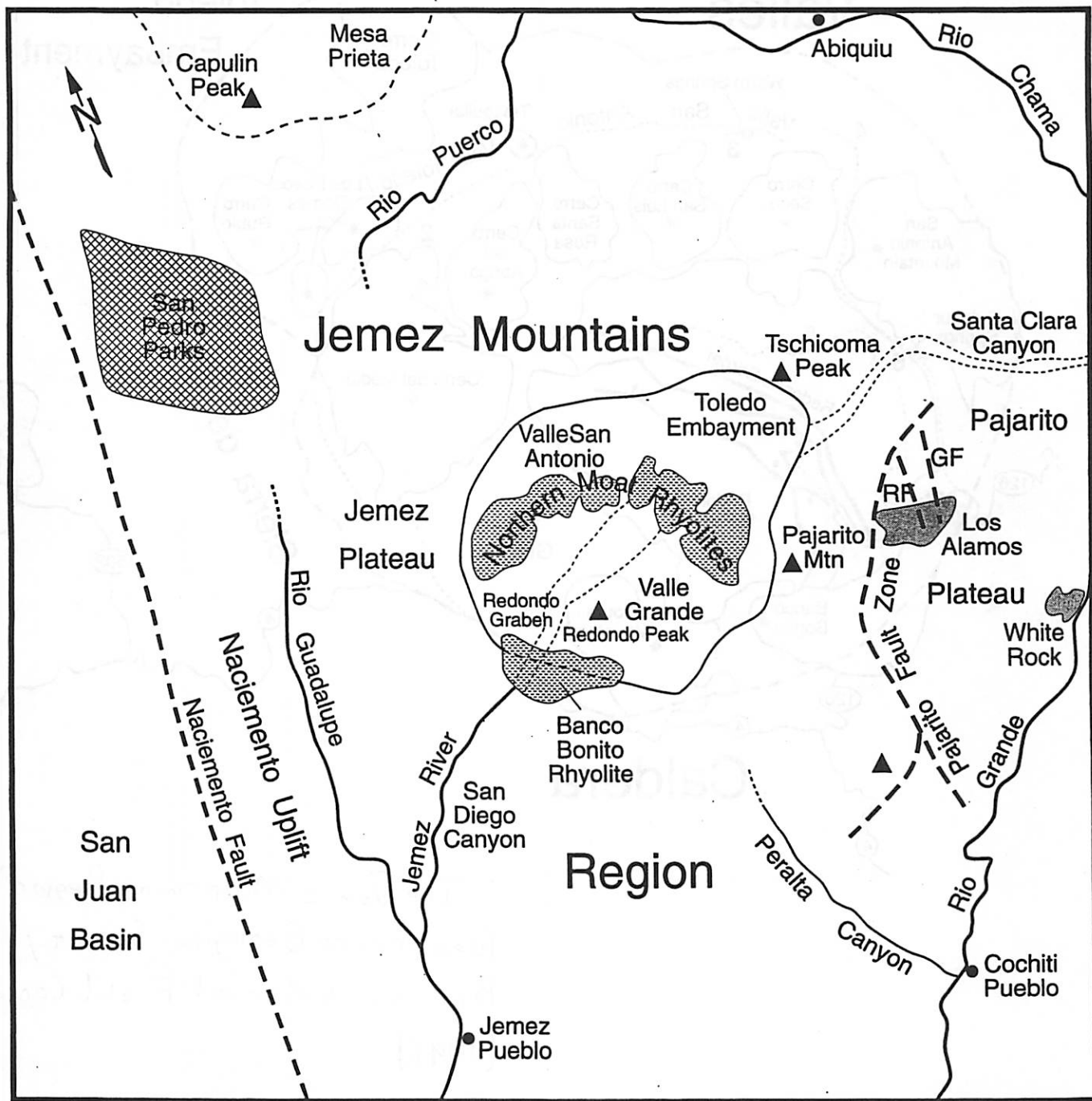
At Deming, take I-10 west to Tucson (216 miles)

Arrive back in Tucson in the late afternoon or early evening



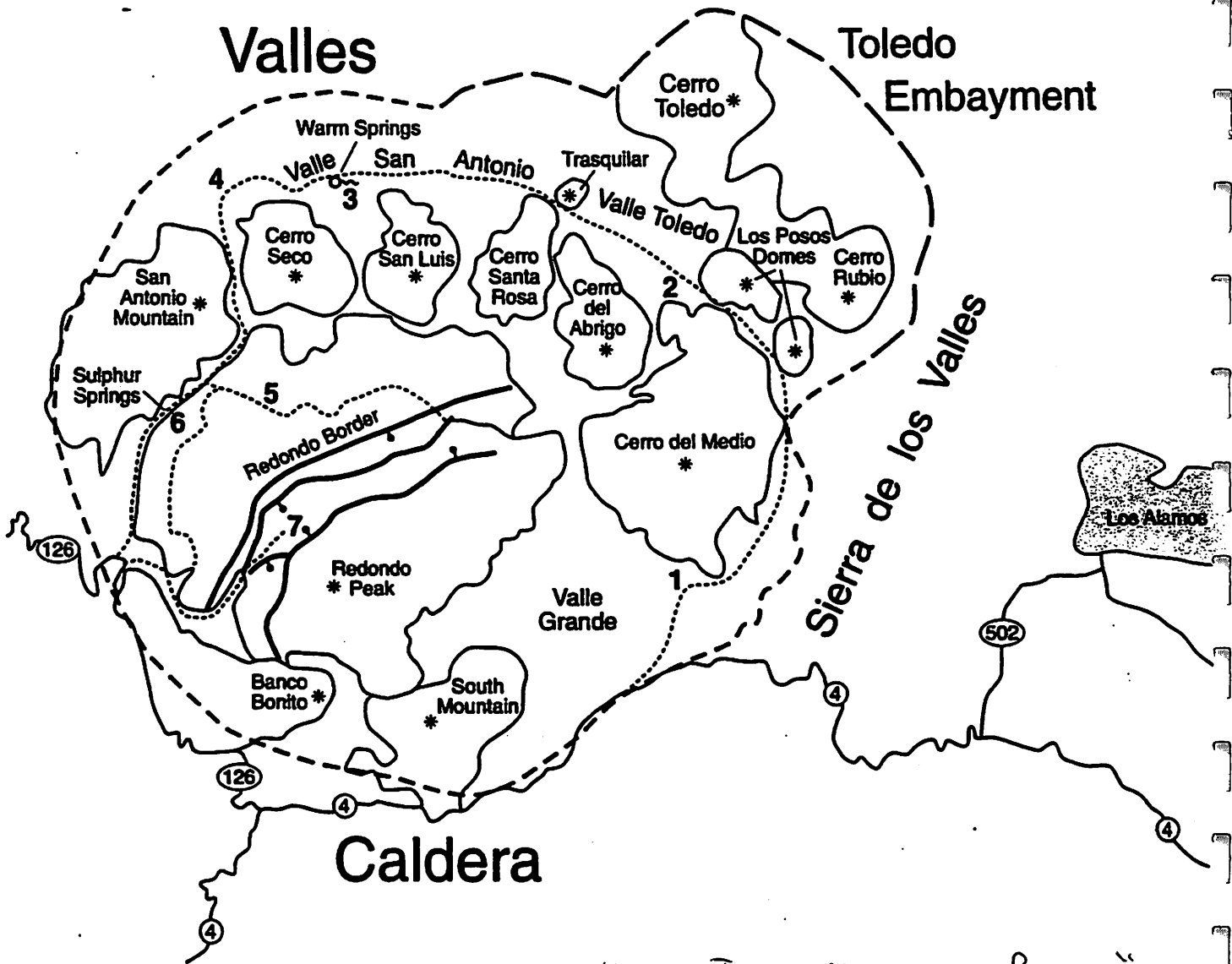
Day 2, 3

5



Line drawing map of area shown in facing LANDSAT photo.

"The Jemez Mountains Region."
 New Mexico Geological Society,
 Proc. 47th Annual Field Conference.
 (1996)



"The Jemez Mountains Region"
 New Mexico Geological Society,
 Proc. 47th Annual Field Conference.
 (1996)

Uniform Time Scale	Subdivisions Based on Strata/Time		Radiometric Dates (millions of years ago)	Outstanding Events			
	Systems/Periods	Series/Epochs		In Physical History	In Evolution of Living Things		
PHANEROZOIC	CENOZOIC	Quaternary	Recent or Holocene Pleistocene	0	Several glacial ages Making of the Great Lakes; Missouri and Ohio Rivers	<i>Homo sapiens</i>	
		Tertiary	Pliocene		2?		Later hominids
Miocene				6	Beginning of Colorado River Creation of mountain ranges and basins in Nevada	Primitive hominids Grasses; grazing mammals	
Oligocene				22			
Eocene				36	Beginning of volcanic activity at Yellowstone Park	Primitive horses	
Paleocene				58			
PHANEROZOIC	MESOZOIC	Cretaceous	Many	65	Beginning of making of Rocky Mountains	Spreading of mammals Dinosaurs extinct	
		Jurassic		145	Beginning of lower Mississippi River	Flowering plants Climax of dinosaurs	
		Triassic		210	Beginning of Atlantic Ocean	Birds	
	PALEOZOIC	Permian		250	Climax of making of Appalachian Mountains	Conifers, cycads, primitive mammals Dinosaurs	
		Pennsylvanian (Upper Carboniferous)		290		Mammal-like reptiles	
		Mississippian (Lower Carboniferous)		340		Coal forests, insects, amphibians, reptiles	
		Devonian		365	Earliest economic coal deposits	Amphibians	
	PHANEROZOIC	PALEOZOIC		Silurian	415		Land plants and land animals
				Ordovician	465	Beginning of making of Appalachian Mountains	Primitive fishes
				Cambrian	510	Earliest oil and gas fields	Marine animals abundant
575							
PRECAMBRIAN	PRECAMBRIAN (Mainly igneous and metamorphic rocks; no worldwide subdivisions.)		1,000		Primitive marine animals Green algae		
			2,000				
			3,000				
			4,650	Oldest dated rocks	Bacteria, blue-green algae		
~4,650		Birth of Planet Earth					

8

Flint and Skinner. "Physical Geology":
2nd (1977)

Stratigraphy of the Jemez Volcanic Field

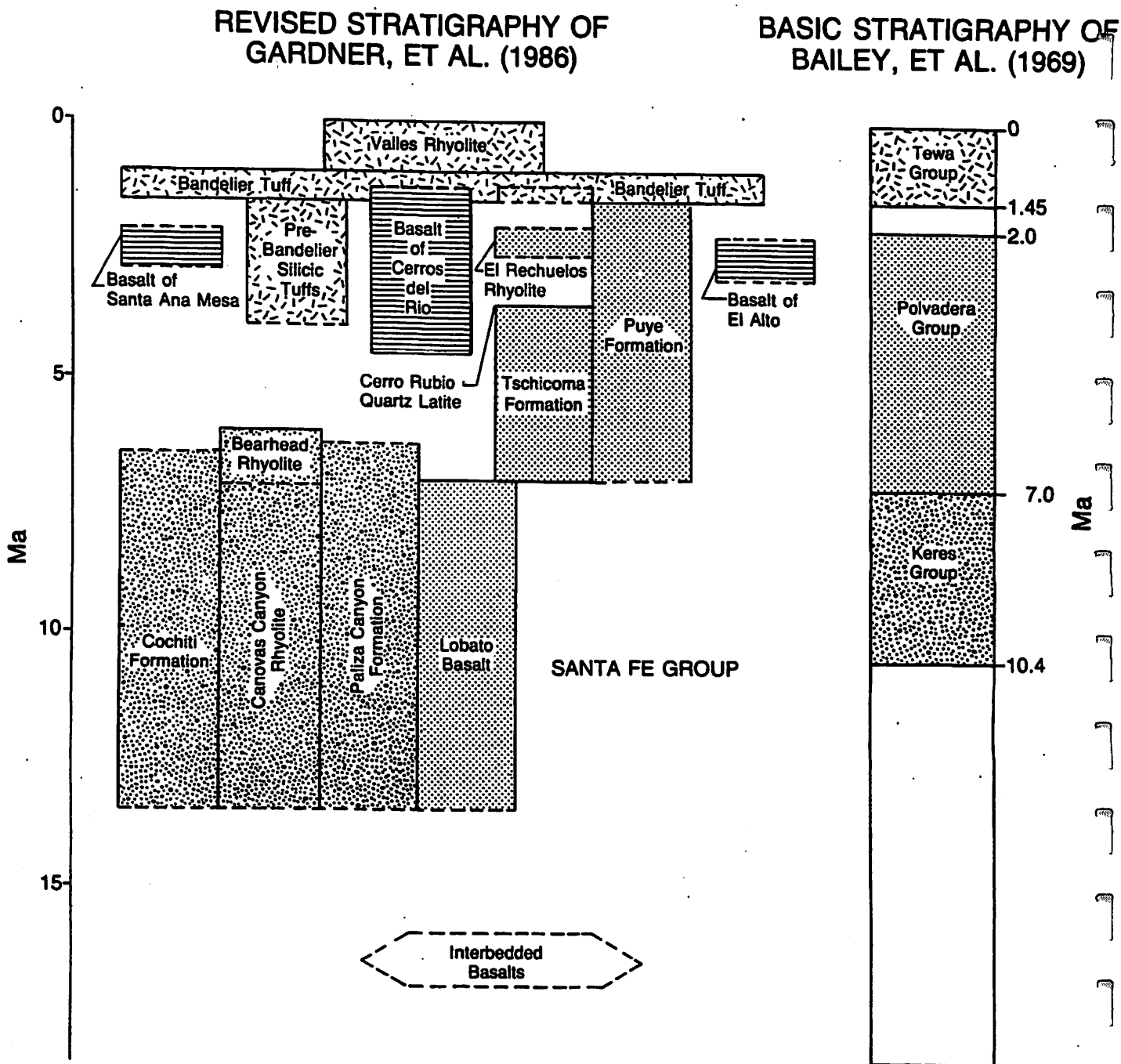


FIGURE 4—Basic stratigraphy of the Jemez volcanic field (Bailey et al., 1969) compared to revised stratigraphy of Gardner et al. (1986); patterns are the same as Fig. 2. Dashed lines indicate uncertainty and more revisions may be forthcoming (see Fig. 27, Day 2). The figure is also a schematic south-to-north (left-to-right) section through the volcanic field.

NM Bureau of Mines + Mineral Resources Memoir 46, May 1989.

"Volcanic and Hydrothermal Evolution of Valles Caldera and Jemez Volcanic Field." P. 381

MINERAL NAMES

Mineral	Formula	Mineral	Formula
Åkermanite	$\text{Ca}_2\text{MgSi}_2\text{O}_7$	Hematite	Fe_2O_3
Alabandite	$(\text{Mn,Fe})\text{S}$	Hercynite	$(\text{Fe,Mg})\text{Al}_2\text{O}_4$
Albite	$\text{NaAlSi}_3\text{O}_8$	Hibonite	$\text{CaAl}_{12}\text{O}_{19}$
Andradite	$\text{Ca}_3\text{Fe}_2\text{Si}_3\text{O}_{12}$	Ilmenite	FeTiO_3
Anorthite	$\text{CaAl}_2\text{Si}_2\text{O}_8$	Kaersutite	$\text{Ca}_2(\text{Na,K})(\text{Mg,Fe})_4\text{TiSi}_6\text{Al}_2\text{O}_{22}\text{F}_2$
Apatite	$\text{Ca}_5(\text{PO}_4)_3$	Kamacite	$\alpha\text{-(Fe,Ni)}$
Aragonite	CaCO_3	Krinovite	$\text{NaMg}_2\text{CrSi}_3\text{O}_{10}$
Armalcolite	$\text{FeMgTi}_2\text{O}_5$	Lawrencite	$(\text{Fe,Ni})\text{Cl}_2$
Augite	$\text{Mg}(\text{Fe,Ca})\text{Si}_2\text{O}_6$	Lonsdaleite	C
Awaruite	Ni_3Fe	Mackinawite	FeS_{1-x}
Baddeleyite	ZrO_2	Maghemite	Fe_2O_3
Barringerite	$(\text{Fe,Ni})_2\text{P}$	Magnesiochromite	MgCr_2O_4
Bassanite	$\text{CaSO}_4 \cdot 1/2\text{H}_2\text{O}$	Magnesite	$(\text{Mg,Fe})\text{CO}_3$
Bloedite	$\text{Na}_2\text{Mg}(\text{SO}_4)_2 \cdot 4\text{H}_2\text{O}$	Magnetite	Fe_3O_4
Brezinaite	Cr_3S_4	Majorite	$\text{Mg}_3(\text{MgSi})\text{Si}_3\text{O}_{12}$
Brianite	$\text{CaNa}_2\text{Mg}(\text{PO}_2)$	Marcasite	FeS_2
Buchwaldite	NaCaPO_4	Melilite solid solution	
Calcite	CaCO_3	åkermanite (Ak)	$\text{Ca}_2\text{MgSi}_2\text{O}_7$
Carlsbergite	CrN	gehlenite (Ge)	$\text{Ca}_2\text{Al}_2\text{SiO}_7$
Caswellsilverite	NaCrS_2	Merrhueite	$(\text{K,Na})_2\text{Fe}_2\text{Si}_{12}\text{O}_{30}$
Chalcopyrite	CuFeS_2	Merrillite	$\text{Ca}_9\text{MgH}(\text{PO}_4)_7$
Chamosite	$\text{Fe}_2\text{Mg}_3[(\text{Si}_4\text{O}_{10})(\text{OH})_2]$	Mica	$(\text{K,Na,Ca})_2\text{Al}_4[\text{Si}_6\text{Al}_2\text{O}_{70}]$
Chaoite	C		$(\text{OH,F})_4$
Clinopyroxene	$(\text{Ca,Mg,Fe})\text{SiO}_3$	Molybdenite	MoS_2
Chlorapatite	$\text{Ca}_5(\text{PO}_4)_3\text{Cl}$	Monticellite	$\text{Ca}(\text{Mg,Fe})\text{SiO}_4$
Chromite	FeCr_2O_4	Montmorillonite	$\text{Al}_4(\text{Si,Al})_3\text{O}_{20}(\text{OH})_4\text{Mg}_6$
Cohenite	$(\text{Fe,Ni})_3\text{C}$		$(\text{Si,Al})_3\text{O}_{20}(\text{OH})_4$
Copper	Cu	Nepheline	$\text{NaAlSi}_3\text{O}_8$
Cordierite	$\text{Mg}_2\text{Al}_4\text{Si}_5\text{O}_{18}$	Niningerite	$(\text{Mg,Fe})\text{S}$
Corundum	Al_2O_3	Oldhamite	CaS
Cristobalite	SiO_2	Olivine	$(\text{Mg,Fe})_2\text{SiO}_4$
Cronstedtite	$(\text{Mg,Fe})_2\text{Al}_3\text{Si}_5\text{AlO}_{18}$	Olivine solid solution	
Cubanite	CuFe_2S_3	fayalite (Fa)	Fe_2SiO_4
Daubreelite	FeCr_2S_4	forsterite (Fo)	Mg_2SiO_4
Diamond	C	Orthoclase	KAlSi_3O_8
Diopside	$\text{CaMgSi}_2\text{O}_6$	Orthopyroxene	$(\text{Mg,Fe})\text{SiO}_3$
Djerfisherite	$\text{K}_3\text{CuFe}_{12}\text{S}_{14}$	Osbornite	TiN
Dolomite	$\text{CaMg}(\text{CO}_3)_2$	Panethite	$(\text{Ca,Na})_2(\text{Mg,Fe})_2(\text{PO}_4)_2$
Enstatite	MgSiO_3	Pentlandite	$(\text{Fe,Ni})_9\text{S}_8$
Epsomite	$\text{MgSO}_4 \cdot 7\text{H}_2\text{O}$	Perovskite	CaTiO_3
Farringtonite	$\text{Mg}_3(\text{PO}_4)_2$	Perryite	$(\text{Ni,Fe})_5(\text{Si,P})_2$
Fassaite	$\text{Ca}(\text{Mg,Ti,Al})(\text{Al,Si})_2\text{O}_6$	Pigeonite	$(\text{Fe,Mg,Ca})\text{SiO}_3$
Fayalite	Fe_2SiO_4	Plagioclase	
Feldspar solid solution		albite	$\text{NaAlSi}_3\text{O}_8$
albite (Ab)	$\text{NaAlSi}_3\text{O}_8$	anorthite	$\text{CaAl}_2\text{Si}_2\text{O}_8$
anorthite (An)	$\text{CaAl}_2\text{Si}_2\text{O}_8$	Portlandite	$\text{Ca}(\text{OH})_2$
orthoclase (Or)	KAlSi_3O_8	Potash feldspar	$(\text{K,Na})\text{AlSi}_3\text{O}_8$
Ferrosilite	FeSiO_3	Pyrite	FeS_2
Forsterite	Mg_2SiO_4	Pyrope	$\text{Mg}_3\text{Al}_2(\text{SiO}_4)_3$
Gehlenite	$\text{Ca}_2\text{Al}_2\text{SiO}_7$	Pyroxene solid solution	
Gentnerite	$\text{Cu}_9\text{Fe}_3\text{Cr}_{11}\text{S}_{18}$	enstatite (En)	MgSiO_3
Graftonite	$(\text{Fe,Mn})_3(\text{PO}_4)_2$	ferrosilite (Fs)	FeSiO_3
Graphite	C	wollastonite (Wo)	CaSiO_3
Greigite	Fe_3S_4	Pyrrhotite	Fe_{1-x}S
Grossular	$\text{Ca}_3\text{Al}_2\text{Si}_3\text{O}_{12}$	Quartz	SiO_2
Gypsum	$\text{CaSO}_4 \cdot 2\text{H}_2\text{O}$	Rhönite	$\text{Ca}_4(\text{Mg,Al,Ti})_{12}(\text{Si,Al})_{12}\text{O}_{40}$
Haxonite	Fe_{23}C_6	Richterite	$\text{Na}_2\text{CaMg}_5\text{Si}_4\text{O}_{22}\text{F}_2$
Heazlewoodite	Ni_3S_2	Ringwoodite	$(\text{Mg,Fe})_2\text{SiO}_4$
Hedenbergite	$\text{CaFeSi}_2\text{O}_6$	Roaldite	$(\text{Fe,Ni})_4\text{N}$
Heideite	$(\text{Fe,Cr})_{1+x}(\text{Ti,Fe})_2\text{S}_4$		

MINERAL NAMES *continued*

Mineral	Formula	Mineral	Formula
Roedderite	$(K,Na)_2Mg_5Si_{12}O_{30}$	Stanfieldite	$Ca_4(Mg,Fe)_5(PO_4)_6$
Rutile	TiO_2	Suessite	Fe_3Si
Sanidine	$KAlSi_3O_8$	Sulfur	S
Sarcopside	$(Fe,Mn)_3(PO_4)_2$	Taenite	$\gamma-(Fe,Ni)$
Scheelite	$CaWO_4$	Tetrataenite	$FeNi$
Schöllhornite	$Na_{0.3}(H_2O) [CrS_2]$	Thorianite	ThO_2
Schreibersite	$(Fe,Ni)_3P$	Tridymite	SiO_2
Serpentine (or chlorite)	$(Mg,Fe)_6Si_4O_{10}(OH)_8$	Troilite	FeS
Sinoite	Si_2N_2O	Ureyite	$NaCrSi_2O_6$
Smythite	Fe_9S_{11}	V-rich magnetite	$(Fe,Mg)(Al,V)_2O_4$
Sodalite	$Na_8Al_6Si_6O_{24}Cl_2$	Valleriite	$CuFeS_2$
Sphalerite	$(Zn,Fe)S$	Vaterite	$CaCO_3$
Spinel	$MgAl_2O_4$	Whewellite	$CaC_2O_4 \cdot H_2O$
Spinel Solid Solution		Wollastonite	$CaSiO_3$
spinel	$MgAl_2O_4$	Yagiite	$(K,Na)_2(Mg,Al)_5(Si,Al)_{12}O_{30}$
hercynite	$FeAl_2O_4$	Zircon	$ZrSiO_4$
chromite	$FeCr_2O_4$		
magnesiocromite	$MgCr_2O_4$		
V-rich magnetite	$(Fe,Mg)(Al,V)_2O_4$		

"Meteorites and the Early Solar System". Kerridge & Matthews, ed. U of A Press (1988).

Igneous Rocks

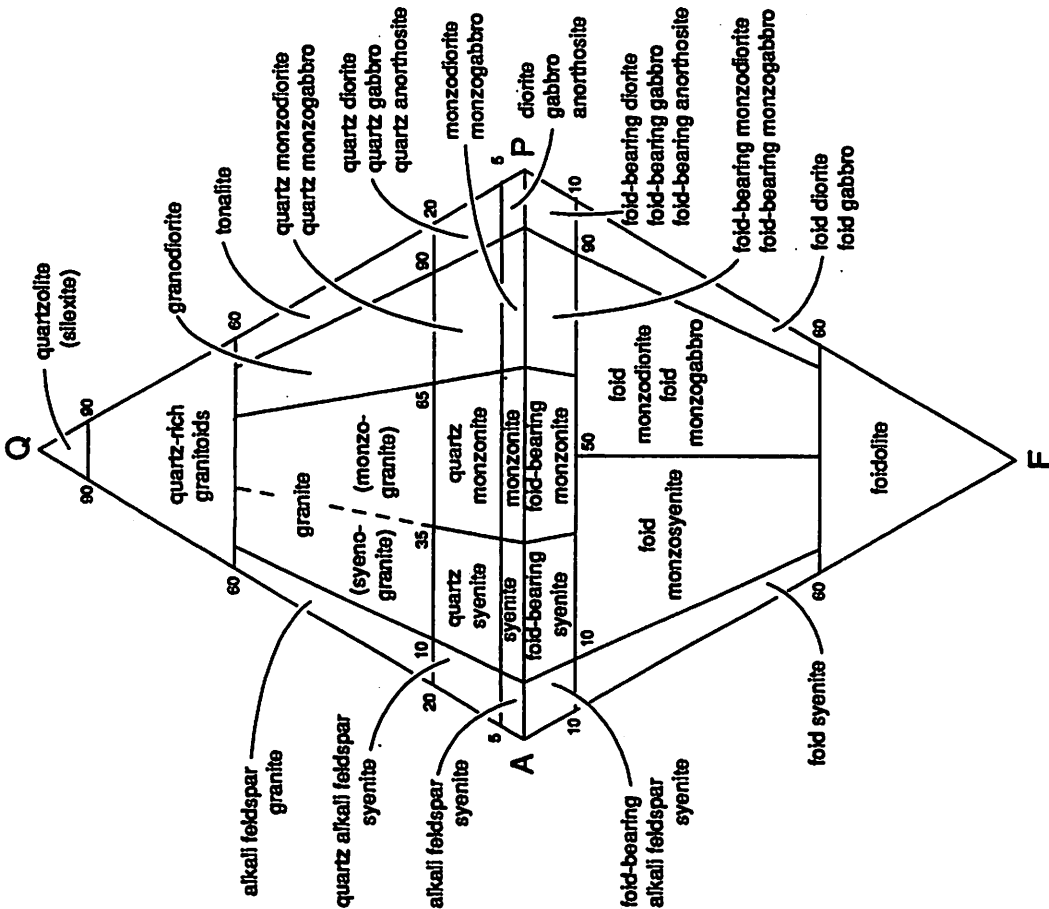


Fig. B.4. Classification and nomenclature of plutonic rocks according to their modal mineral contents using the QAPF diagram (based on Streckeisen, 1976, Fig. 1a). The corners of the double triangle are Q = quartz, A = alkali feldspar, P = plagioclase and F = feldspathoid. However, for more detailed definitions refer to section B.2. This diagram must not be used for rocks in which the mafic mineral content, M, is greater than 90%.

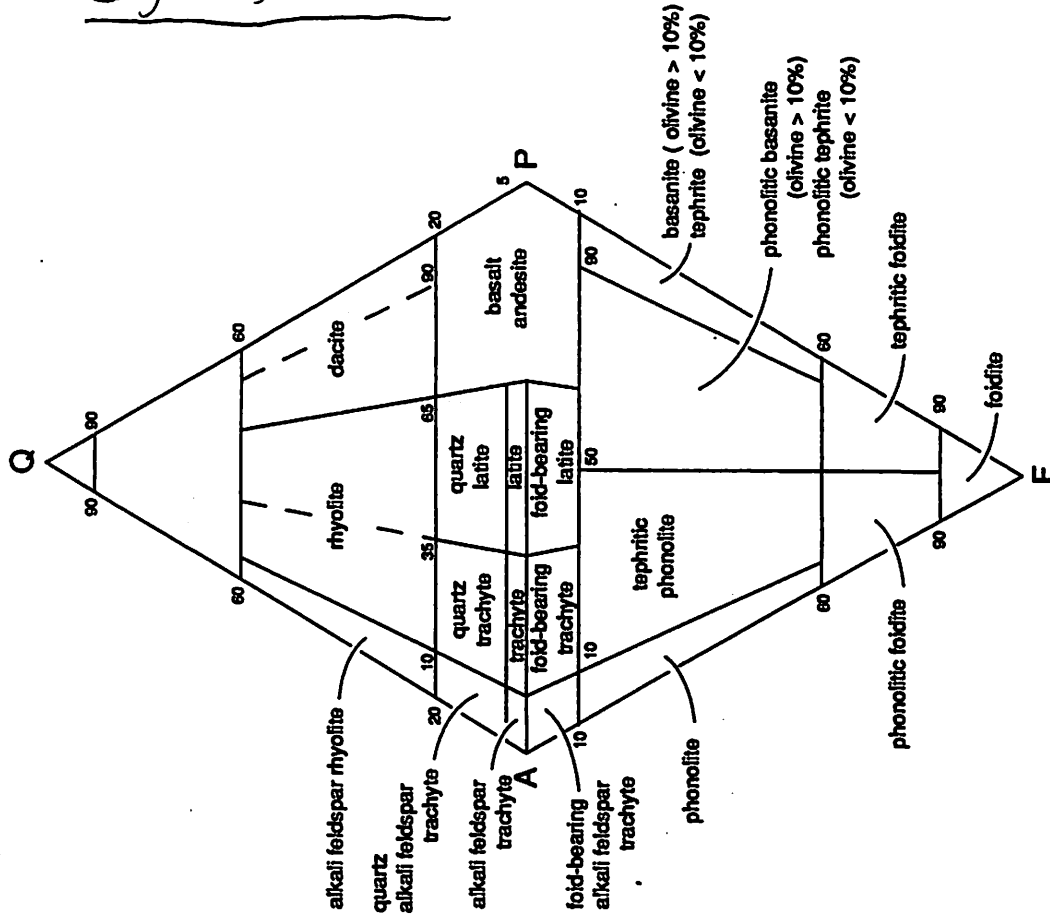


Fig. B.10. Classification and nomenclature of volcanic rocks according to their modal mineral contents using the QAPF diagram (based on Streckeisen, 1978, Fig. 1). The corners of the double triangle are Q = quartz, A = alkali feldspar, P = plagioclase and F = feldspathoid. However, for more detailed definitions refer to section B.2.

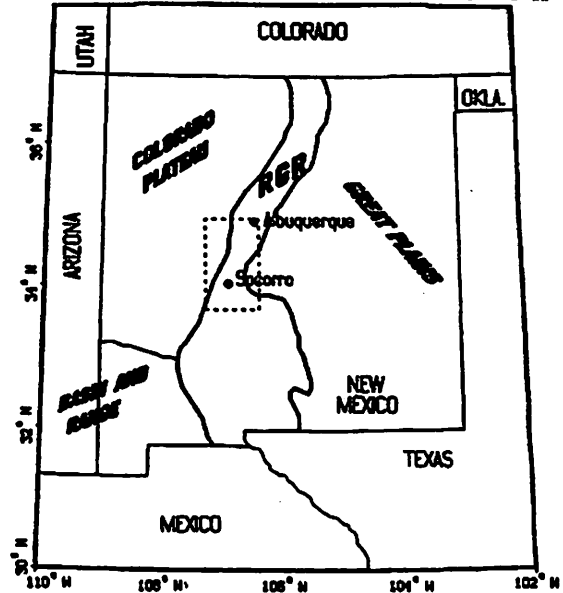
The Rio Grande Rift

Josh

May 12, 2000

Introduction

The geology in the central part of the great state of New Mexico is dominated by the Rio Grande Rift, which is at least partially responsible for most of the volcanic structures we'll see. As we will be spending most of our driving time in this region, it behooves us to briefly review some aspects of this ever expanding feature. The Rio Grande Rift (RGR) cuts the entire way through New Mexico, extending from southern Colorado southward deep into the Mexican state of Chihuahua. It is bordered on the east by the Great Plains, on the northwest by the Colorado Plateau, and on the southwest by the Basin and Range province. The rift is comprised of a series of presently interconnected basins, and it widens to the south where it is physiographically indistinguishable from the adjacent Basin and Range. The RGR is characterized by a thinning crust, high heat flow, above average seismic activity, and a relative high in gravity anomaly data.



Brief Highlights of what I would have written if I weren't lazy

- The rift developed in 2 main phases:
 - late Oligocene to Early Miocene (~30-18 Ma) – low angle faulting
 - late Miocene to Pliocene (~9-3 Ma) – high and low angle normal faulting
- Formed along previously existing zone of weakness
 - Ancestral Rockies and Laramide orogenies
- Began as series of isolated, shallow depressions which later deepened, then were filled in by erosion of surroundings.
 - Present river formed when these basins connected (Rio Grande did not cut the Rio Grande valley, just followed best path)
- Crust in rift is up to 2 km thinner than adjacent regions
- Regional gravity low associated with Rockies is partially reversed within rift
 - crustal intrusion???????
- Very high heat flow and lots of seismic activity (low intensity) in the Socorro area
 - rift still active

Tectonic model for rift formation

Phase 1: Normal Subduction

Continental arc volcanism

Phase 2: Early Slab Retreat, Lithospheric Magmatism, and Basin Formation

Widespread crustal melting, emplacement of silicic magmas into large chambers

Voluminous outflow sheets from large calderas

Eruption of mafic to intermediate lavas formed by partial melting of lithosphere

Phase 3: Rapid Basin Subsidence and Asthenospheric Magmatism

Continued foundering of slab

- emptied space filled by asthenosphere, establishes convection cell

Decompression melting of asthenosphere when cell sufficiently large

- asthenospheric magmatism supplants lithospheric magmatism

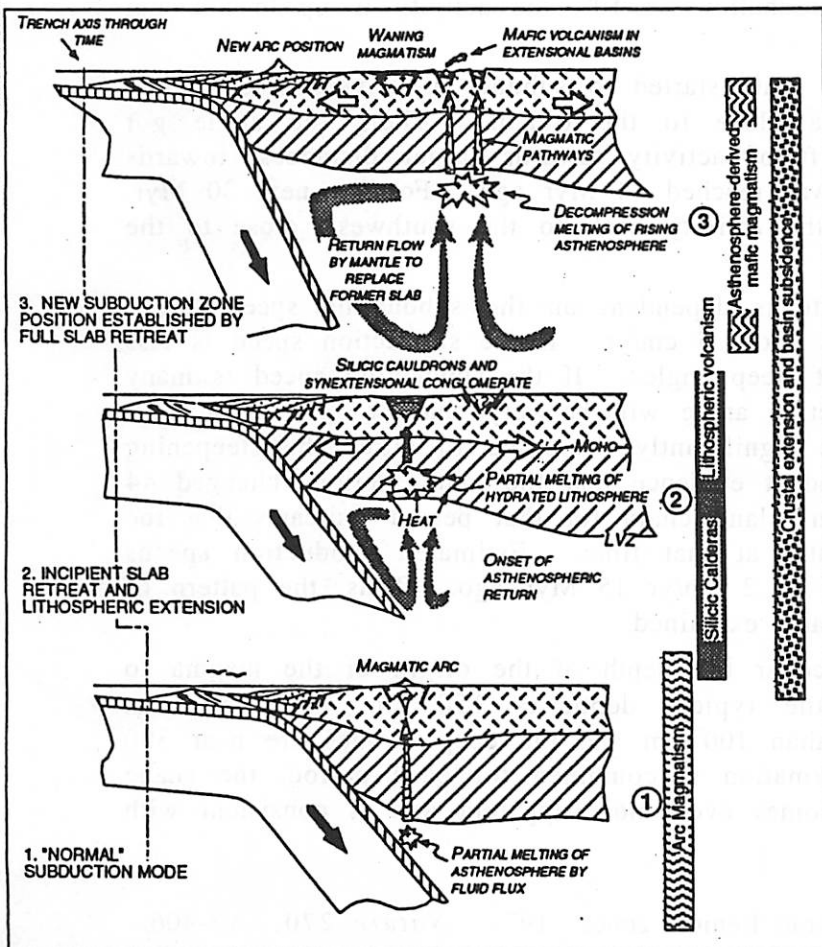


Figure 4. Tectonic model for creation of passive continental rift above foundering subducted slab.

Southern Rio Grande Rift Stratigraphy

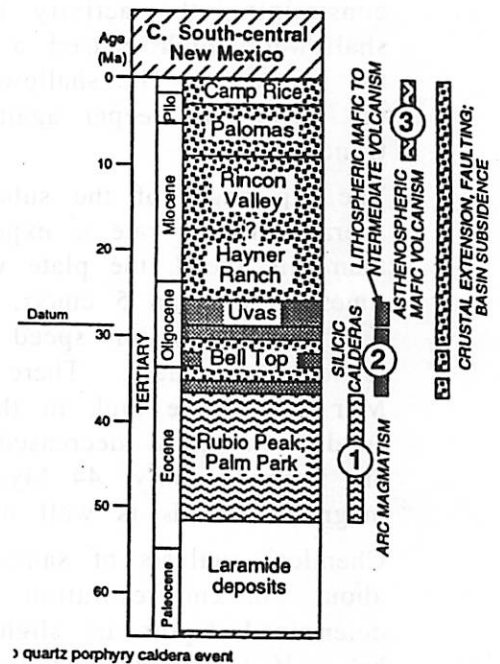


Figure 2. Comparative tectonic stratigraphy of Mexican Borderland and Rio Grande rifts and interpretation of their tectonic significance. Correlation of units after Chapin and Seager (1975), Dickinson et al. (1986, 1989), and Lawton and Olmstead (1995). Mesozoic time scale is from Gradstein et al. (1994); Cenozoic time scale is from Cande and Kent (1992).

East-West Magmatic Trends Across Southwestern US./Northern Mexico

Erich Karkoschka

Dating of magmatic rocks in southeastern California, southern Arizona, southwestern New Mexico, and northern Mexico yielded an interesting distribution of ages versus location. At each epoch, volcanic activity occurred only at specific distances from the San Andreas trench line. On the other hand, the distributions in Mexico and the US. are quite similar (Coney and Reynolds 1977, Clark *et al.* 1982).

The oldest ages found are 140-160 Myr BP at sites all across the investigated area. Then, starting 140 Myr BP, the volcanic activity occurred only within 80 km of the trench line. During the period from 100 to 44 Myr BP, the distance of activity from the trench line increased to about 800 km. Then, the migration stopped and reversed to within 100 km of the trench line by 15 Myr BP. Few samples are younger.

The interpretation is the following. The subducting Pacific plate is melting and causing volcanic arcs once it reaches a depth of about 150 km. If the subduction angle is steep, as steep at 80°, the activity is less than 100 km from the trench line. If the subduction angle is shallow, as shallow as 10°, the activity is up to 800 km from the trench line.

140 Myr ago, the shallow subducting plate started to subduct at a very steep angle, constraining the activity to the area close to the trench. Then, the angle got shallower which caused a steady drift of activity towards larger distances, towards the northeast. The shallowest angle was reached 44 Myr ago. For the next 30 Myr, the angle got steeper again moving the activity back to the southwest, close to the trench line.

The dip angle of the subducting plate is dependent on the subducting speed. The average sinking rate is expected to be about 5 cm/yr. If the subduction speed is less than this speed, the plate will sink at steep angles. If the subduction speed is many times larger than 5 cm/yr, the subduction angle will be very shallow. Thus, 44 Myr ago, the subduction speed must have significantly decreased to allow the steepening angle of the plate. There is independent evidence that the plate motions changed 44 Myr ago. The kink in the Hawaiian island chain for that period indicates that the subduction speed decreased significantly at that time. Estimated subduction speeds are from 15 cm/yr 44 Myr BP down to 2 cm/yr 15 Myr ago. Thus, the pattern of magmatic trends is well understood and explained.

Chemical analysis of samples can recover the depth of the origin of the magma to about 50 km resolution. While the typical depth is 150 km, the shallowest determined depths are slightly lower than 100 km and the deepest ones are near 300 km. If the depth and location information is combined for each period, the shape and angle of the subducted plate becomes even more apparent and is consistent with the explanation given above.

Coney, P.J. and S.J. Reynolds. Cordilleran Benioff zones 1977. *Nature* 270, 403-406.

Clark, K.F., C.T. Foster, and P.E. Damon 1982. Cenozoic mineral deposits and subduction-related magmatic arcs in Mexico. *Geolog. Soc. of Amer. Bull.* 93, 533-544.

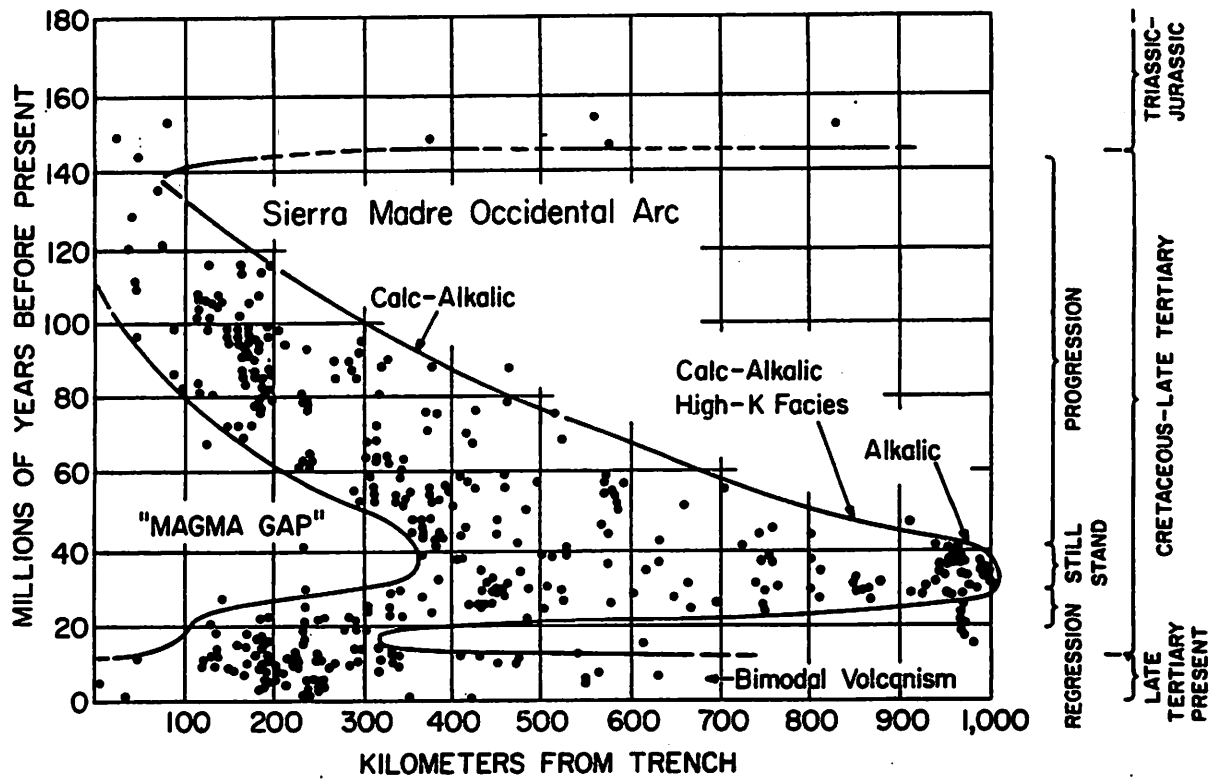


Figure 2. Magma distribution in space and time in northern Mexico (from Clark and others, 1979b).

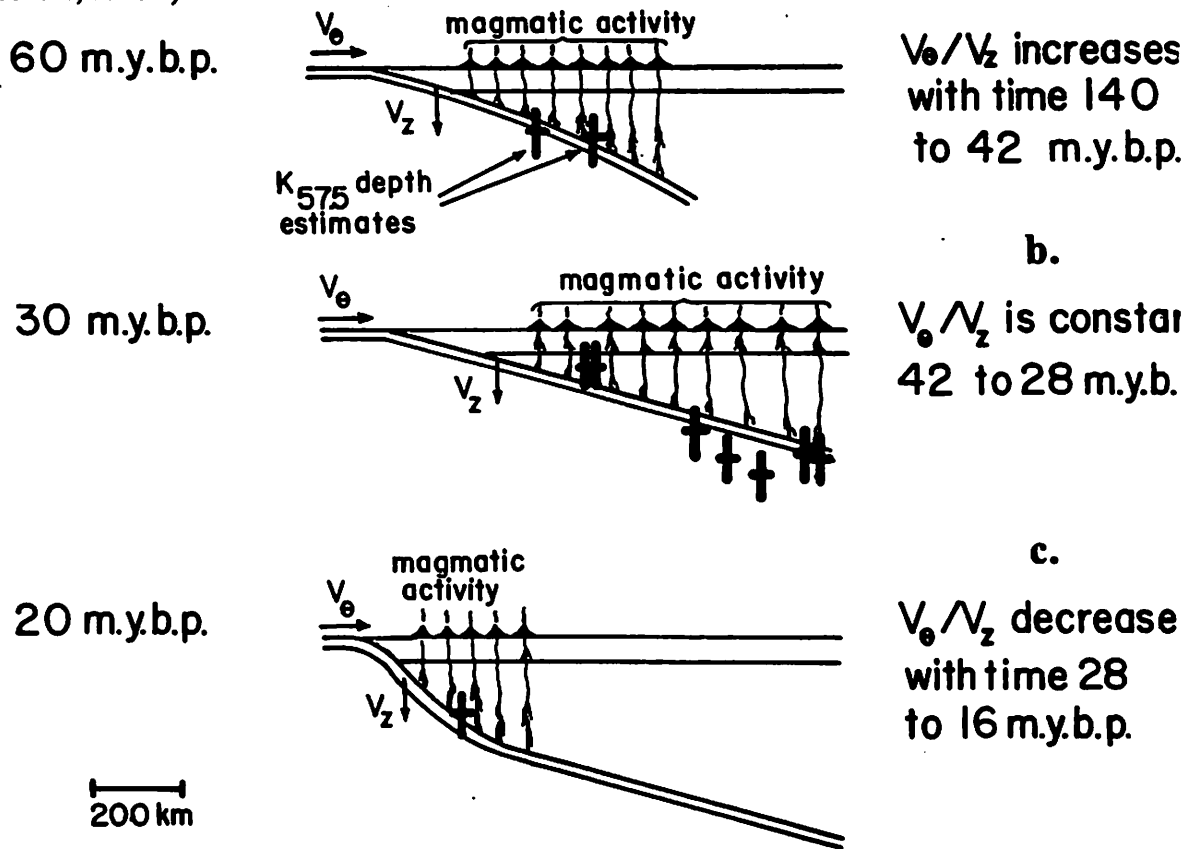
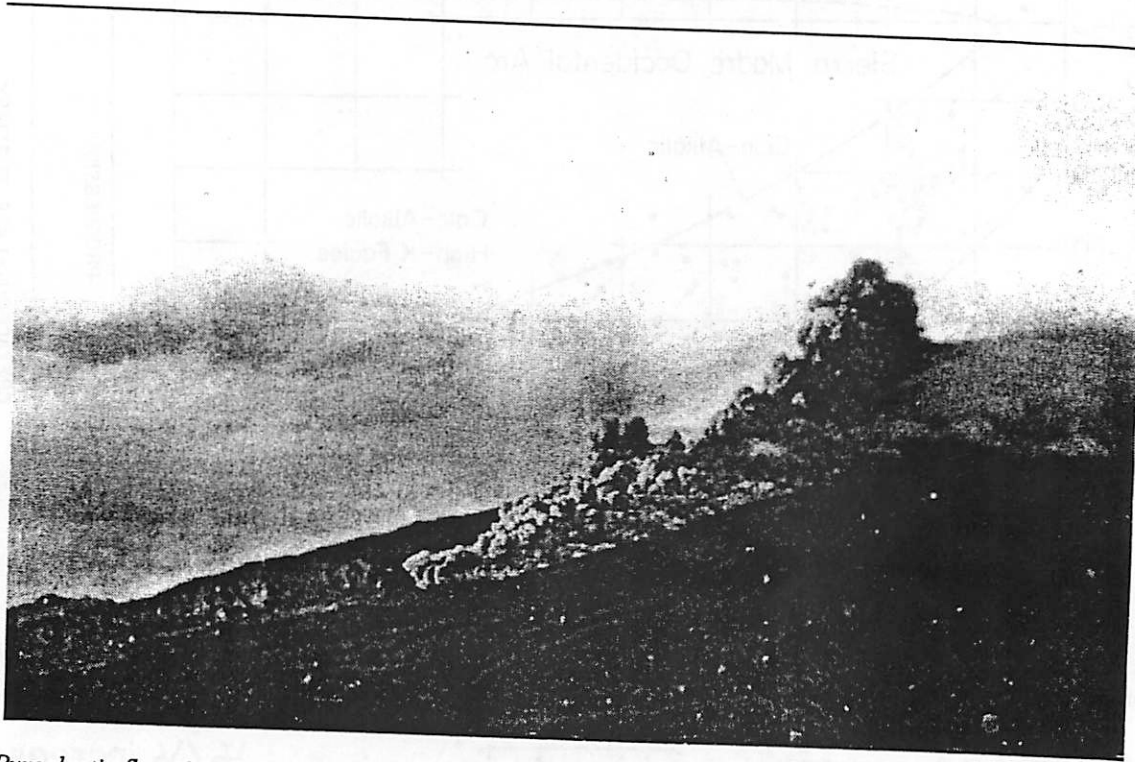


Figure 4. Calculated depths to Benioff zone for 15 magmatic suites listed in Table 1 using the Dickinson (1975) $K_{57.5}$ -h relationship. Magma envelope from Figure 2 show times of the three cross sections shown in Figure 4.

Eruption and Deposition of Ass – I mean “Ash” - Flows

Pete “Where the hell did my hair go?” Lanagan



Pyroclastic flow, Mt. Pelée, 25 January 1903 [LaCroix 1904, pl. XII]. Stolen from Volcanic Phenomena at Pompeii (<http://urban.arch.virginia.edu/struct/pompeii/images/pages/pl-XII-flow-2.html>) (Martini, 1997)

Possibly Helpful Definitions

ash flow: see *glowing avalanche*

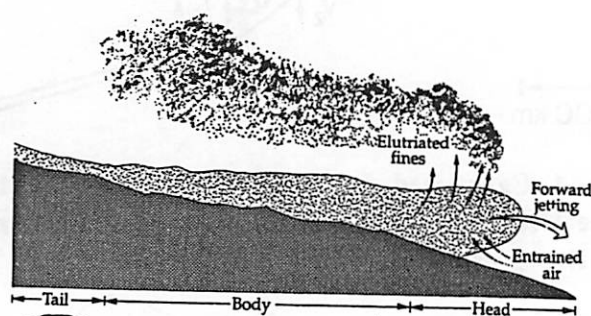
glowing cloud: see *nuée arente*

glowing avalanche: see *glowing cloud*

nuée arente: see *pyroclastic flow*

pyroclastic flow: see *ash flow*

Fig. 11.7 A generic pyroclastic flow, showing usually recognized components of head, body, and tail. Head is most highly fluidized and turbulent; body moves mostly in laminar mode. Most deposition takes place from body, not head. Here, forward-springing jets are shown, which may be involved in formation of some ground surge deposits.



(Francis, 1993)

17

Possibly More Helpful Definitions

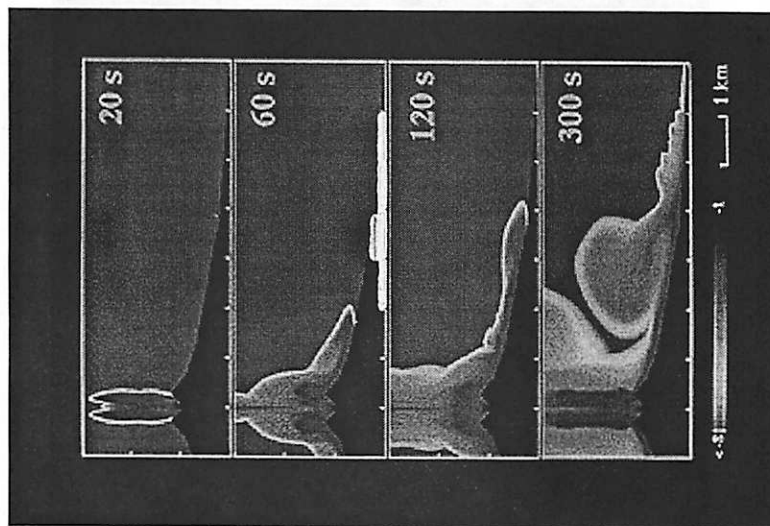
ash flow: A density current, generally a highly heated mixture of volcanic gases and ash, traveling down the flanks of a volcano or along the surface of the ground; it is produced by the explosive disintegration of viscous lava in a volcanic center or by the explosive emission of gas-charged ash from a fissure or group of fissures. The solid materials contained in a typical ash flow are unsorted and ordinarily include pumice, scoria, and blocks in addition to ash.

ignimbrite: The rock formed by the widespread deposition and consolidation of ash flows and nuée ardentes. The term includes *welded tuff* and nonwelded but recrystallized ash flows.

nuée ardente: A swiftly flowing, turbulent gaseous clouds, sometimes incandescent, erupted from a volcano and containing ash and other pyroclastics in its lower part; a *density current* of pyroclastic flow. The lower part of nuée ardente is comparable to an *ash flow*, and the terms are sometimes used synonymously.

welded tuff: A glass-rich pyroclastic rock that has been indurated by the welding together of its glass shards under the combined action of the heat retained by particles, the weight of overlying material, and hot gases. It is generally composed of silicic pyroclasts and appears banded or streaky.

- from *Dictionary of Geologic Terms: Third Edition*, AGI 1984



Computer simulation of plume collapse from Vesuvius-type plinian eruption. (Dobran, 1996)

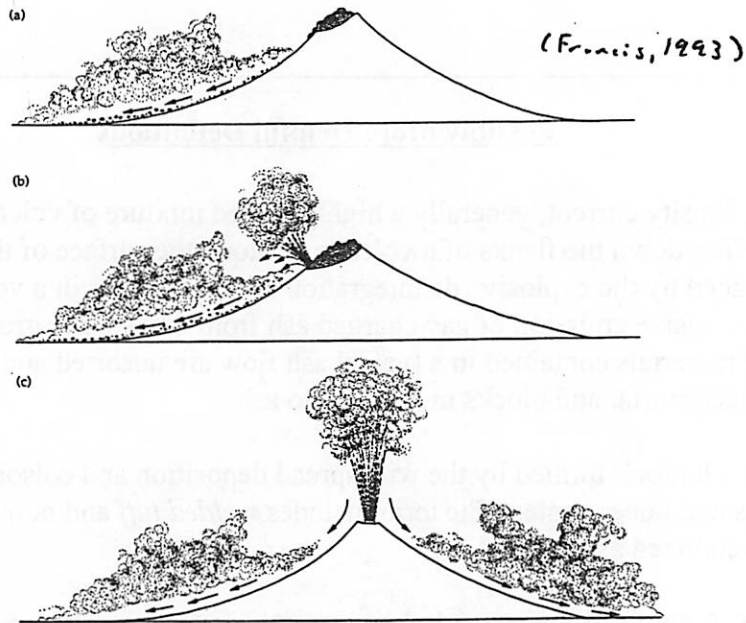
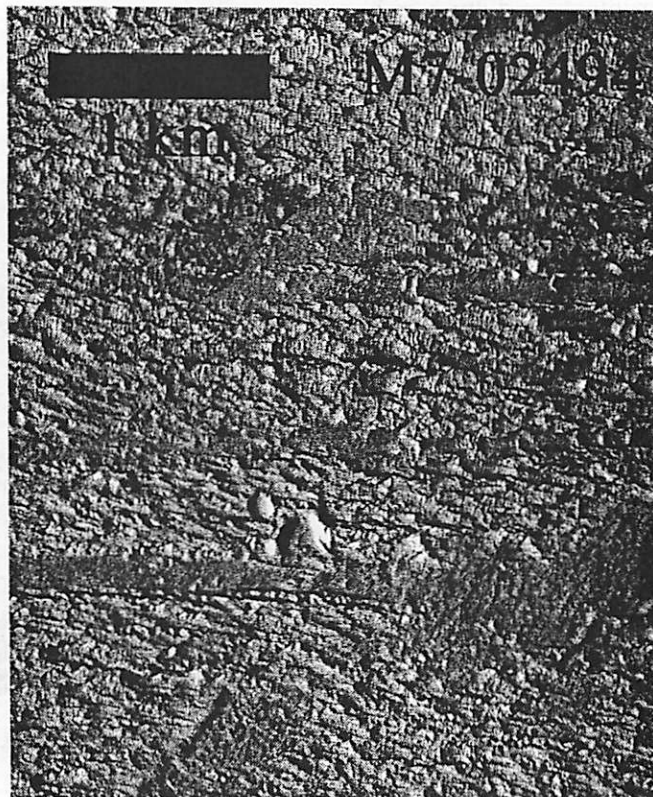


Fig. 12.1 Three common mechanisms for generating *nuées ardentes*. (a) Simple gravitational collapse of a growing lava dome or flow on a volcano (merapi type). (b) Explosive disruption of growing lava dome (pelécan type). (c) Collapse from eruption column (soufrière type).

The Planetary Connection

Mars: The Medusae Fossae Formation...???



References

- Bates, R.L. and J.A. Jackson (eds) 1984. *Dictionary of Geologic Terms: Third Edition*, American Geological Institute. New York.
- Dobran, Flavio. 1996. *Prevention of a Catastrophe in the Vesuvius Area*, WWW document, Global Volcanic and Environmental Systems Simulation (GVES), Napoli, Italy. <http://tribeca.ios.com/~dobran/HPrest.html>.
- Fagents, S.A. and L. Wilson. Numerical Modeling of Ejecta Dispersal from Transient Volcanic Explosions on Mars. *Icarus*, 123, 284-295.
- Francis, Peter. 1993. *Volcanoes: A Planetary Perspective*. Clarendon Press: New York.
- Macdonald, G.A. 1972. *Volcanoes*. Prentice-Hall Inc.: Englewood Cliffs.
- Martini, K. 1997. *Volcanic Phenomena at Pompeii*. WWW document, University of Virginia. <http://urban.arch.virginia.edu/struct/pompeii/images/pages/pl-XII-flow-2.html>.
- Williams, H. and A.R. McBirney. 1969. *An Investigation of Volcanic Depressions*. Progress Report: NASA Research Grant NGR-38-033-012.
- Wilson, L. and J.W. Head III. 1994. Mars: Review and Analysis of Volcanic Eruption Theory and Relationships to Observed Landforms. *Rev. Geophys.*, 32, 221-263.

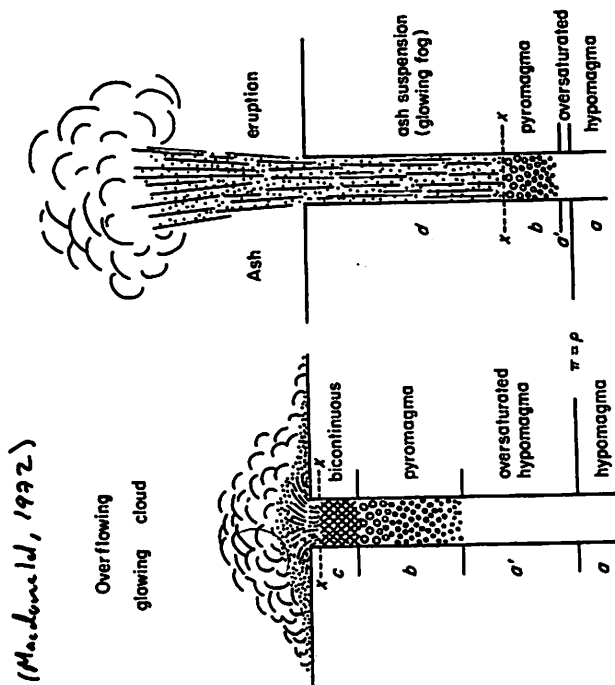


FIGURE 8-4. Diagram illustrating the difference between a normal ash eruption and an ash-flow eruption. (From Rittman, 1988a.) The hypomagma at depth (zone a) is saturated or undersaturated with gas. As it rises into zones of lower pressure it becomes oversaturated (zone a') and bubbles start to form in it (pyromagma, zone b) but the expansion of the liquid-and-gas mixture is restrained by the high viscosity of the liquid. In zone c the gas becomes so abundant that there are present two continuous phases, instead of a gas phase dispersed in a liquid. Eventually, with further rise, the eruption level (X-X') is reached, and the gas rushes out, bearing in it a cloud of liquid and solid particles. In the ash eruption (right) the eruption level is deep, and the expanding gas is directed upward as though by a gun barrel. In the ash-flow eruption (left) the shallow eruption level results in an overflow of the gas-and-ash mixture with ash flows and glowing clouds spreading out from the vent. The higher the viscosity of the magma, the lower the external pressure that is required to initiate eruption, hence the shallower the eruption level, so that the more viscous siliceous magmas (e.g. rhyolite) are more apt to produce ash flows than are the less viscous basaltic ones.

COOLING UNITS of the BANDELIER TUFF

Jani Radebaugh May 2000

A **cooling unit**, as first described by Robert L. Smith in 1960, prior to his comprehensive study of Valles Caldera and the Bandelier Tuff in 1966, is a collection of pyroclastic material that is erupted together and almost immediately cooled. Generally a cooling unit is one ash flow, although this could also be several flows erupted successively, as long as they cool simultaneously as a single sheet.

We will discuss some of the major cooling units of the **Bandelier Tuff** (See Figures on following pages). The first of two major members of the Bandelier Tuff, the **Otowi Member**, was erupted about 1.4 my ago, and was comprised of about 300 km³ of 76% to 77% SiO₂ rhyolite magma. This eruption also resulted in the formation of the **Toledo Caldera**. Over the next 300,000y a series of air fall deposits were lain on top of the Otowi member. Then about 1.1 my ago, the second major member of the Bandelier Tuff was erupted, the 300 km³ **Tshirege Member**, and the resulting collapse of Valles Caldera erased the previous Toledo Caldera. The Tshirege Member is composed largely of vitric pumice, of approximately 76% SiO₂.

After the Tshirege was erupted, **resurgence** (post-caldera eruptions that generally lead to formation of viscous silicic domes within the caldera) produced a 74% SiO₂ porphyritic rhyolite glass. The trace element (Nb, Ta, U, Th, Rb, etc.) composition of these later eruptions are anomalously low in comparison with the rest of the sequences; the interpretation follows that the magma chamber composition was imbalanced after the Tshirege eruption and caldera formation. The magma equilibrium was later recovered upon eruption of aphyric (nonporphyritic) **obsidians** within the caldera. **Quartz latite domes** of identical composition, 68% SiO₂ are found both immediately before (underlying) and immediately after (overlying) the Tshirege flows. These are probably cogenetic, yet separate from the Bandelier flows. It is possible these rose from greater depths than the magma chamber feeding the main caldera tuffs.

Some confusion exists over why certain trace element (Nb, Ta, U, Th, Rb, etc.) abundances start high and then grade to low in these magmas; some argue that fractional crystallization can explain the enrichment, yet others hold that this is not a sufficient mechanism to bring this about. Smith (1979) argues that the gradients shown are a function of changing boundary-layer conditions at the top of a **large magma chamber**. The compositional and temperature gradients, as well as the movement or convection styles of these large silicic magma chambers, are not well known (See magma chamber figure). This problem is also addressed by Wes Hildreth in study of the Bishop Tuff of Long Valley Caldera (1979). Study of the ash flow units, however, can lead to a better understanding of their properties and evolutions.

Bandelier Tuff/ Cooling Units, ctd.

Further Reading:

Best, M. G., 1982, *Igneous and Metamorphic Petrology*: Blackwell Science, Mass., 630 p.

Christiansen, R. L., 1979, Cooling units and composite sheets in relation to caldera structures: Geological Society of America Special Paper 180, p. 29-42.

Heiken, G., F. Goff, J. Stix, S. Tamanyu, M. Shariqullah, S. Garcia, and R. Hagan, 1986, Intracaldera volcanic activity, Toledo Caldera and embayment, Jemez Mountains, New Mexico: *Journal of Geophysical Research*, v. 91, no. b2, p. 1799-1815.

Hildreth, W., 1979, The Bishop Tuff: Evidence for the origin of compositional zonation in silicic magma chambers: Geological Society of America Special Paper 180, p. 43-75.

Smith, R. L., 1960, Ash flows, Geological Society of America Special Paper 180, p. 125-136.

Smith, R. L., and R. A. Bailey, 1966, The Bandelier Tuff—A study of ash-flow eruption cycles from zoned magma chambers: *Bulletin of Volcanology* 29, p. 83-104.

Smith, R. L., and R. A. Bailey, 1968, Resurgent cauldrons, *in* R. R. Coats, R. L. Hay, and C. A. Anderson, eds., *Studies in volcanology*: Geological Society of America Special Memoir 116, p. 153-210.

Smith, R. L., 1979, Ash-flow magmatism: Geological Society of America Special Paper 180, p. 5-27.

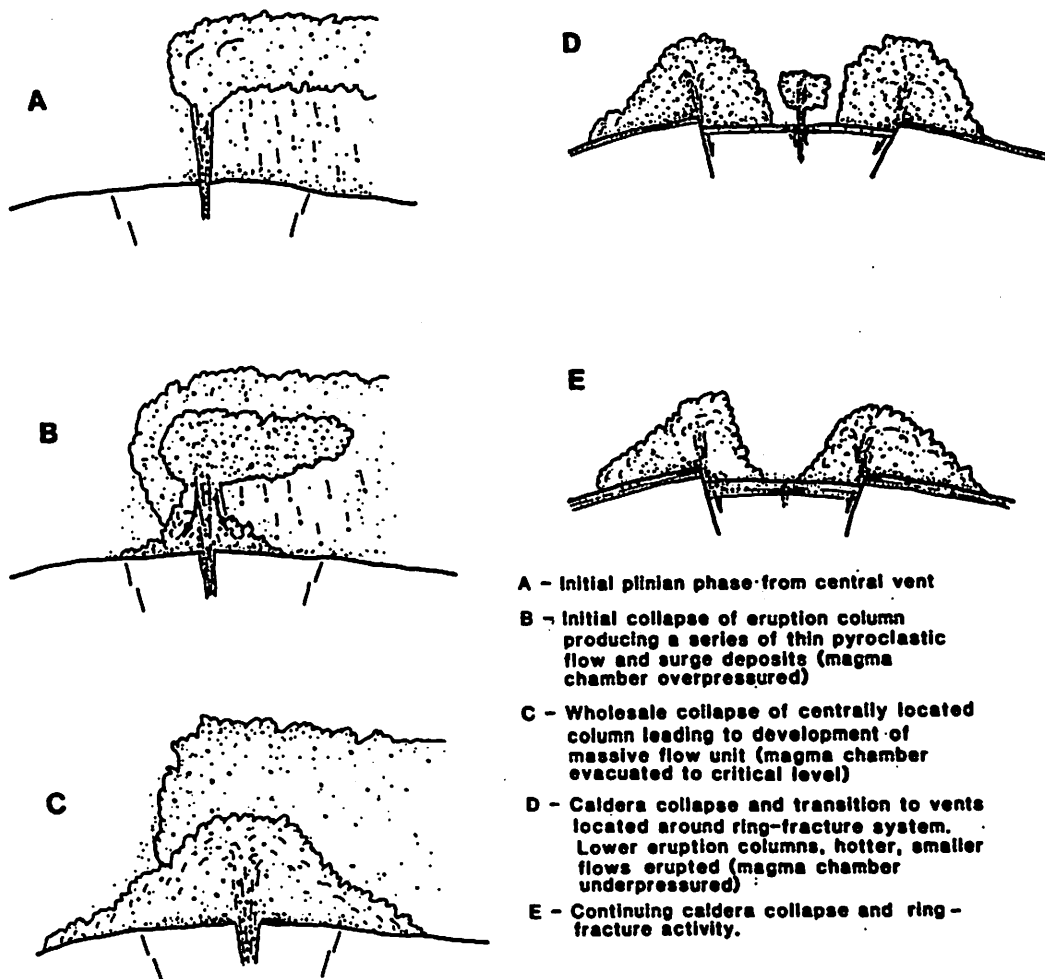
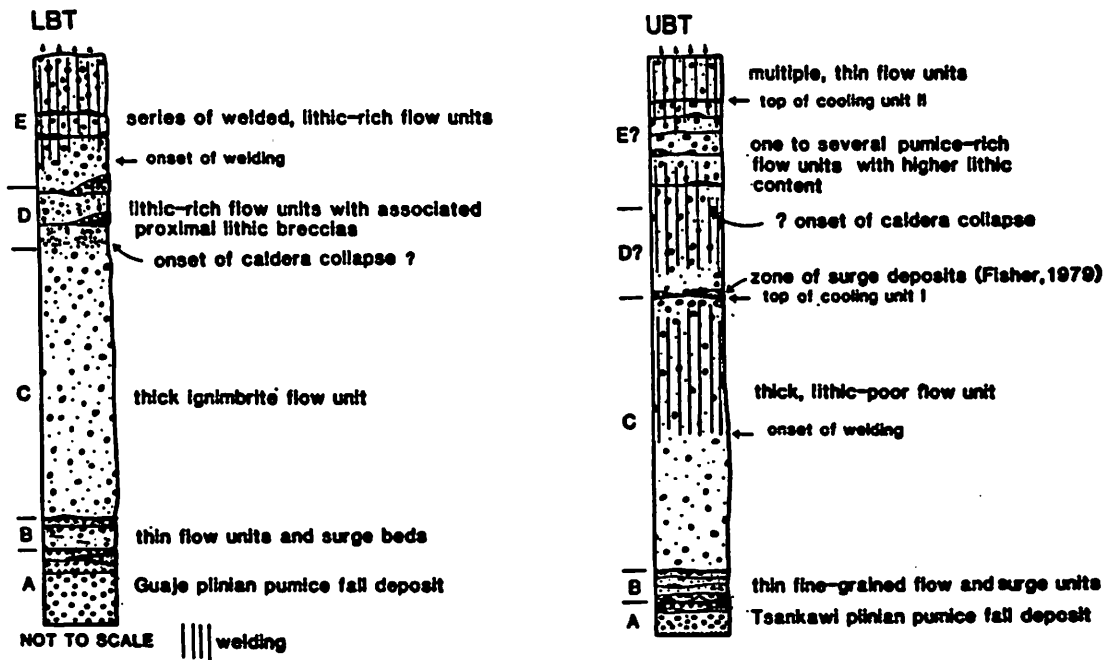


Fig. 15. Standardized composite sections through the Lower and Upper Bandelier tufts (UBT and LBT), showing major zones and interpretation of dominant eruptive mechanisms operating during the deposition of each zone. Interpretation of the eruptive sequence from zone A to E is shown in the cartoon below, based on the LBT. Phases in the eruption are keyed to the sections above.

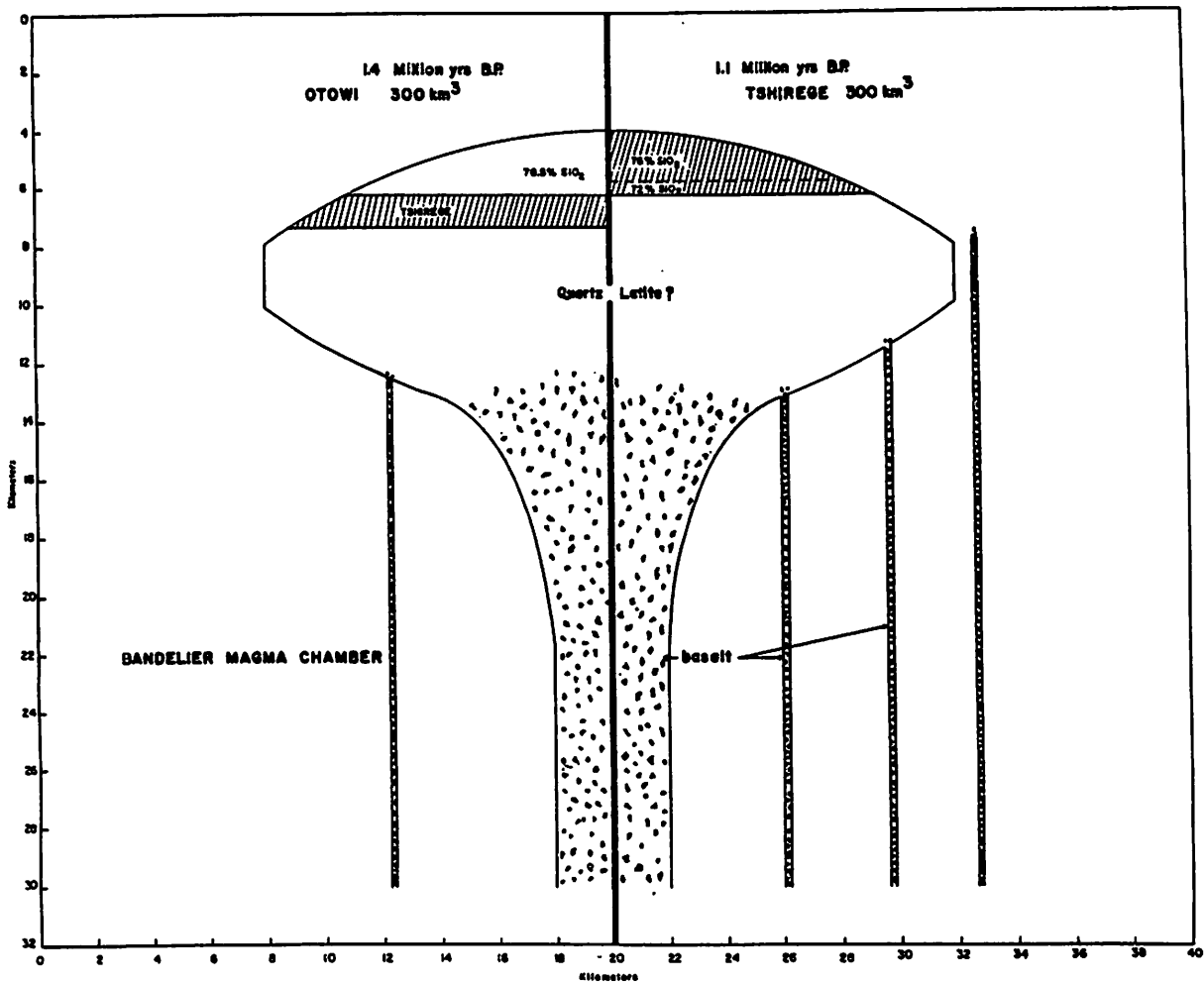


Figure 9. Schematic cross section of the Bandelier magma chamber as it may have existed at two points in time.

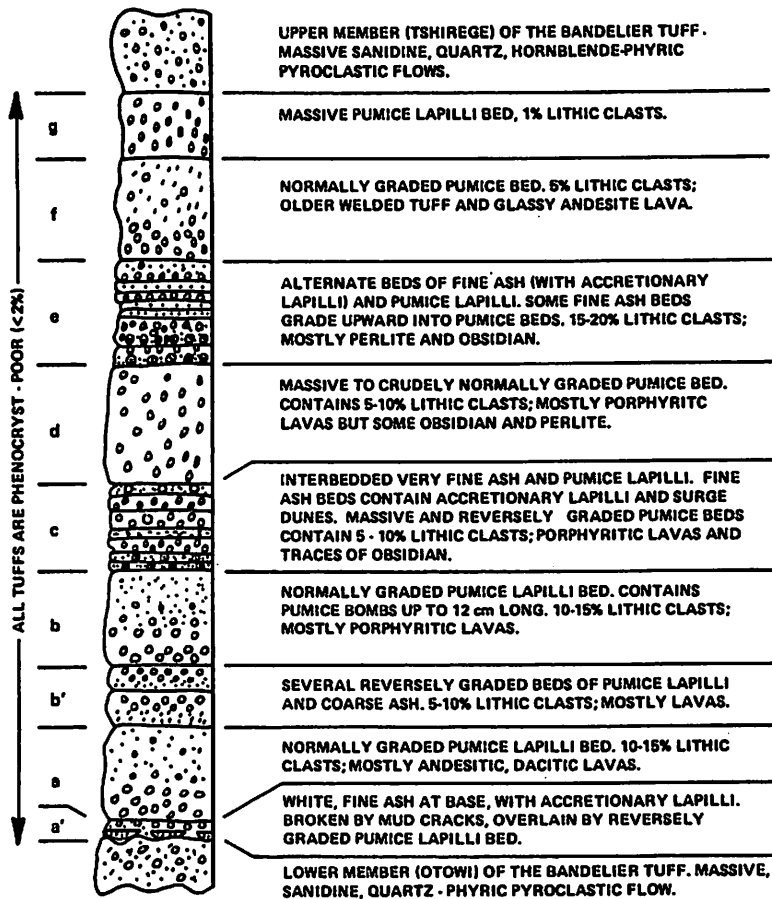


Fig. 2. Composite stratigraphic section, Cerro Toledo tuffs.

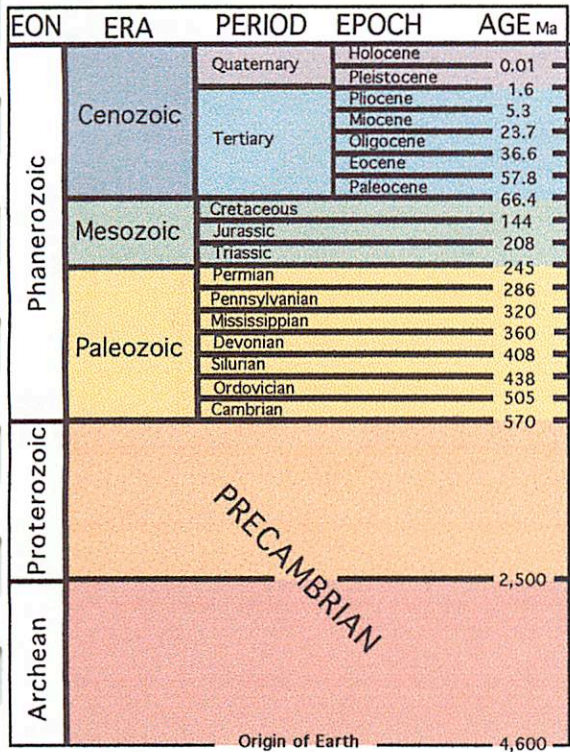


Figure 1a. Geologic timescale. (after McGeary and Plummer, 1992)

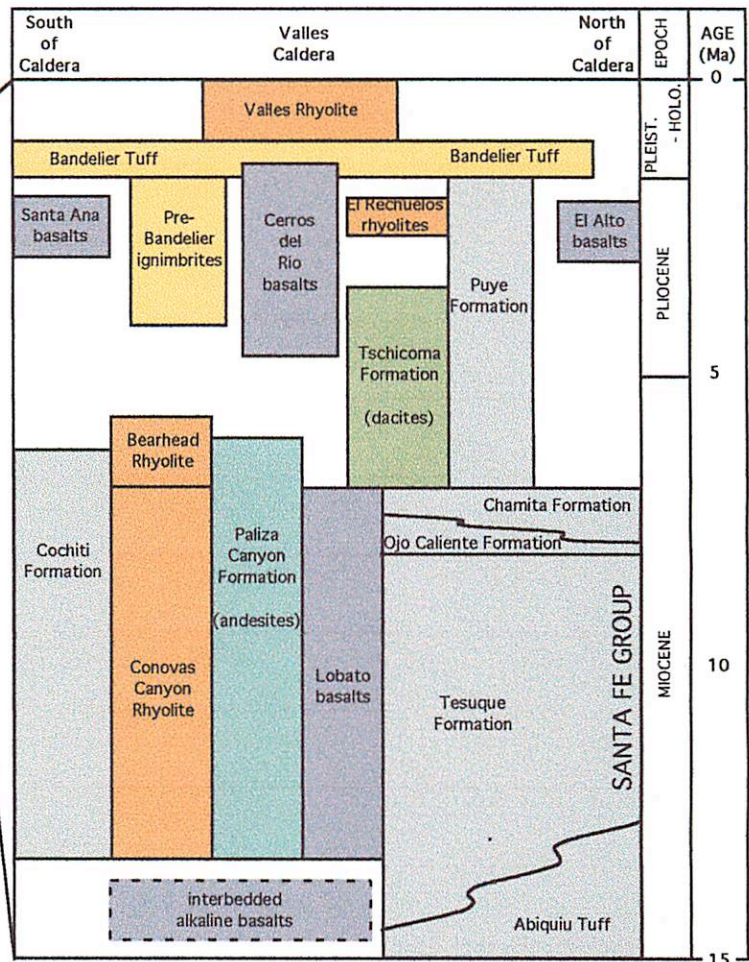


Figure 1b. Chronostratigraphic chart of major units along a south to north (left to right) transect through the Jemez Mountains. (adapted from Gardner *et al.*, 1986 and Self *et al.*, 1986)

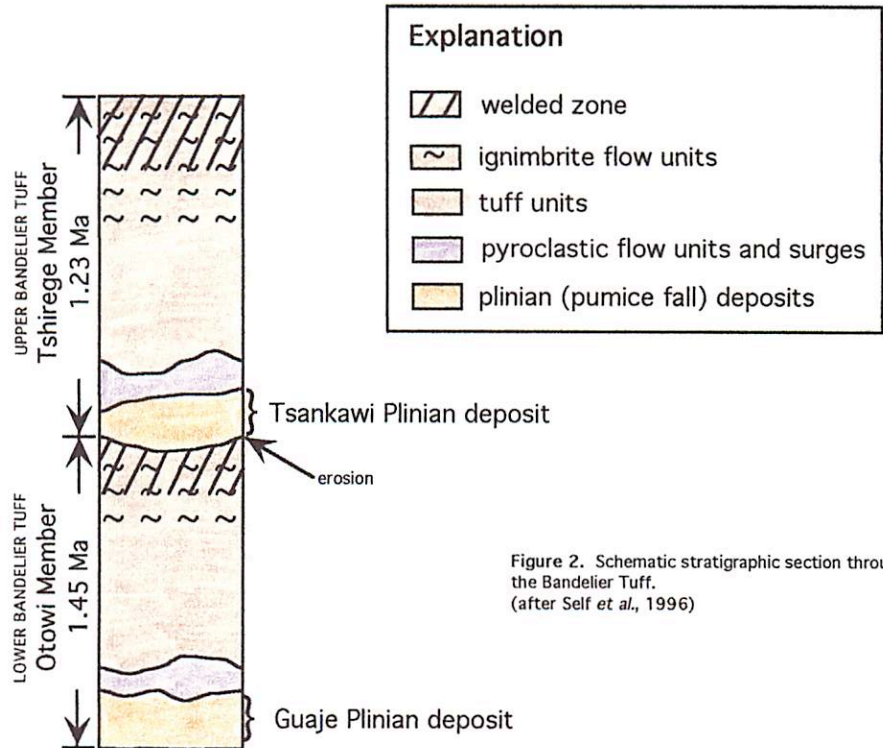


Figure 2. Schematic stratigraphic section through the Bandelier Tuff. (after Self *et al.*, 1996)

Resurgent Domes

Joe Spitale

**JEMEZ
MTN. LOOP**

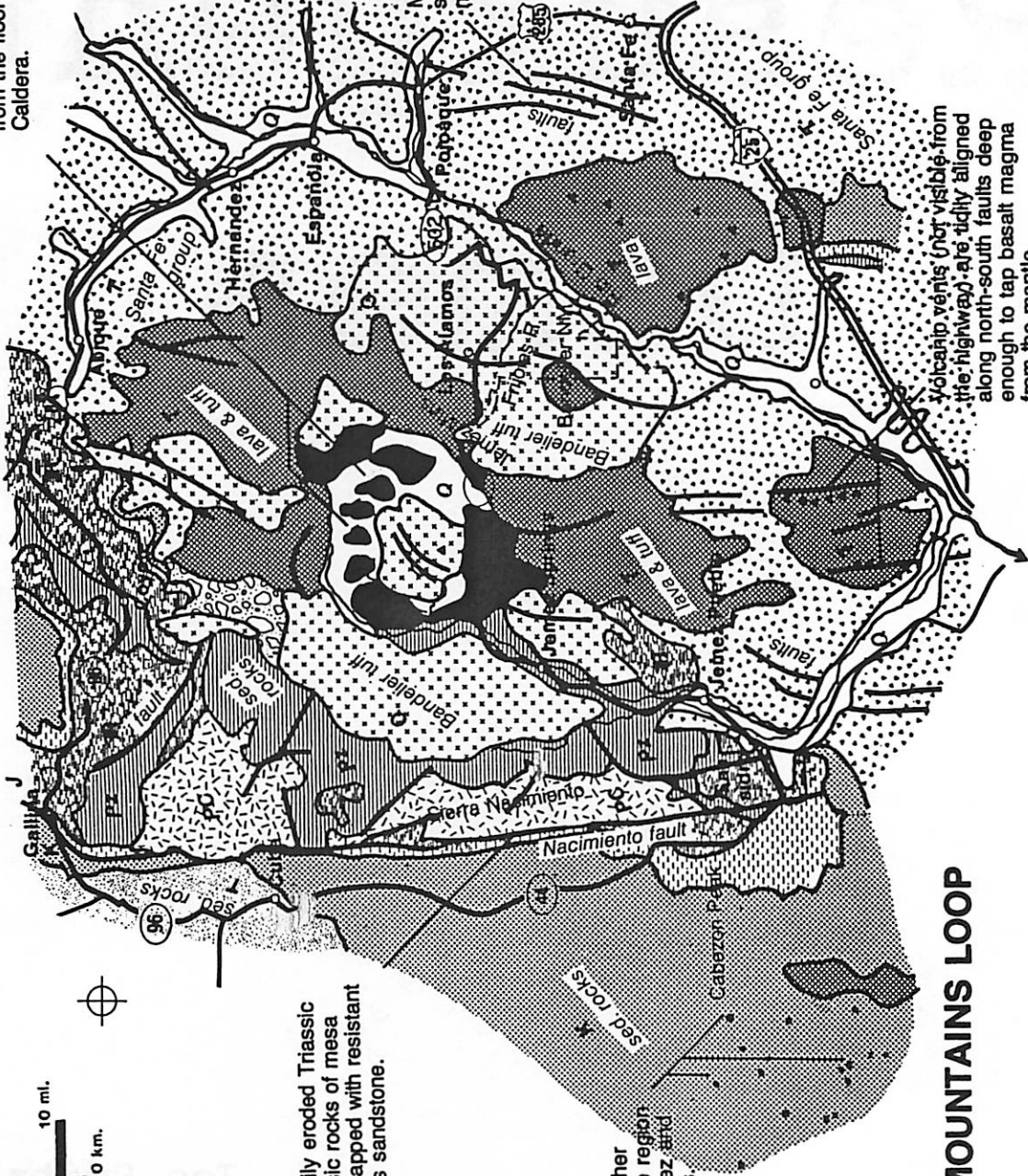
A few miles north on US 84 is Ghost Ranch, site of dinosaur finds. An exhibit explains local geology.

A cirlet of lava domes and a central resurgent dome rise from the floor of the Jemez Caldera.

Many rift valley faults are not shown. These reflect north-south trend.

lava dome

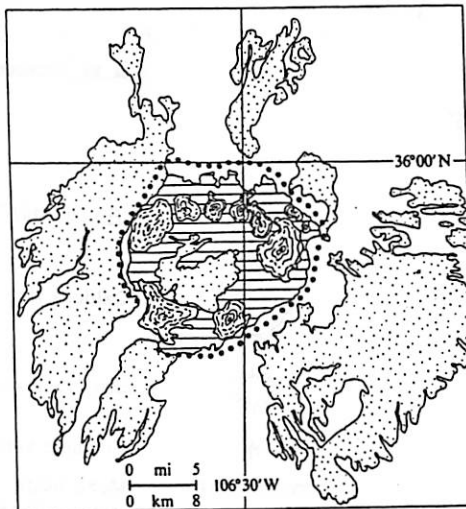
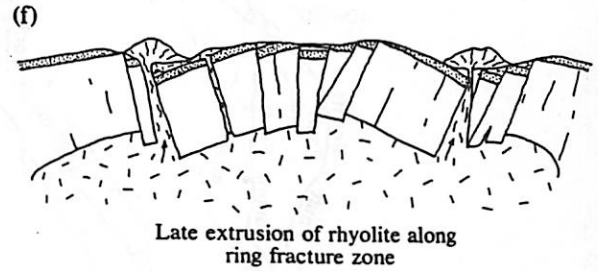
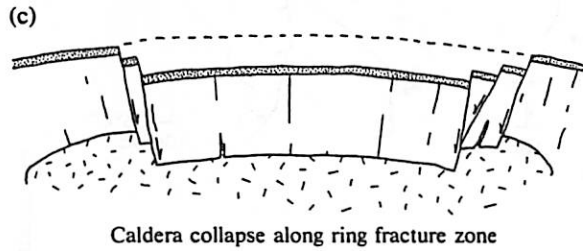
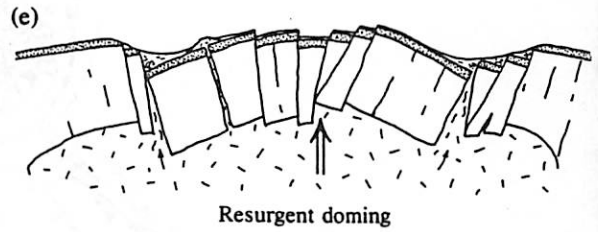
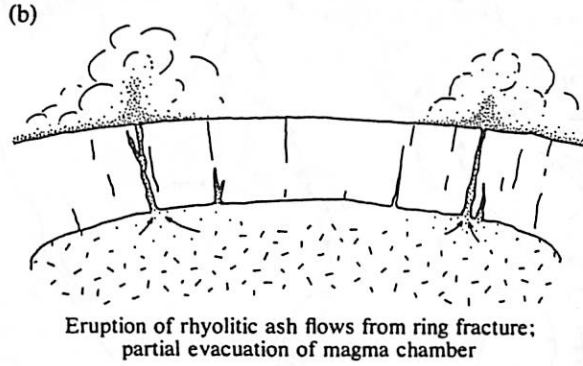
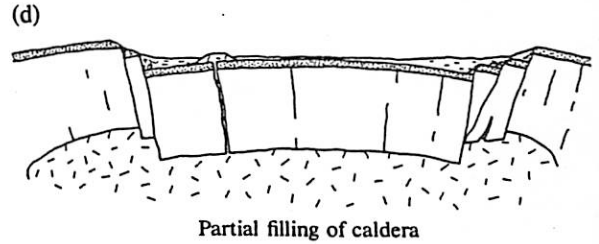
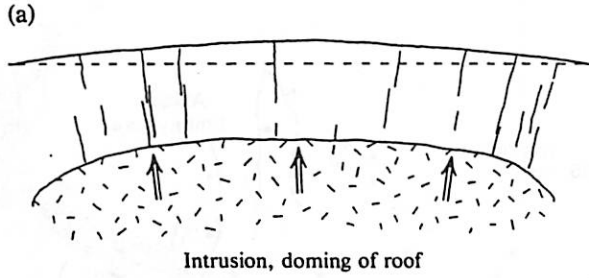
Volcanic vents (not visible from the highway) are tidily aligned along north-south faults deep enough to tap basalt magma from the mantle.

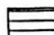





Weak, easily eroded Triassic and Jurassic rocks of mesa walls are capped with resistant Cretaceous sandstone.

Cabezon Peak and other volcanic necks dot the region southwest of the Jemez and Nacimiento Mountains.

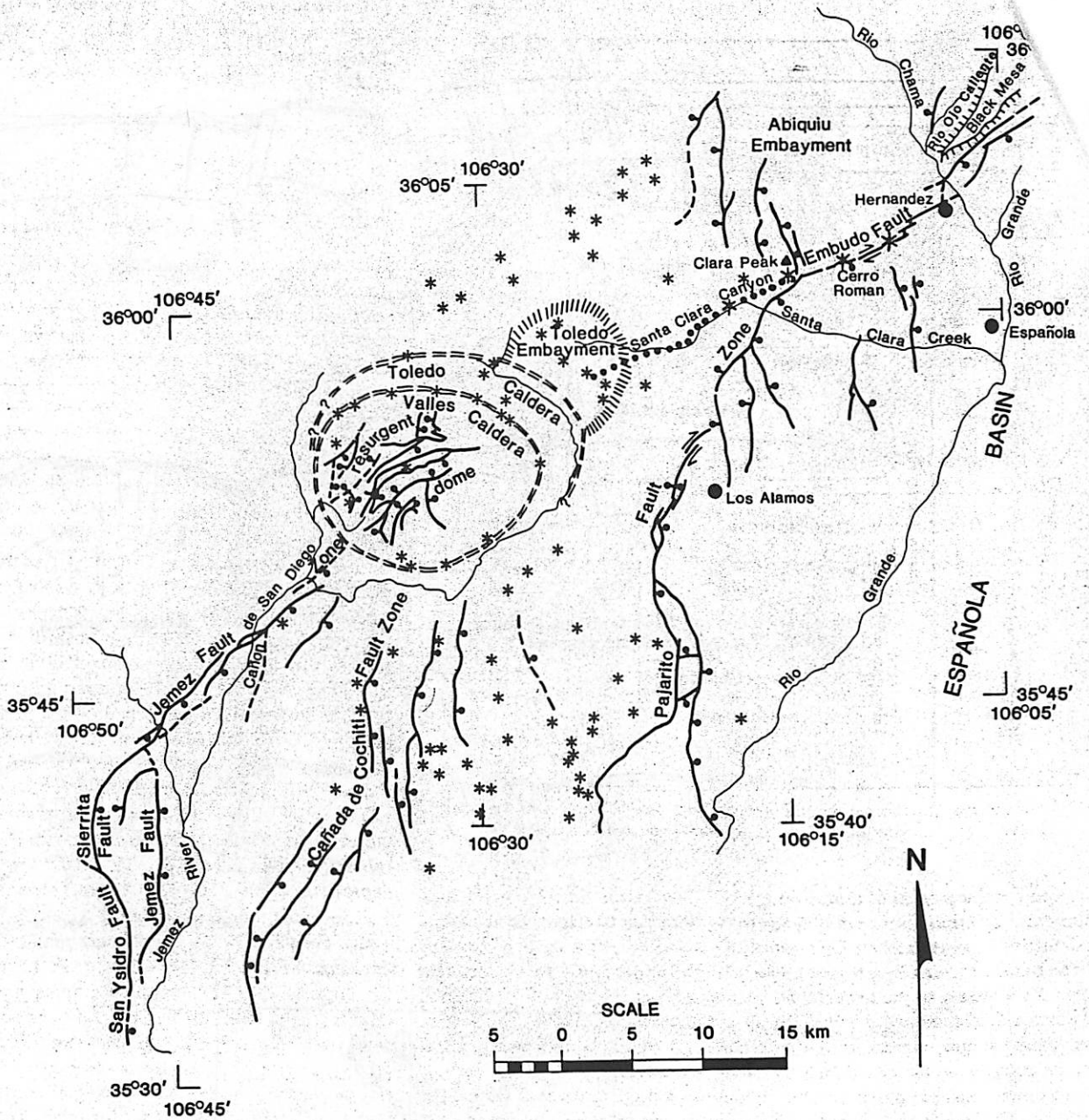
JEMEZ MOUNTAINS LOOP









-  Caldera fill (tuffs, lake sediments, alluvium, lavas)
-  Rhyolite domes
-  Ash-flow tuffs
-  Older volcanic and sedimentary rocks

... Topographic rim of caldera

28

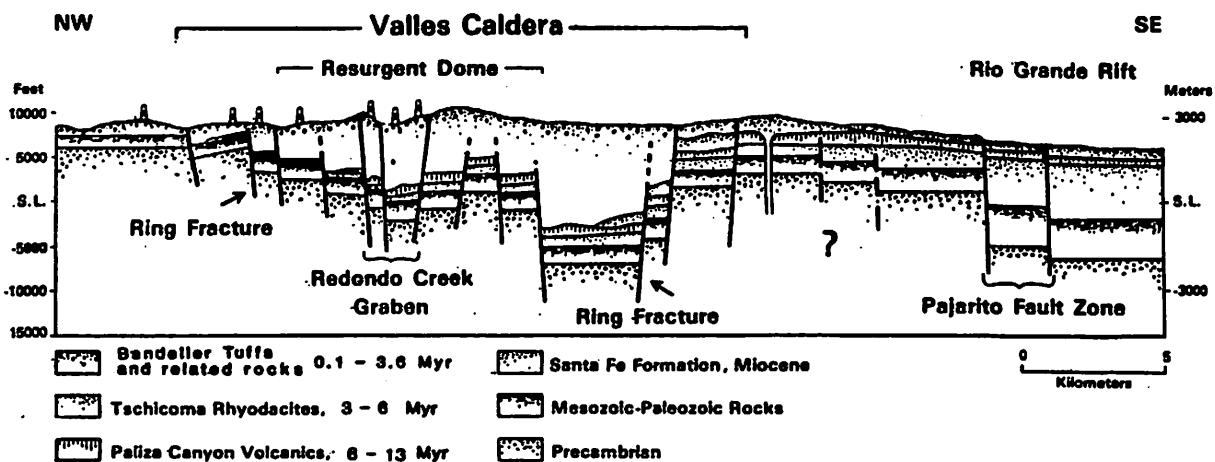
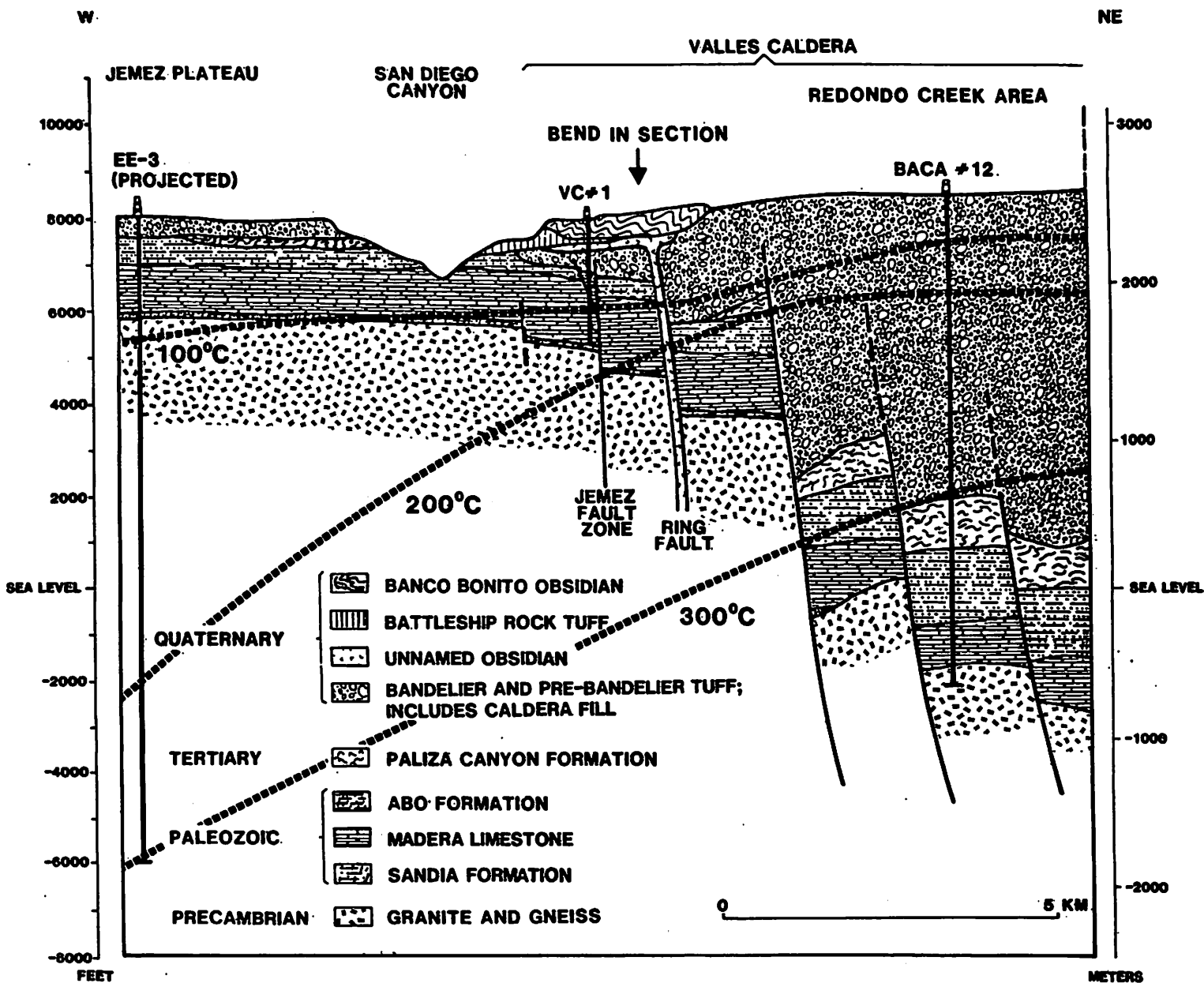


EXPLANATION

-  Caldera ring fracture
-  Structural depression
-  Volcanic vent
-  Mesa edge
hachures on slope
-  High angle fault
dumbbell on downthrown side
arrows show relative offset
-  Structural discontinuity

85

29



REFERENCES

- Best, M. G. 1982. *Igneous and Metamorphic Petrology* W. H. Freeman and Co., New York
- Suppe, J. 1985. *Principles of Structural Geology* Prentice Hall, Inc., Englewood Cliffs, NJ
- Chronic, H. 1987. *Roadside Geology of New Mexico* Mountain Press Publishing Co., Missoula
- Aldrich, M. J., Jr. 1986. Tectonics of the Jemez Lineament Mountains and Rio Grande Rift. *Journal of Geophysical Research* **91B2**, 1753-1762.
- Goff, F., Rowley, J., Gardner, J. N., Hawkins, W., Goff, S., Charles, R., Wachs, D., Maasan, L., Heiken, G. 1986. Initial Results from VC-1, First Continental Scientific Drilling Program Core Hole in Valles Caldera, New Mexico. *Journal of Geophysical Research* **91B2**, 1742-1752.
- Self, S., Goff, F., Gardner, J. N., Wright, J. V., Kite, W. M. 1986. Explosive Rhyolitic Volcanism in the Jemez Mountains: Vent Locations, Caldera Development and Relation to Regional Structure. *Journal of Geophysical Research* **91B2**, 1779-1798.

“Moat” Rhyolites

Rhyolite Domes & Flows Around Valles Caldera

By Ingrid Daubar

The Tewa Group represents the last phase of volcanism near Valles Caldera. It is almost entirely rhyolitic. The Bandelier Tuffs are included in this group; they are related to the formation of the caldera. The Valles Rhyolite Formation includes all the stuff erupted after the caldera was formed. The oldest of these, the Deer Canyon member, was formed before the uplift of the resurgent dome. The Redondo Creek member formed during the uplift, and consequently these two members were affected (deformed and tilted) by the resurgence. Later eruptions were all vented from spots on the Valles Caldera ring fracture.

Valle Grande Member Rhyolites

This group includes eight domes which define the ring fracture around the caldera. They range in age from the time of the caldera collapse to ~0.45Ma. A general trend of decreasing ages is seen from the oldest (Del Medio) dome continuing counterclockwise around the caldera.

Chemistry and dating analysis indicates that these rhyolites originated in (at least) three separate magma chambers, *not* one single long-lived chamber. They are also probably not comagmatic with either the preceding or following rhyolitic eruptions.

GROUP	Formation and Member	
TEWA GROUP	Valles Rhyolite	Banco Bonito Member
		Battleship Rock Member
		El Cajete Member
		Valle Grande Member
		Redondo Creek Member
Bandelier Tuff	Deer Canyon Member	
	Tahirege Member	
	Cerro Toledo Rhyolite	
POLVADERA GROUP	Otowi Member	
	El Rechuelos Rhyolite	
	Tschicoma Formation	
KERES GROUP	Lobato Basalt	
	Bearhead Rhyolite	
KERES GROUP	Paliza Canyon Formation	
	Canovas Canyon Rhyolite	

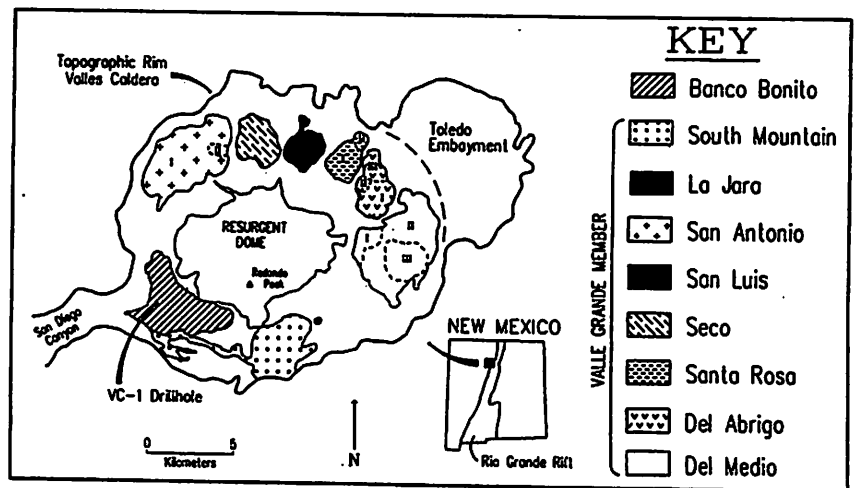
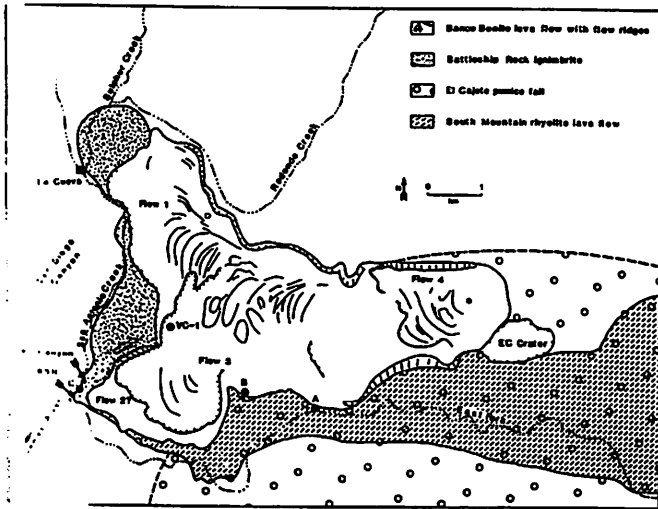


Fig. 1. Location map of the Jemez Mountains Volcanic Field and the Valles Caldera. Individual domes and dome complexes which make up the Valle Grande Member are illustrated by patterns.

Bibliography

- S. Self et al. (1988) *JGR* 93, 6113-6127.
- T.L. Spell & P.R. Kyle (1989) *JGR* 94, 10,379-10,396.
- S. Self et al. (1991) *JGR* 96, 4107-4116.



El Cajete series

The El Cajete Series consists of three eruptive units. They have less silica than the Valle Grande Group, and they are the youngest rhyolites found in the area (170-240 ka). They have similar chemical compositions, mineralogies and morphologies, which indicates a comagmatic origin, although this is debated.

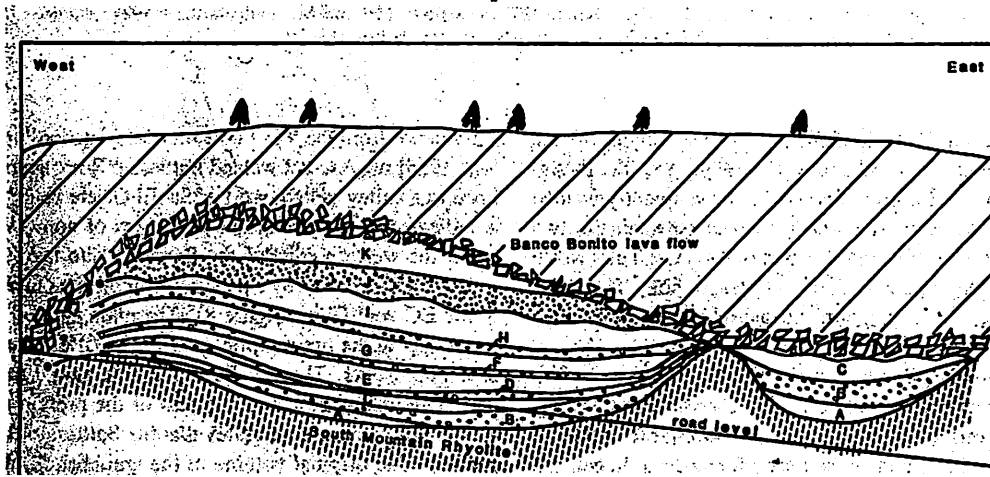
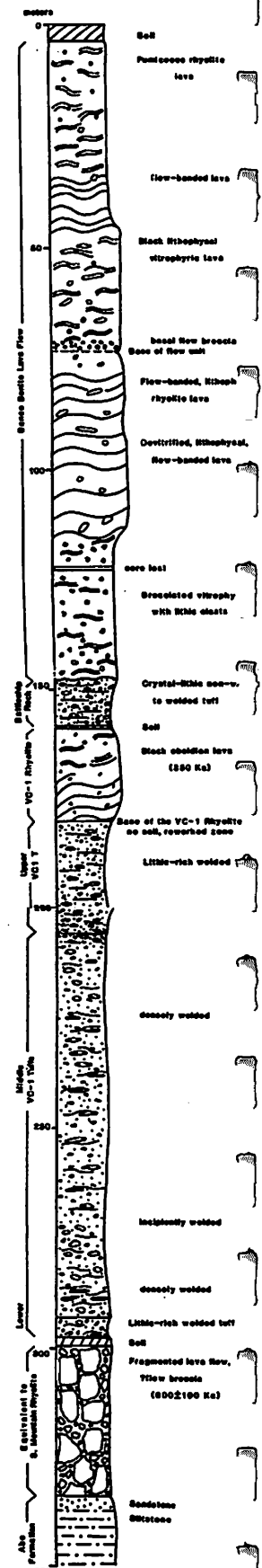
These rhyolites are generally porphyritic, with phenocrysts of plagioclase and biotite. Mafic minerals are mostly biotite and hornblende.

The El Cajete Plinian deposit consists of interbedded pyroclastic flows and surge deposits. The beds are white to pink, thin, and nonwelded, with varying grain and lithic sizes. Tan to white rhyolitic pumice is also present. The lower surge deposits show impact sags, indicating simultaneous ballistic emplacement and surge deposition.

The plinian column responsible for this deposit was unstable. It occasionally collapsed, followed by pyroclastic flow deposits. The column was of moderate height (~28 km) and had low to moderate muzzle velocities (150-350 m/s).

Battleship Rock was once believed to be a separate member, however now it is thought to have nearly the same age and source as the El Cajete deposit. The two are chemically and mineralogically nearly identical. However, the morphologies differ slightly: Battleship rock is a welded ignimbrite which was confined to a narrow canyon as it cooled, thus giving it its distinct steep-sided shape. The deposit was substantially eroded prior to Banco Bonito emplacement, indicating a significant amount of time separated the two eruptions.

Banco Bonito is the last phase of volcanism in Valles Caldera. It is an obsidian lava flow which extends 7 km south of the vent and 8.5 km north. This makes it an unusually long flow for a rhyolite, since high silica content generally increases viscosity, making it a sticky, slow lava. There are three or four distinct flows, which are distinguishable on aerial photographs. The flows are quite varied in texture, including microcrystalline rhyolite, glassy obsidian, and inflated pumice.



A-K are El Cajete units:
 [Symbol] plinian fall units
 [Symbol] pyroclastic flows & surge units

33

Hydrothermal Activity and Travertine Deposits in Valles Caldera

Paul Withers

Valles Caldera is the youngest major episode (1.0 – 0.13 Mya) of the Jemez volcanic field (>13 – 0.13 Mya.) The high heat content and subsurface temperatures associated with shallow, crystallizing magma in this pluton cause convection of hot ground waters in overlying rock. This water leaches minerals from subsurface rocks and forms hot springs and fumaroles. Heat flow within Valles Caldera is approximately 4 times greater than a typical continental crustal value of 80 mWm^{-2} .

Analysis of water, surface geology, and 40 drill holes lead to a model for the Valles Caldera hydrothermal system [fig]. Some fluids escape in acid springs and mud pits (Sulphur Springs) within the caldera. Some flow laterally southwest from the caldera, dissolving Palaeozoic limestone, until they escape in hot springs in the Soda Dam area.

The mineral-laden hot springs precipitate mineral deposits as they cool, specifically travertine. Travertine is a freshwater, calcium carbonate deposit. We saw lots of travertine, or tufa if you prefer, in Havasupai Canyon. Bacteria, via their effects on the partial pressure of CO_2 , can be important in its deposition.

One such deposit is Soda Dam, a 100 m long, 25 m wide formation that extends across the narrow San Diego Canyon of the Jemez River and has an estimated volume of 15,000 m^3 [figs]. Travertine was being deposited on Soda Dam until the NM Highways Dept blasted a notch in it around 1970. Now it is slowly disintegrating. Approximately 20 hot springs and thermal seeps presently occur in the Soda Dam area. The Main Spring occurs in a dynamited notch at the northwest end of Soda Dam on the west side of NM State Highway 4 where it issues from a shear zone between Precambrian granite-gneiss and vertically standing Palaeozoic rock. Its temperature remained constant at $47 - 48^\circ\text{C}$ during 1973 – 1987. Total discharge in the Soda Dam system has averaged ~ 1000 litres/min over the past century. Chemically, the Soda Dam hot springs contain 1500 mg/kg HCO_3 , 1500 mg/kg Cl, 340 mg/kg Ca, and 25 mg/kg Mg out of a total dissolved solids content of 4600 mg/kg. The high Ca and Mg values indicate the presence of dissolved Palaeozoic limestone.

Thermal waters issue from various points along the base of Soda Dam, from sheared rock on the west side of the highway, and from several mounds of travertine within and adjacent to the river just downstream. A warm spring (Hidden Warm Spring, 32°C) flows from a marshy flat 100 m upstream on the east side of the river. A very picturesque spring issues from a 1 m high mound of travertine inside a cave at the southeast end of Soda Dam (Grotto Spring, 32°C .) All springs presently deposit travertine.

Three nearby deposits of travertine (A, B, C in a figure) are substantially older than Soda Dam and provide constraints on the evolution of the hydrothermal system. A has a volume of 13 million m^3 (1000 times larger than Soda Dam), B has a volume of 3000 m^3 (5 times smaller than Soda Dam) and C is smaller than 30 m^3 . The range of ages found in samples from A is ~ 0.5 – 1.0 My old (^{234}U - ^{238}U), in samples from B and C is ~ 50 – 110

ky old (^{230}Th - ^{234}U), and Soda Dam samples range from 0 – 5 ky old (^{230}Th - ^{234}U). C and O isotope measurements suggest that the maximum temperature of the Soda Dam hot spring system has never been much greater than the current temperature and probably no greater than 60 °C. A is located at an elevation ~ 100m above Soda Dam and B/C are ~ 20m above Soda Dam.

Three constraints follow from age determinations and stable isotope data:

- 1) The hydrothermal system was established relatively soon after formation of the Valles Caldera and its lateral outflow has operated for at least 1.0 My.
- 2) The deep circulation of hydrothermal fluids and buffering capacity of Palaeozoic limestone have caused the isotopic composition of the hot springs water to vary negligibly during that time.
- 3) The temperature of the Soda Dam hot springs has probably never been greater than 60 °C.

We can suggest the following evolution of the Valles Caldera hydrothermal system, noting that we appear to have episodic travertine deposition despite constant plumbing. Travertine deposition in A (large volume, high elevation) began soon after the formation of Valles Caldera 1.1 Mya. Lacustrine deposits in Valles Caldera suggest that a lake existed within Valles Caldera from this time until 0.5 Mya, and then escaped via a breach in the southwest wall of the caldera by 0.4 Mya, cutting upper San Diego Canyon and lowering the water table. The loss of hydraulic head caused deposition of travertine to cease. 0.1 Mya the last rhyolite eruption in Valles Caldera partially filled the breach in the caldera and reactivated the hot springs for a short time, forming B and C (small volume, slightly elevated above Soda Dam.) A recent thermal pulse (for which the evidence is unconvincing) then initiates the current depositional phase.

If you want to be argumentative:

- Why are these episodes correlated with climatic events such as glaciation?
- Why are B and C, deposited over a period of 50 ky, so much smaller than Soda Dam?
- Are these all the travertine deposits that were ever formed due to this caldera?
- Is there really a thermal pulse causing Soda Dam?

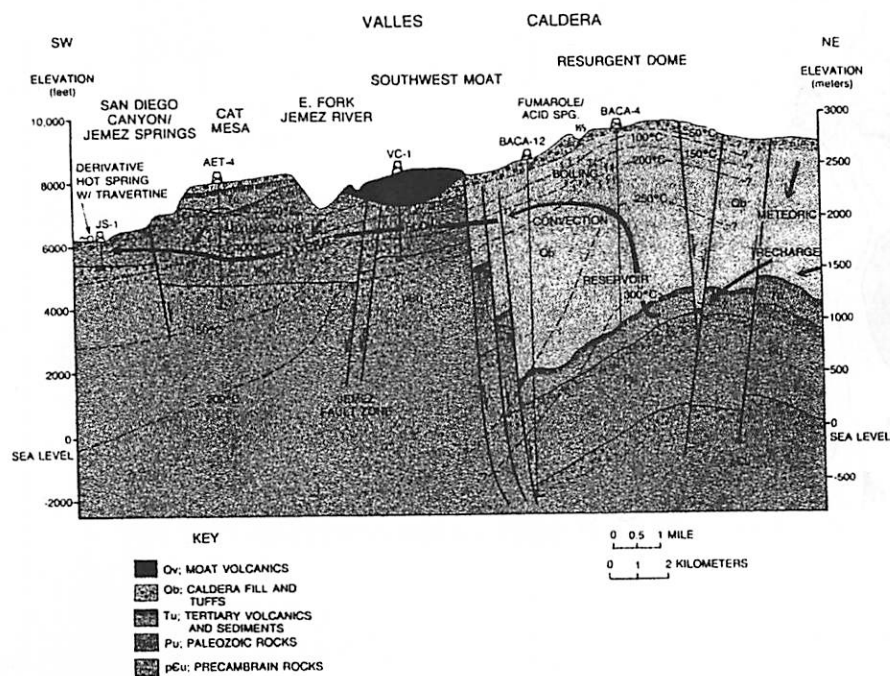
The Valles/Toldedo Caldera complex, Jemez Volcanic Field, New Mexico, 1990, Heiken et al, *Ann. Rev. Earth Planet. Sci.*, **18**, 27-53.

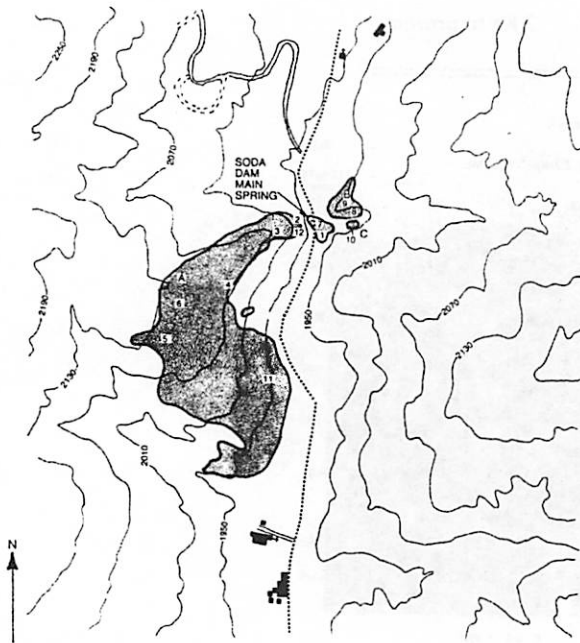
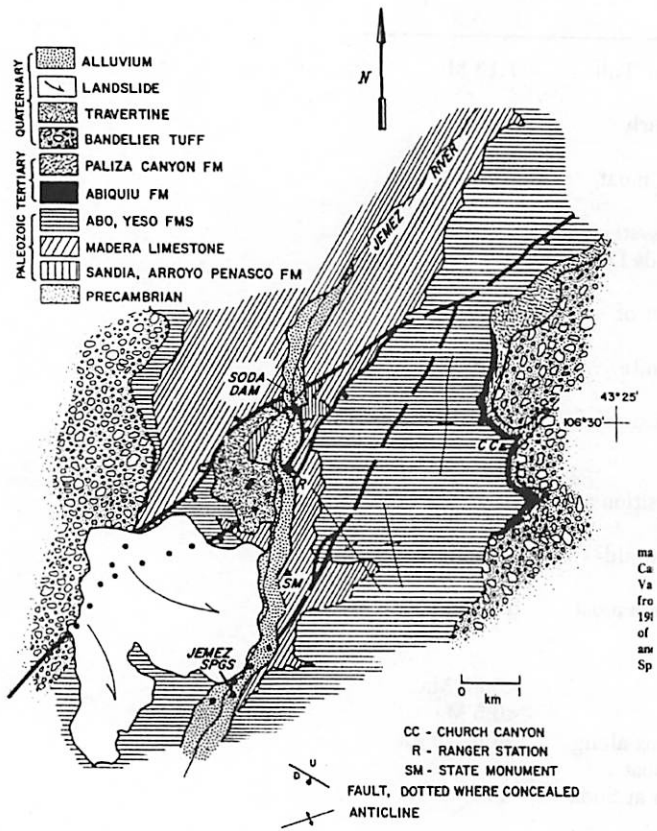
Evolution of a mineralized geothermal system, Valles Caldera, New Mexico, December 1994, Goff and Gardner, *Economic Geology*, **89**, (8), 1803-1832.

Travertine deposits of Soda Dam, New Mexico, and their implications for the age and evolution of the Valles Caldera hydrothermal system, August 1987, Goff and Shevenell, *GSA Bull.*, **99**, (2) 292-302.

Tufa Dams of Havasupai Canyon, Ingrid Daubar, PTYS594 Field Trip Handout, September 1999.

Event	Age
1. Eruption of Tshirege Member, Bandelier Tuff; formation of Valles caldera	1.13 Ma
2. Uplift of resurgent dome; eruption of early rhyolites	~1.0 Ma
3. Eruption of northern arc of postcaldera moat rhyolites	1.04-0.45 Ma
4. Initial formation of Valles hydrothermal system and voluminous travertine deposit at Soda Dam	~1.0 Ma 1.0 Ma >0.97 Ma
5. Initial formation of Sulphur Springs part of hydrothermal system	≤1.09 Ma
6. Formation of Sulphur Springs molybdenite deposit	≥0.66 Ma
7. Breaching of SW caldera wall; deep erosion of SW caldera moat zone	~0.5 Ma
8. Cessation of voluminous travertine deposition at Soda Dam	~0.5 Ma 0.48 Ma
9. Initial formation of vapor zone above liquid-dominated hydrothermal system	≤0.5 Ma
10. Eruption of southern cluster of postcaldera moat rhyolites	0.49-0.13 Ma
11. Partial filling of SW caldera breach	≤0.65 Ma <0.5 Ma
12. Formation of hydrothermal calcite veins along Jemez fault zone beneath SW caldera moat	>400-95 Ka
13. Second period of travertine deposition at Soda Dam	110-60 Ka
14. Last pulse of thermal activity at Fenton Hill (SW caldera margin)	40-10 Ka
15. Final period of travertine deposition at Soda Dam	7 Ka to present





Life in Hot Water: Astrobiology and Hydrothermal Environments

by ®

Ever since the discovery of unexpected and diverse ecological systems surrounding deep sea hydrothermal vents, the concept of “livable” environment has been turned on its ear. After an expedition to the Galapagos Spreading Center, John Corliss presented a model of abiotic synthesis of organic molecules at deep sea vents. The non-equilibrium state of the hydrothermal vent system attracted many models for the origin of life. However, other groups still believe that hydrothermal systems are too hot for complex organic molecules to be stable long enough to form life. Since then, the debate has continued with out a clear solution.

Review: Types of Hydrothermal Environments

Deep Sea

Galapagos Type 293 K vent water in 275 K surroundings

Sulfide-mound hot-water 653 K vent water in 275 K surroundings. The high pressure conditions makes it possible to have liquid water at these temperatures. This is thought to be more common on the early earth, everyone says it but never explains why. Figure 1.

Terrestrial hot springs ~310 K with fluctuating pH

The Question: Did life form in a deep sea vent?

The arguments for:

Free food

Thermal gradients provide energetic pathways for synthesis of organics¹. Organic molecules can be formed by a “quenching” process. Complex molecules form in a high temperature setting where the energy barrier is low and then are mixed into lower temperature water where they are stable². Abiotic synthesis of complex organic compounds by reduction of CO₂ and N₂ depends strongly on the host rock^{3,4}. Lot of organics mean free food.

Our oldest ancestor

Phylogeny – the earliest forms of life probably did not use photosynthesis and fed on inorganic sources⁵. Also, the Last Common Ancestor is (LCA) thought to be a thermophile or even a hyperthermophile⁶.

Amino Acids

The high temperatures also allows easy synthesis of amino acids theoretically⁷, and experimentally⁸. The theoretical work looked on amino acid production based on temperature, assuming the presence of the appropriate enzymes. The experimental work was preformed from 473-548 K. Amino acids are used by RNA to build proteins. There are 20 amino used by living organisms. See Figure 3.

The arguments against:

Amino Acid Decomposition

The theoretical work above assumed that the system was in equilibrium, which is not at all realistic. Kinetics should dominate instead of equilibrium. Several groups measured the decomposition of amino acids at high temperature: at 500 K and pH of 8.48⁹, 373-493 K and up to 265 atm, shows that both amino acid and peptide decomposition increase with temperature and pressure¹⁰.

No RNA

Experimental work performed at 373 K show that most of the nucleobases are unstable, and decompose within 100 years¹¹. Therefore there is not enough A U G C to make RNA. The work also showed that A U G T are stable at 273 K. Clarke, et al. performed experiments from 200-500 K, the nucleobases were unstable above 398 K¹². A – adenine, U uracil, G - guanine, C – cytosine, T – thymine, see Figure 2.

Re-thinking Phylogeny

The phylogenetic tree has been re-“rooted” since the first one appeared. The root appears to depend on what kind of genetic material you are mapping (rRNA vs. metabolic genetic material). Pre-biotic chemistry and some phylogeny argue against origin at high temperature¹³.

Terrestrial Hot Springs – Some groups look at life forming at the lower temperatures of a terrestrial spring. In this setting RNA can form on zeolites and clays¹⁴ and eventually organize into living organisms. This model of the origin of life is called the RNA world.

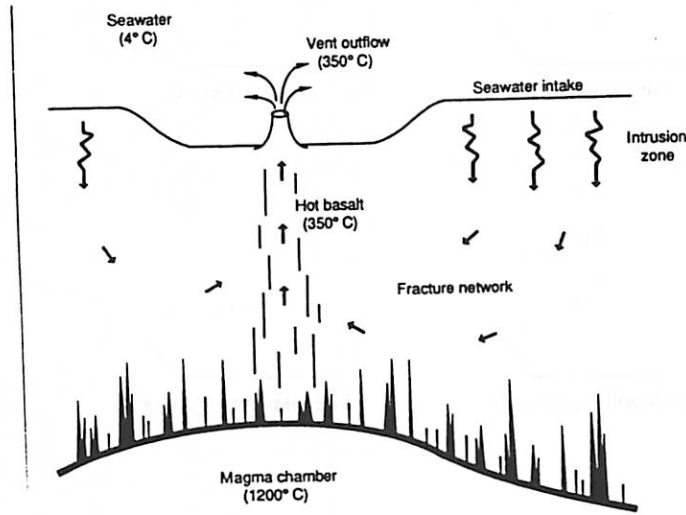
Planetary context

Mars – Several groups look at hydrothermal environments for ancient or extant life on Mars^{15, 16, 17}. Europa, too but I was too lazy to find a reference.

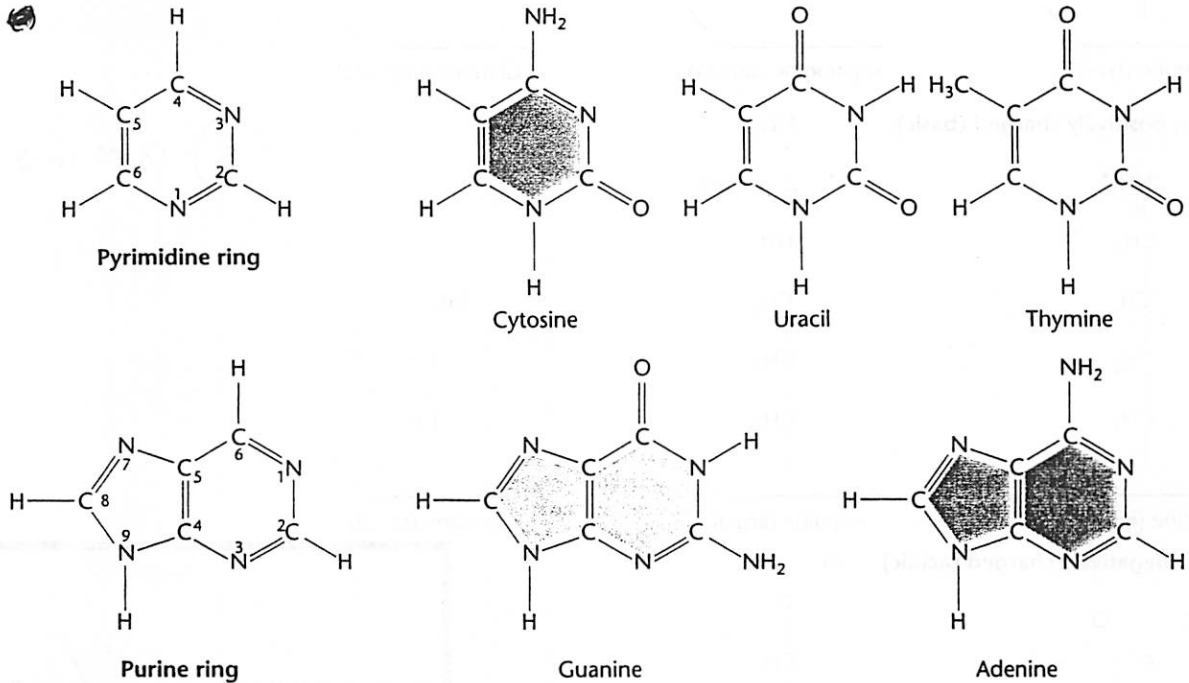
Impacts - It has been shown on Earth that Impacts can create temporary (10⁵ year) hydrothermal systems¹⁸. Therefore, you might get these kinds of environments for short periods of time on terrestrial planets.

References (Brought to you be Endnote, my new god)

1. Baross, J. A. & Hoffman, S. H. *Origins of Life and Evolution of the Biosphere* **15**, 327-345 (1985).
2. Corliss, J. B. *Nature* **347**, 624 (1990).
3. Shock, E. L. *Origins of Life and Evolution of the Biosphere* **20**, 331-367 (1990).
4. Shock, E. L. & Schulte, M. D. *Journal of Geophysical Research* **103**, 28,513-28,527 (1998).
5. Pace, N. R. *Science* **276**, 734-740 (1997).
6. Baross, J. A. & Holden, J. F. *Advances in Protein Chemistry* **48**, 1-34 (1996).
7. Amend, J. P. & Shock, E. L. *Science* **281**, 1659-1662 (1998).
8. Marshall, W. L. *Geochimica et Cosmochimica Acta* **58**, 2099-2106 (1994).
9. Bada, J. L., Miller, S. L. & Zhao, M. *Origins of Life and Evolution of the Biosphere* **25**, 111-118 (1995).
10. Qian, Y., Engel, M. H., Macko, S. A., Carpenter, S. & Deming, J. W. *Geochimica et Cosmochimica Acta* **57**, 3281-3293 (1993).
11. Levy, M. & Miller, S. L. *Proceedings of the National Academy of Sciences of the United States of America* **95**, 7933-7938 (1998).
12. Clarke, R. G. & Tremaine, P. R. *Journal of Physical Chemistry B* **103**, 5131-5144 (1999).
13. Miller, S. L. & Lazcano, A. *Journal of Molecular Evolution* **41**, 689-692 (1995).
14. Nisbet, E. G. *Nature* **322**, 206 (1986).
15. Shock, E. L. *Journal of Geophysical Research* **102**, 23,687-23,694 (1997).
16. Walter, M. R. & Des Marais, D. J. *Icarus* **101**, 129-143 (1993).
17. Boston, P. J., Ivanov, M. V. & McKay, C. P. *Icarus* **95**, 300-308 (1992).
18. Kring, D. A. *Catastrophic Events and Mass Extinctions: Impacts and Beyond* (2000).

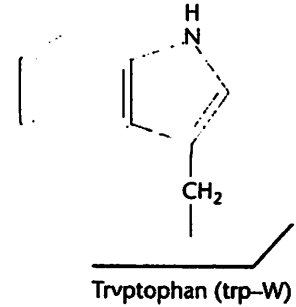
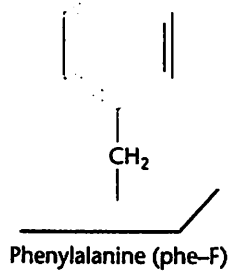
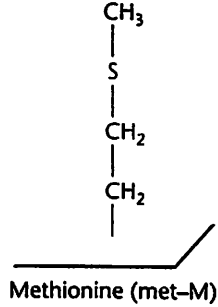
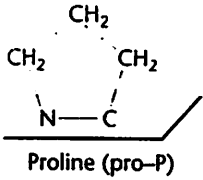
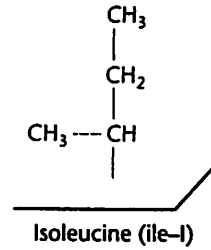
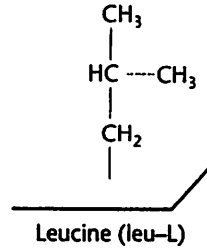
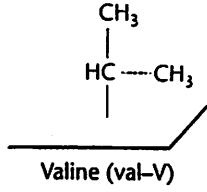
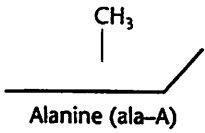


1) Schematic of a deep sea vent.

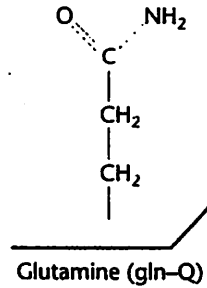
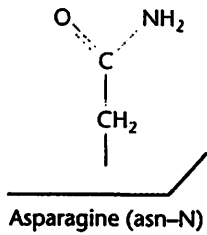
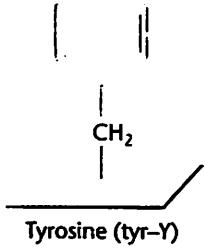
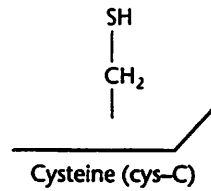
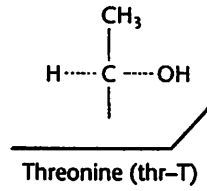
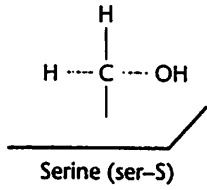
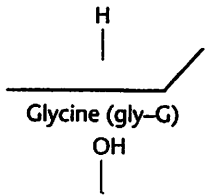


2) The nucleobases

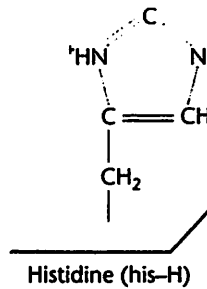
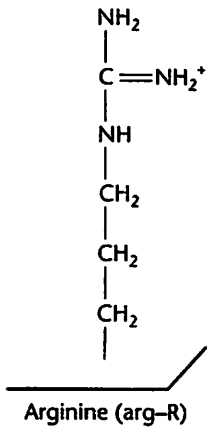
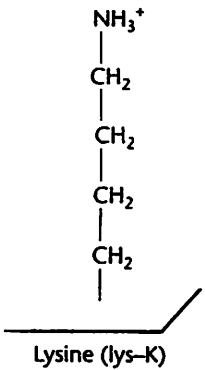
1. Nonpolar: Hydrophobic



2. Polar: Hydrophilic

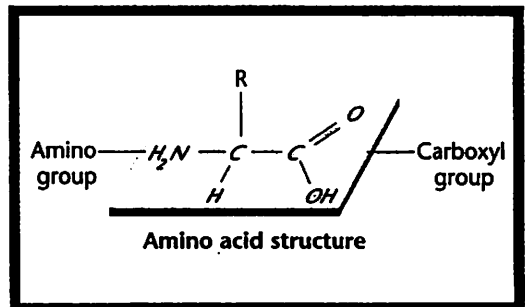
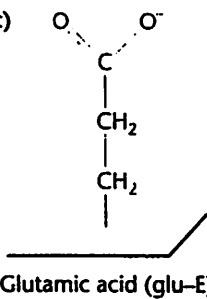
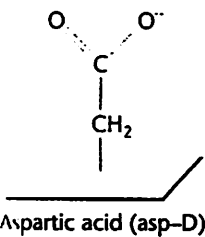


4. Polar: positively charged (basic)



3) amino acids

5. Polar: negatively charged (acidic)



Erosion and Deposition on the Pajarito Plateau, New Mexico

Gwen Bart

Spring 2000 Field Trip

The Pajarito Plateau has much evidence of Quaternary landscape changes. Several diverse locations have been studied to determine age and composition of the rocks. These locations include mesa tops (figure 2, 3), canyon walls (figure 4), and canyon bottoms (figures 5, 6, 7). Figure one shows the location of these study sites on the Pajarito Plateau. Effects of regional climatic changes (figure 8) are also discussed.

➤ *Main Reference*

Reneau, S. L., et al., Erosion and Deposition of the Pajarito Plateau, New Mexico, and Implications for Geomorphic responses to Late Quaternary Climatic Changes, *New Mexico Geological Society Guide Book, 47th Field Conference, Jemez Mountains Region*, 391-397, 1996.

➤ *Additional References*

Broxton, D. E. and Reneau, S. L., Buried Early Pleistocene Landscapes Beneath the Pajarito Plateau, Northern New Mexico, *New Mexico Geological Society Guide Book, 47th Field Conference, Jemez Mountains Region*, 325-333, 1996.

Drakos, P. G. et al., Holocene Evolution of Canyons and Implications For Contaminant Transport, Pajarito Plateau, *New Mexico Geological Society Guide Book, 47th Field Conference, Jemez Mountains Region*, 399-406, 1996.

Formento-Trigilio, M. L. and Pazzaglia, F. J., Quaternary Stratigraphy, Tectonic Geomorphology and Long-Term Landscape Evolution of the Southern Sierra Nacimiento, *New Mexico Geological Society Guide Book, 47th Field Conference, Jemez Mountains Region*, 335-345, 1996.

McFadden, L. D. et al., General Soil-Landscape Relationships and Soil-Forming Processes in the Pajarito Plateau, Los Alamos National Laboratory Area, New Mexico, *New Mexico Geological Society Guide Book, 47th Field Conference, Jemez Mountains Region*, 357-365, 1996.

Reneau, S. L. and Dethier, D. P., Pliocene and Quaternary History of the Rio Grande, White Rock Canyon and Vicinity, New Mexico, *New Mexico Geological Society Guide Book, 47th Field Conference, Jemez Mountains Region*, 317-324, 1996.

Rogers, J. B. and Smartt, R. A., Climatic Influences on Quaternary Alluvial Stratigraphy and Terrace Formation in the Jemez River Valley, New Mexico, *New Mexico Geological Society Guide Book, 47th Field Conference, Jemez Mountains Region*, 347-355, 1996.

Wilcox, B. P., Runoff and Erosion on the Pajarito Plateau: Observations From the Field, *New Mexico Geological Society Guide Book, 47th Field Conference, Jemez Mountains Region*, 433-439, 1996.

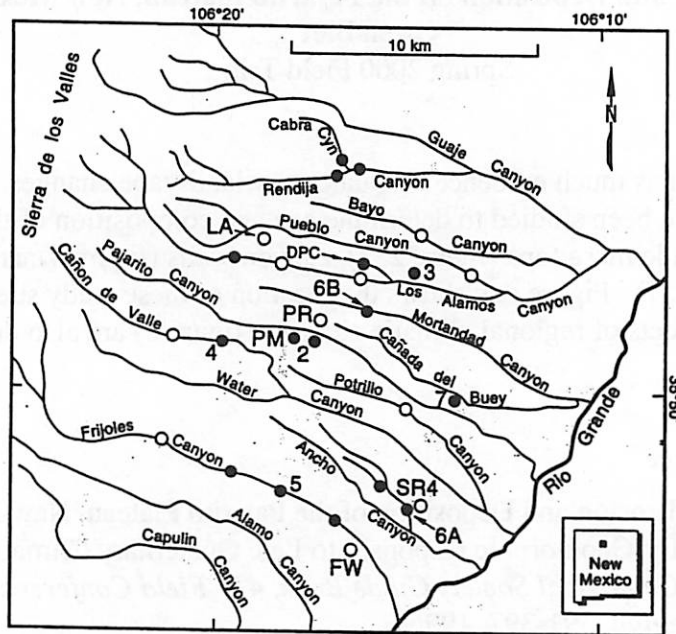


FIGURE 1. Map showing selected drainages on the Pajarito Plateau and location of sites discussed in text. Filled circles indicate sites with radiocarbon age control mentioned in this paper, and open circles indicate other sites mentioned in text. Numbers indicate sites of Figures 2-7. DPC, DP Canyon; FW, Frijolito watershed; LA, Los Alamos; PM, Pajarito Mesa; PR, Pajarito Road trench sites; SR4, State Road 4 site.

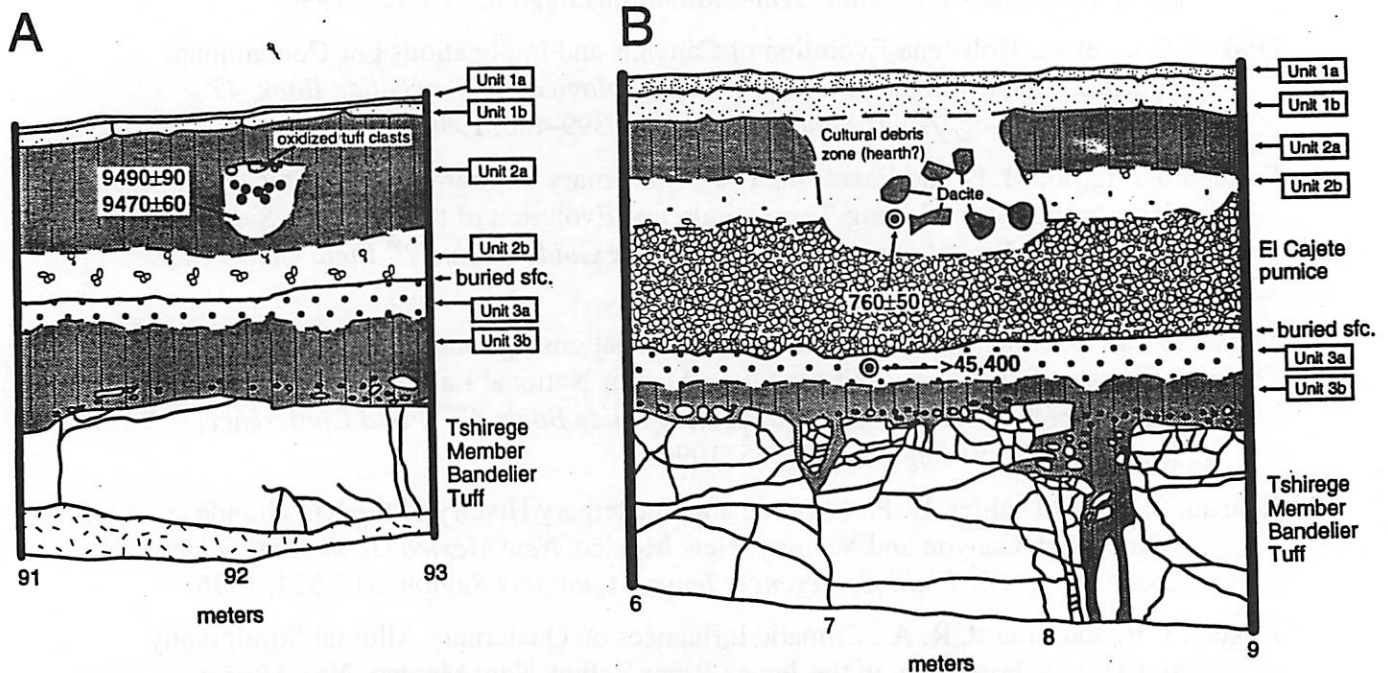


FIGURE 2. Soil-stratigraphic units in Pajarito Mesa trenches and buried archaeological sites. A, Log of part of trench E1, showing Paleo-Indian fire pit (10,525 yrs B.P.) in fine-grained early Holocene eolian (?) deposit. B, Log of part of trench E8, showing Anasazi site (715 yrs B.P.) excavated into late Pleistocene and Holocene units, and buried by fine-grained late Holocene (eolian?) deposits (unit 1b, with typical ages of 540-710 ^{14}C yr BP; 706-586 cal yr B.P.). A distinctive buried soil (unit 3) underlies the ca. 50-60 ka El Cajete pumice and is present throughout the trenches; unit 2b is bioturbated El Cajete pumice, and unit 2a includes soils and deposits above the pumice which have yielded ages of 2-30 ^{14}C ka. Horizontal axis indicates trench distance. No vertical exaggeration. (From Kolbe et al., unpubl. report for Los Alamos National Laboratory, 1994, and Reneau et al., in press).

43

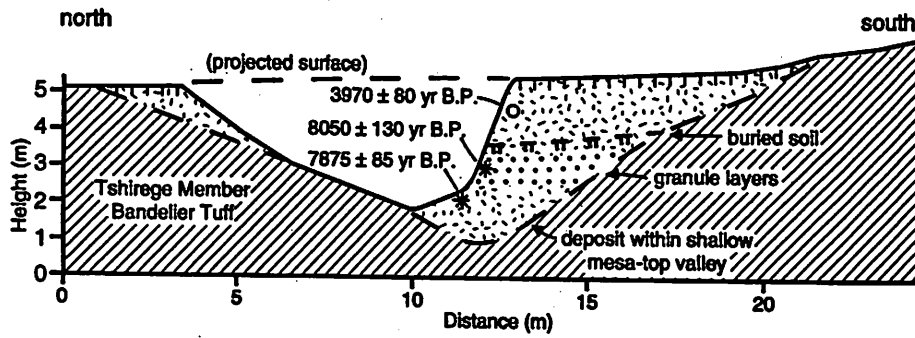


FIGURE 3. Cross section showing stratigraphy and radiocarbon dates at "EG&G gully" (informal name), in a shallow mesa-top drainage east of the Los Alamos townsite (from Longmire et al., in press). The deposit is generally an unstratified loam or silt loam, except for sand and granule layers that occur in the ca. 8 ka unit and which may record relatively high energy surface runoff.

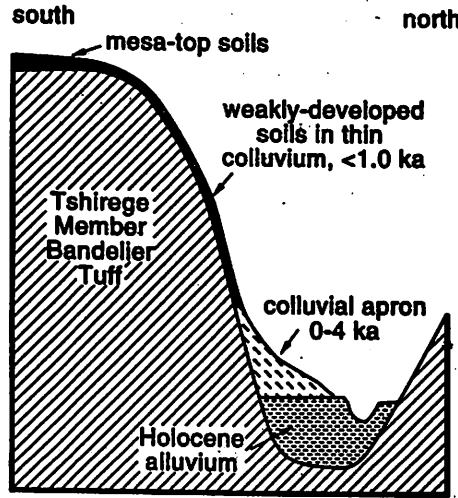


FIGURE 4. Schematic cross section across Cañon de Valle (stream elevation 2240 m), showing relations of colluvial soils on canyon walls, colluvial aprons at slope base, and Holocene alluvial fill. Canyon is about 70 m deep and 190 m wide here. (Thicknesses of surficial units are not to scale).

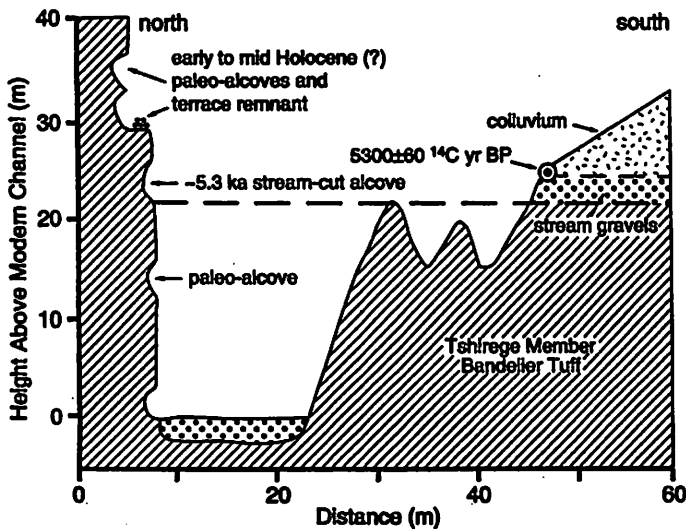


FIGURE 5. Schematic cross section across bottom of Frijoles Canyon about 8 km upstream of the Rio Grande (stream elevation 1945 m), showing mid-Holocene terrace remnant and location of ^{14}C date in basal part of overlying colluvium. Stream-cut alcoves are formed in this canyon during periods of local base level stability and floodplain development (including about 5.3 ^{14}C ka and today), and become stranded on cliff walls following renewed incision, recording former stream levels.

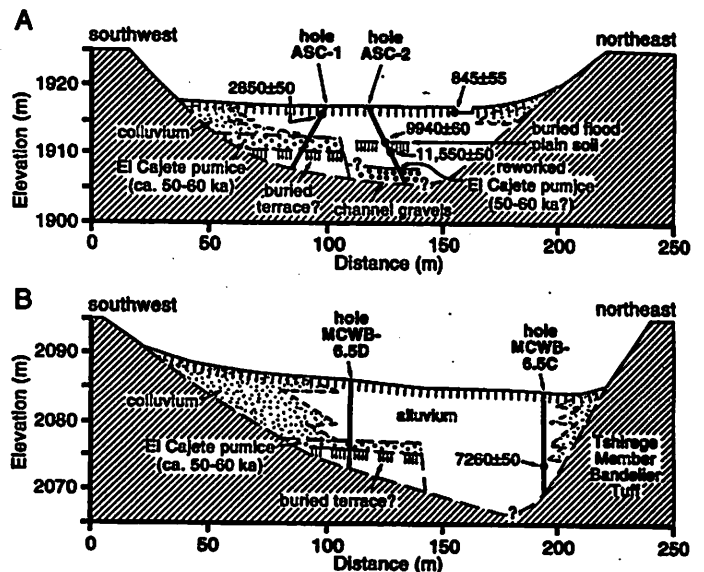


FIGURE 6. Cross sections across (A) north fork of Ancho Canyon and (B) Mortandad Canyon, showing radiocarbon dates and inferred stratigraphic context of units exposed in core holes. Stratigraphy modified from unpublished core logs (K. Shisler et al., unpubl. 1994; S. McLin et al., unpubl. 1994). Bedrock in (A) includes the Tshirege and Otowi Members of the Bandelier Tuff and alluvium of the intervening Cerro Toledo interval.

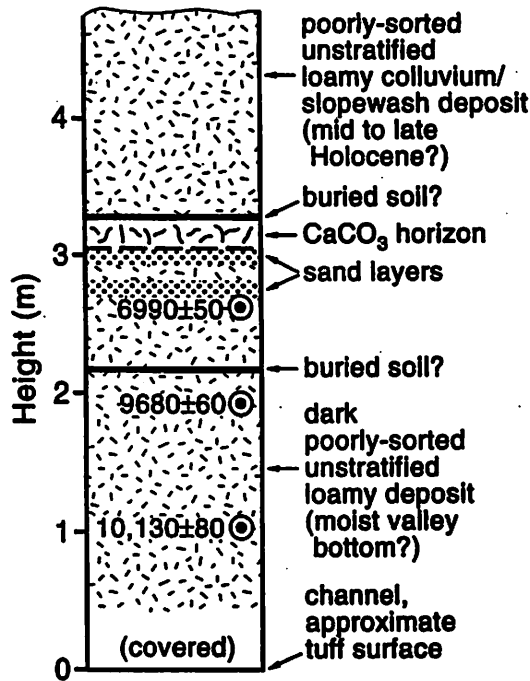


FIGURE 7. Sketch showing stratigraphy and radiocarbon dates at the head of a minor tributary to Cañada del Buey, at the east end of Mesita del Buey. This early to mid-Holocene fill has been extensively dissected and eroded, and the modern channel is close to tuff bedrock.

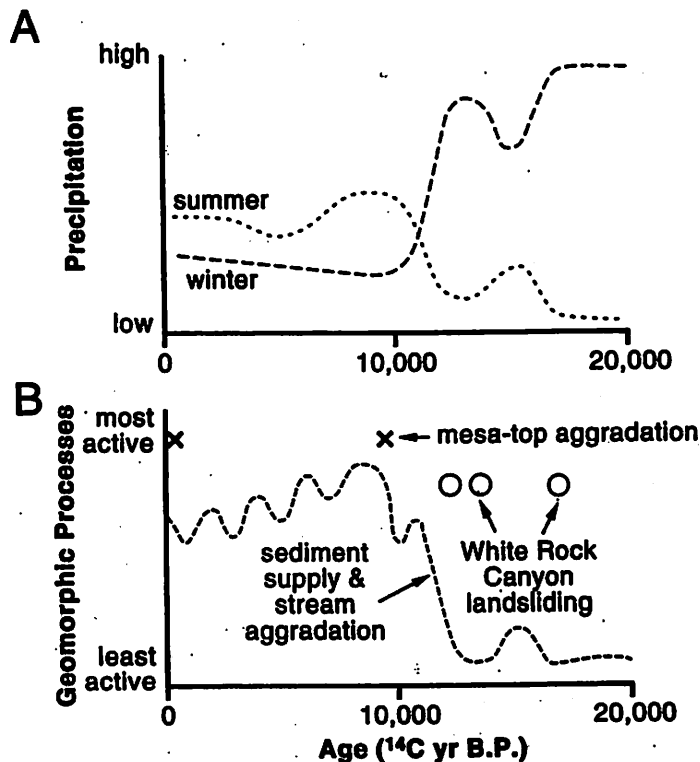


FIGURE 8. Schematic representations of possible gross variations in (A) precipitation and (B) geomorphic processes on the Pajarito Plateau and in surrounding areas for the last 20,000 years, illustrating inferred temporal relations between climatic changes and the geomorphic record. Geomorphic processes presented here include the supply of sediment to channels derived from erosion throughout the basins, and associated aggradation of channels; local mesa-top aggradation that probably records increased eolian influx; and large-scale landsliding. Vertical scales are intended to show relative differences between the late Pleistocene and the Holocene, as inferred from regional paleoclimatic records and from local geomorphic evidence, and not absolute values. Because available records are incomplete, the plotted curves are of necessity partly speculative.

(45)

The Late Cretaceous Global Environment

Dave O'Brien

Introduction

The Late Cretaceous is characterized by a cooling episode which decreased global temperatures and increased the equator-to-pole thermal gradients compared to the mid-Cretaceous, while still remaining warmer overall than the current climate. This summary will outline the evidence for the Late Cretaceous global climate, explore possible reasons for such a climate, and discuss the relevance of such a climate in relation to the environmental effects of the K/T impact.

Evidence for a warm climate

1) Stable isotope data.

The ratio of oxygen-18 to oxygen-16 in oceanic sediments records varying levels of fractionation, which serve as an indicator of the oceanic temperatures at a given time. Sediments at different latitudes can give an estimate of the equator-pole temperature gradient. The equatorial temperature during the Late Cretaceous was approximately the same as the present value, but the equator-pole temperature gradient was between 0.14 and 0.3 degrees Celsius per degree of latitude, compared to the current value of 0.73 (Pierazzo 1997).

2) The fossil record.

The Mid Cretaceous was characterized by the presence of tropical organisms extending to high latitudes, and an absence of cold-water species. Coral reef and carbonate formations extended from 5 to 15 degrees latitude higher than present, and alligator and crocodile fossils are found as high as 60 degrees latitude (Lunine 1999). The Late Cretaceous fossil record shows the beginnings of a global climate cooldown. Tropical species began to recede from the high latitudes they occupied during the Mid Cretaceous. Ferns and other tropical plants in Europe and Asia began to decline and be replaced with conifers and angiosperms, which are more adapted to cooler climates (Levin 1978).

As tree ring growth rates and leaf morphology change in a predictable manner in response to different temperatures, the analysis of fossil tree rings and fossil leaves can be used to infer temperature on the continents (Pierazzo 1997). Studies of North American vegetation during the Late Cretaceous yield an equator-pole temperature gradient of approximately 0.30 degrees Celsius per degree of latitude, similar to the upper end of estimates for the oceanic gradient.

3) The geological record.

The main evidence for a warm Late Cretaceous in the geologic record is the lack of glacial erosion features from the time, especially at high latitudes (Deconto *et. al.* 2000). The early Cretaceous shows evidence for glaciation, but by the Mid Cretaceous, global temperatures, and especially high-latitude temperatures, were high enough to melt any glaciers. The Late Cretaceous, while somewhat cooler than the Mid Cretaceous, was not cool enough for glaciers to return.

Mechanism for a warm climate

During the Cretaceous, most of the continental mass of the earth was concentrated around the equator, there were no plate collisions leading to high altitude areas that would accumulate snow and ice, and the higher sea level led to shallow inland seas, all contributing to a warm climate. During the Late Cretaceous, the inland seas started to recede and the continents moved somewhat higher in latitude, contributing to a cooler climate than the Mid Cretaceous, but still warmer than today. (Levin 1978).

These factors alone are not capable, in themselves, of causing the increased global temperature and especially the low equator-pole temperature gradient observed during the Late Cretaceous. Ocean currents must have played a role, in that continent positions can lead to greater heat transport from equator to pole, but this is still difficult to model. A factor that must be taken into account is the carbon dioxide level during this time. Climate models indicate that to get the same mean temperature as the Late Cretaceous, around 4 times the present level of carbon dioxide is necessary. This tends to increase temperatures globally, however, rather than decreasing the equator-pole temperature gradient (Deconto *et. al.* 2000).

It seems that the combined effects of increased carbon dioxide in the atmosphere and increased equator-pole heat transport, possibly due to ocean currents, are needed to achieve the Late Cretaceous climate. Further modeling, however, is necessary.

Conclusion

The Late Cretaceous was characterized by equatorial temperatures similar to today's and polar temperatures significantly higher, as inferred from stable oxygen isotope analysis, the fossil record, and the geologic record. This is due in part to the equatorial position of the continents at that time, but almost certainly requires a higher carbon dioxide level than today, possibly by as much as a factor of 4. While the Chixilub impact would have released a large amount of carbon dioxide from the target material, this would represent less than 20% of the Late Cretaceous carbon dioxide abundance due to the already high levels (Pierazzo 1997). A similar impact today would result in a much greater perturbation to the climate in terms of greenhouse effect.

References

Deconto, R. M., E. C. Brady, J. Bergengren, and W. W. Hay. Late Cretaceous climate, vegetation, and ocean interactions. *Warm Climates in Earth History*. Huber *et. al.* eds. Cambridge University Press (2000).

Levin, H. L. *The Earth Through Time*. W. B. Saunders Company (1978).

Lunine, J. I. *Earth: Evolution of a Habitable World*. Cambridge University Press (1999).

Pierazzo, E. *The Chixilub impact and the environmental catastrophe at the end of the Cretaceous period*. Thesis, University of Arizona (1997).

Press, F. and R. Seiver. *Earth*. W. H. Freeman and Company (1974).

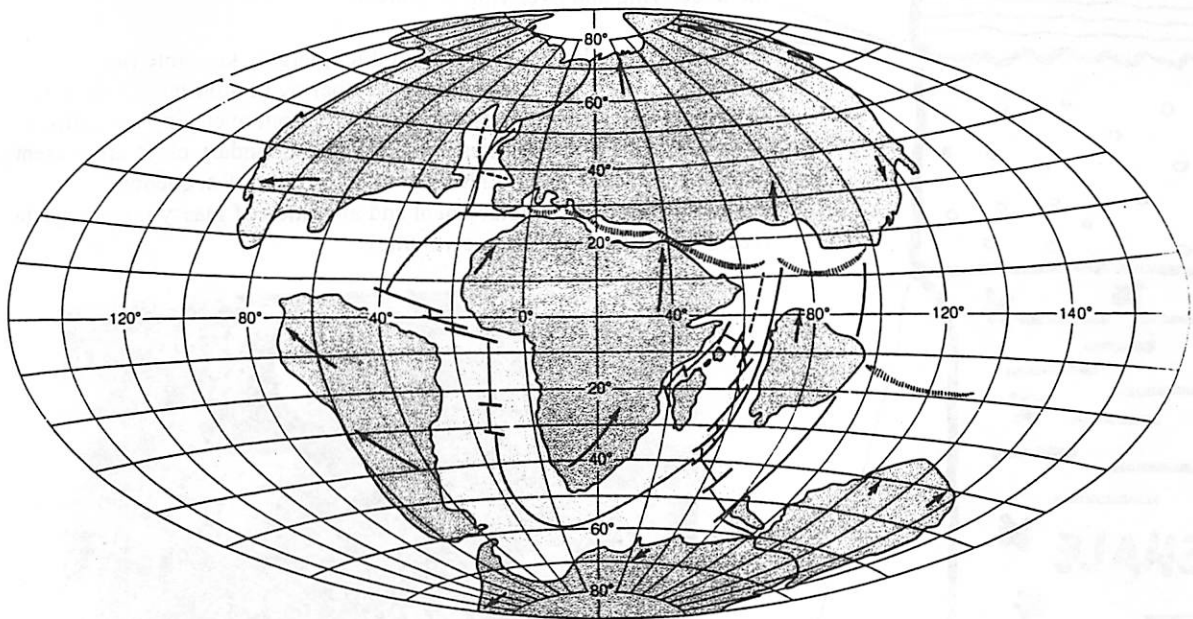


Figure 21-19

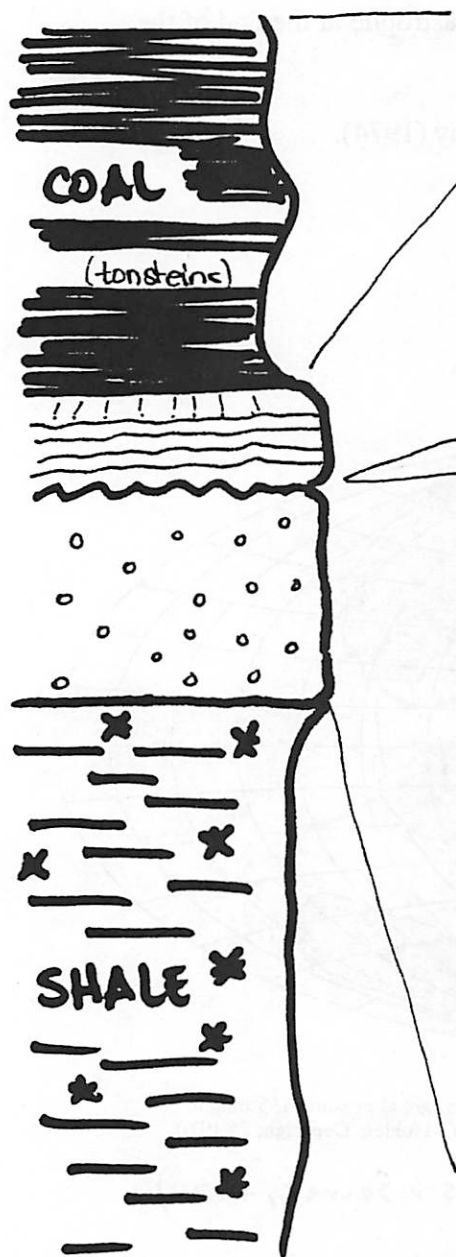
World geography at the end of the Cretaceous Period, 65 million years ago, after some 135 million years of drift. [After "The Breakup of Pangaea" by R. S. Dietz and J. C. Holden. Copyright © 1970, by Scientific America, Inc. All rights reserved.]

(From Press & Seiver, 1974)

KT boundary layers in the Raton Basin: A shocking tale

✿✿Barbara Cohen✿✿

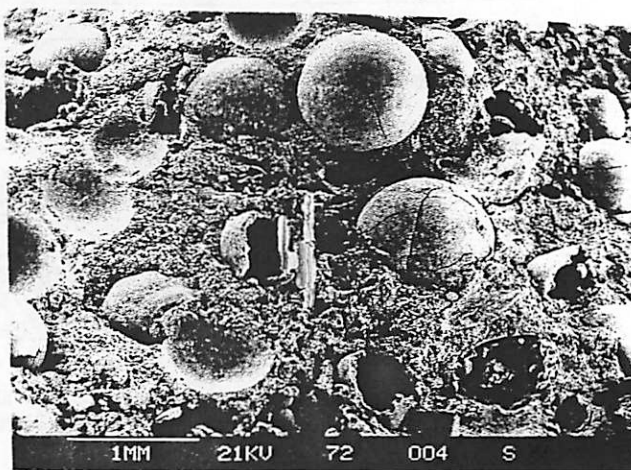
The Rocky Mountain region contains the most shockingly complete and examined terrestrial K-T sections known. The KT boundary interval in the Raton Basin is not a simple unit, but instead, a shockingly complex couplet composed of a lower *Boundary Claystone* and an overlying *Boundary Impact Layer*. These two units are separated by a depositional hiatus of unknown duration. The Impact Layer is itself directly overlain by the *Boundary Coal Bed*. The sequence overlies carbonaceous Shale beds. The boundary units have been identified at sites in Wyoming, Montana, and Canada.



Boundary Coal Bed: 4-16 cm thick, formed by accumulation of organic debris in low-energy, swampy environment. Contains tonsteins, or clay layers formed from weathering of volcanic ash. The composition of the tonsteins is different from the clay in the Boundary layers.

K-T Boundary Impact Layer: 4 to 8 mm thick, largely smectitic (clay minerals with K, Ca, and Mg cations, including the well known swelling purple bentonite). This layer contains the maximum iridium abundance and shock-metamorphosed grains; the latter constitute ~2% by volume and are evenly distributed throughout the layer. Its microlaminated structure contrasts with the underlying Boundary Clay. Microlaminations are warped over and under clastic mineral grains reflecting soft sediment compaction. The composition contrasts with the underlying and overlying clay layers.

K-T Boundary Claystone: 1 to 2 cm thick, largely kaolinite (an aluminous clay mineral, formed by weathering of aluminous minerals like feldspar). Clay composition is distinct from overlying tonsteins. Spherules resembling tektites in marine K-T boundary clays are present but are completely altered. Not found in EuropeKT sequences. Probably formed by emplacement and alteration of glassy impact ejecta (see other discussions in this volume).



Shale beds: light gray mudstone containing fragments of plant material and leaf impressions on bedding planes. Probably of fluvial and pond origin, low energy environments. No dinosaur bones in the Raton basin, though they do occur in late Cretaceous sediments at other sites.

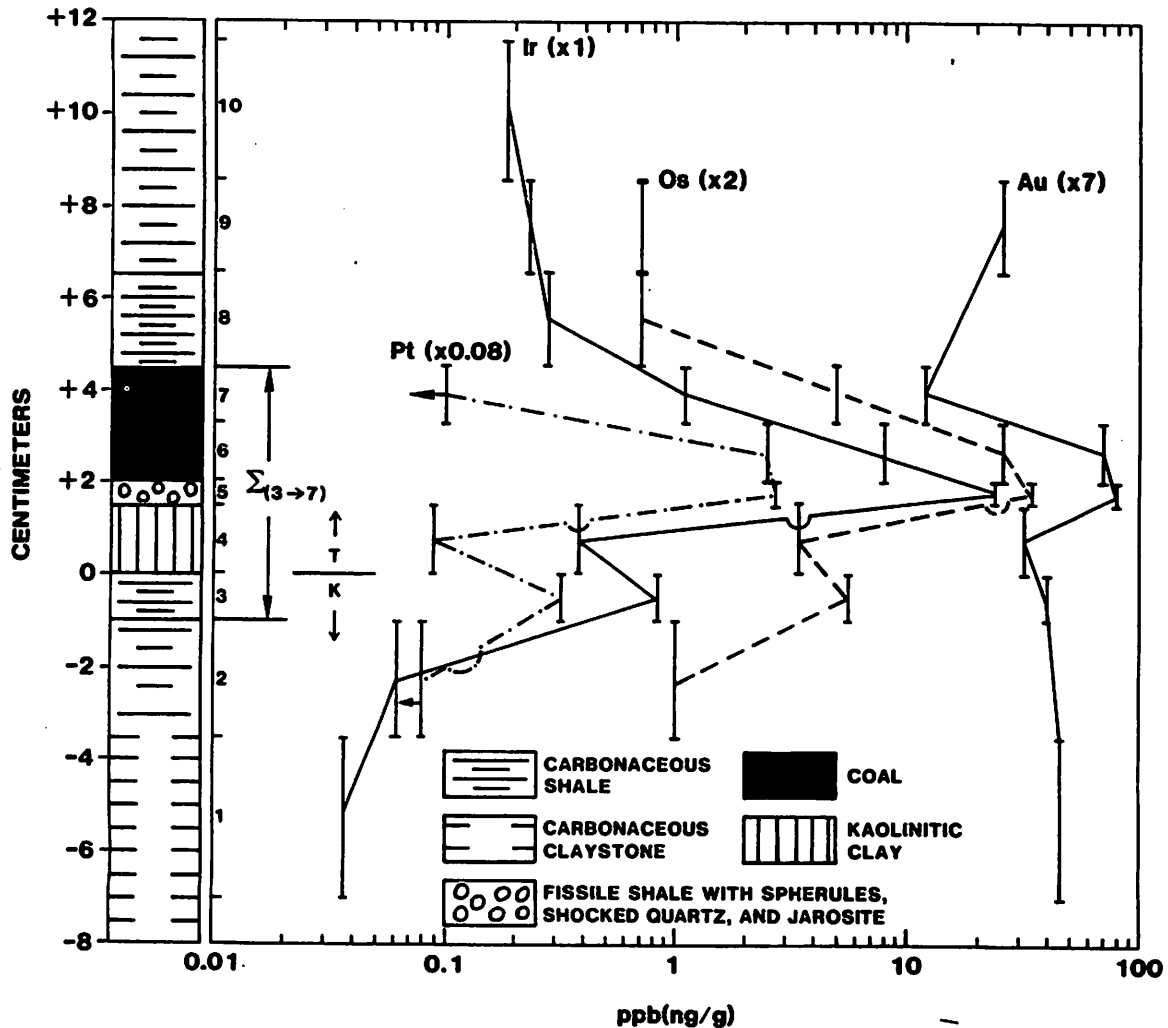
✿ = POLLEN

The original "smoking gun," the *iridium anomaly*, is now detected at marine and continental KT boundary sections all around the world. Ir is a shockingly sensitive tracer of extraterrestrial matter because of its strong depletion in the Earth crust (0.05 ng/g) compared to chondritic abundance (500 ng/g). Most of the Earth's Ir is stored along with Fe in the core. The same is true for other heavy siderophiles, which are enriched in the Boundary Impact Ejecta layer in the Raton Basin. The Ir probably exists as shockingly fine particles, but the carrier phase has so far not been identified. If the excess Ir had been from a continental (instead of meteoritic) source, shockingly high levels of trace elements like Mo, Sm, and Tb would be expected, which are not found. A higher amount of Ni is predicted by the meteoritic source, but the Ni might be tied up in mineral phases (discussed below).

The finding of Ir at the KT boundary has led to searches for other Ir anomalies, in particular at stratigraphic horizons associated with mass extinctions. So far, considering its shocking magnitude and worldwide distribution, the KT boundary Ir anomaly appears to be a unique event in the sedimentary record. Small Ir anomalies (<0.5 ng/g) have been detected at other stratigraphic boundaries marking extinction events, but in many of these cases the platinoid elements are not in chondritic proportions and in some cases the Ir enrichments appear related to anoxic conditions.

Volcanoes also emit Ir, and the shockingly large Deccan Traps in India were being laid down at the time of the KT event, so a volcanic origin was argued for a long time. However, detailed measurements of the Ir content and platinum-group elemental ratios have ruled this out as a source for the clay layer Ir.

HEAVY SIDEROPHILES - K/T BOUNDARY - RATON BASIN



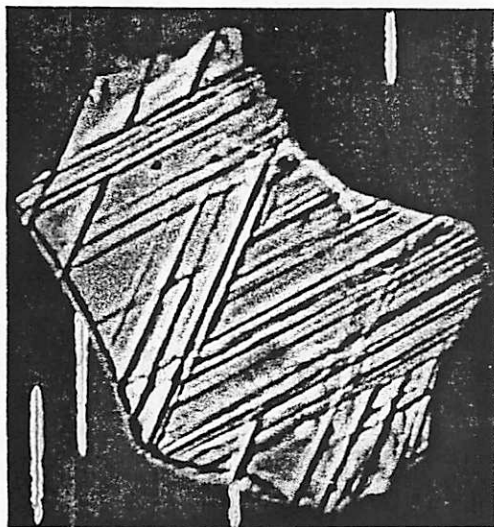
50

Shocked minerals are commonly found in association with the KT boundary event. Similar features occur in minerals at nuclear explosion sites or when material is experimentally shocked to pressures above 5 GPa. The types of shock features and their associations allow estimates of the pressure that was applied to the grain. **Quartz** is a mineral which normally fractures conchoidally, with no regular cleavage planes. High pressure can induce quartz to form parallel pseudo-cleavage planes along low-index crystallographic planes. These fracture planes can be seen in the microscope as planar deformation features (PDFs). Tectonic stresses and volcanic explosions can cause cracks and lamellae that look like PDFs, but there is usually only one set and they are just cracks. In shock experiments, multiple PDF planes can appear, and the cracks are filled with quartz glass. Shocked quartz, with up to nine sets of PDFs, is abundant within the KT boundary clay layer in North America, in deep-sea cores in the Pacific Ocean, and in the polymict breccia from the Chicxulub structure. At other KT sites shocked quartz is less common. **Stishovite** also occurs in the boundary claystones here. **Shatter cones** are formed only in the basement rocks.

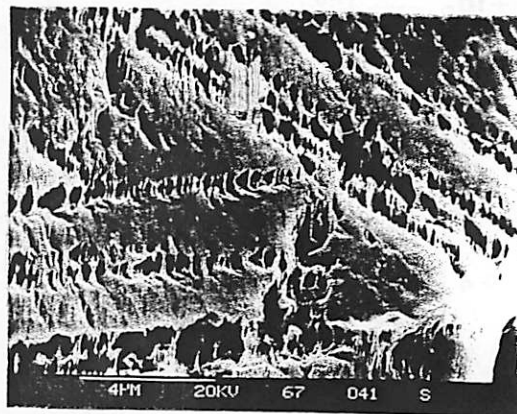
Shock pressures necessary for formation of shock features in quartz (from Turtle, 1998)

Shock Effect	Shock Pressure (GPa)
Shatter cones	2
Basal Planar Deformation Features (PDFs)	5
Rhombohedral PDFs	10
Stishovite	12-15
Coesite	30
Diaplectic Quartz Glass	35-50
Lechatelierite	50
Complete Melting of Quartz	60

Photomicrograph of 0.75 mm shocked quartz grain, showing two sets of PDFs



SEM photo of etched quartz grain with PDFs. The quartz glass fill etches out first.



Zircons also show shock features that are related to increasing degrees of shock metamorphism and correlate with proportionate resetting of the U-Pb isotopic system. Zircons from the KT boundary sections in the US Western Interior, Haiti and from the impact breccia at Chicxulub. The original U-Pb age of the parent material is ~550 Ma and U-Pb isotopic resetting consistent with partial Pb loss took place around 65 Ma. The age for the target rock agrees well with the basement age at Chicxulub in Yucatan but is incompatible with the mid-Proterozoic age of the target beneath the Manson structure in Iowa. **Chromite** and microcline **feldspar** also can show PDFs when shocked, and these shocked minerals are found in small abundances at North American and Caribbean sites. Feldspar grains are often sutured to quartz grains, and the composite grains show shock features. The presence and abundance of the shocked silicates implies a continental source for the target material, rather than oceanic. **Spinel** is a high-pressure mineral that seems to form from the vapor phase of the impactor. They have much more Ni than any terrestrial spinels and are found as tiny euhedral crystals.

Tektites are rounded glass particles. They are formed when the target material melts and is ejected. The molten rock forms small glass beads as it quickly cools and takes on an aerodynamic shape as it flies through the air. Shocked quartz and coesite have been found within tektite layers, and impact glass within the tektites themselves, at sites where the tektites are preserved. In the Raton basin, the tektite glass has devitrified and weathered to clay minerals in the Boundary Clay layer. *Tsunami deposits* and large submarine breccias are preserved in some marine sequences (see J. Barnes, this volume). Fusilinite, or soot, has been detected at the bottom of the Boundary Coal, indicating widespread fires just after the impact time.

Claeys, P. (1995) When the sky fell on our heads: Identification and interpretation of impact products in the sedimentary record. *Rev. Geophys.* Vol. 33 Suppl.,
<http://www.agu.org/revgeophys/claeys00/claeys00.html>

Bohor B. F., Shocked quartz and more; Impact signatures in Cretaceous-Tertiary boundary clays. in *Global catastrophes in Earth history; an interdisciplinary conference on impact, volcanism and mass mortality*, Sharpton, V. L. and Ward P. D., eds., *Geol.Soc. Amer. Spec. Paper*, 247, 335-342, 1990.

Izett, G. A. The Cretaceous-Tertiary (K-T) boundary interval, Raton Basin, Colorado and New Mexico, and its content of shock-metamorphosed minerals: implications concerning the K-T boundary impact-extinction theory, U. S. Geological Survey Open File Report 87-606, 125 pp. 1987.

K/T Layer Cake (var. Raton Basin) From Impact Catering, by H. Jay Melosh

Basic Cake

5 eggs, separated (ambient temperature)
 2 1/4 cups flour
 1 tsp baking soda
 1/2 tsp salt
 2 cups sugar
 1 cup butter
 1 tsp vanilla extract
 1 cup milk
 4 squares of chocolate, melted

Boundary Clay Layer

4 oz cream cheese, softened
 1 egg
 1/2 tsp vanilla
 1 cup sugar
Iridium layer
 3/4 cup frosting
 5-10 ppb iridium (to taste)
 shocked quartz

Preheat oven to 450K. Grease and flour two 23-cm layer cake pans. Combine flour with baking powder and salt, dry sieve and set aside the 10- μ m fraction. At high velocity, beat egg whites until foamy. Gradually add 1/2c sugar and beat until soft peaks form, set aside. Cream butter with rest of sugar and vanilla until the consistency of aerogel. At low speed, beat in flour mixture alternately with milk and melted chocolate, being sure to use a new pipette each time to avoid contamination. Gently fold in egg whites. Divide batter in half, ± 0.2 .

Coal layer: stir in organic detritus and mark layer for future economic exploitation, if you have the foresight. Shale layer: Mix in planktonic foraminifera fossils. If you can find candy ammonites, these are good too. Clay layer: cream together cream cheese, egg, vanilla and sugar until glassy, set outside to weather until smooth.

Pour batter into prepared pans. Bake for 5×10^{-11} Ma, or until cake pulls away from sides. Midway through bake time, remove Shale layer and spread clay over top, return to oven. Cool on wire racks.

Turn Shale layer onto a plate, clay side up. Combine Ir and shocked minerals with 3/4c frosting and ballistically emplace over clay layer. Top with Coal layer. Frost and serve.

(52)

Chemical and Mineralogical Diagenesis of Impact Ejecta

with your hostess with neuroses, Jennifer Grier

"Diagenesis – (1) All of the changes undergone by a sediment after its initial deposition, exclusive of weathering and metamorphism. It includes those processes (such as compaction, cementation, replacement) that occur under conditions of pressure and temperature that are normal in the outer part of the Earth's crust, and according to most U.S. geologists, it includes changes occurring after lithification. There is no universally accepted definition of the term, or if its delimitation, e.g. with metamorphism. (2) The geochemical processes or transformations that affect clay minerals before burial in the marine environment. (Bates and Jackson, 1984)"

Introduction

Almost immediately after ejecta from an impact event has been emplaced, it begins to change and evolve both chemically and mineralogically. The general term for this process of change is "diagenesis". This change encompasses all of the modification undergone by a sediment after it is deposited, other than weathering and metamorphism (and even some of that is included in the loose definition of diagenesis).

Diagenetic interpretation of postimpact events is based on petrologic, mineralogic, and geochemical investigation of materials from the impact site or nearby; including target strata, disturbed and disrupted strata, ejecta, breccias, microbreccias, and impact melt (Crossey and McCarville, 1993), often in the form of drill cores. Here, obviously, we are going to concern ourselves most with postimpact diagenetic events effecting ejecta (and Chicxulub ejecta more specifically).

Postimpact Alteration Processes – Why and How Do Researchers Study Them

Core materials from the Manson impact site were examined by Crossey and McCarville (1993) among others order to evaluate the nature and extent postimpact alteration processes. They looked at impactites (breccias, microbreccias, and melt material), crater fill material (sedimentary clast breccias), disturbed and disrupted target rocks, and reference target material. They also studied drill cores from all over the impact and nearby sites to attempt to develop a regional picture of post-impact thermal history, such as to identify and relate significant postimpact mineral alteration to the postimpact thermal regime (extent and duration). The idea is that large scale studies of impacts of this nature will reveal mineralogical and geochemical

constraints on models for postimpact processes (including infilling of the crater depression; cooling and hydrothermal alteration of melt rocks; and subsequent long-term, low-temperature alteration of target rocks, breccias, and melt rocks). At Manson they found quartz, chlorite, mixed-layer clays, gypsum/anhydrite, calcite, and other indicators of postimpact diagenetic processing in the cores they studied.

Gostin et al. (1999) specifically studied the impact ejecta from the Acraman impact in Australia. This consisted of clast-bearing and sandy sublayers set in a shale host rock. Looking at the average thicknesses and estimated distances of the ejecta from the impact they were able to calculate a transient crater diameter for the Acraman impact of at least 34 km. The ejecta they examined contained numerous grains of quartz and zircon displaying impact-produced features. They also speculated that the coarse-grained ejecta layer embedded within fine-grained sediments allowed easy passage for diagenetic fluids. The result was a porous honeycomb structure in the clays, and an enhancement of the content of elements such as Cu, Pb, Zn, and U. The clay fraction of the ejecta layers consisted of vermiculite and kaolinite, probably formed from alteration and weathering of glassy components (see section on glass and clay). They found that quartz and zircon grains were the only remnants of the ejecta unaltered by diagenetic processes.

Newsom et al. (1986), Allen et al. (1982), and others have keyed in on the diagenetic processes effecting ejecta as a possible clue to what we might find at the Martian surface. Hydrothermal alteration of suevite at the Ries Crater has been examined as a possible source for specific clays hypothesized in Martian soils. An examination of samples of melt rock and breccia from 12 terrestrial impact craters attempted to identify alteration minerals and their conditions of formation. They found in most cases the dominant

"*Clay Mineral* – One of a complex and loosely defined group of hydrous silicate minerals, essentially of aluminum. They have a mono-clinic layered crystal lattice. The extremely small particle size imparts ability to adsorb water and ions on the particle surfaces. Most clay minerals belong to the kaolin, smectite (montmorillonite) and illite groups; the micas and chlorite are close relatives. *Clay* – An earthy, extremely fine grained sediment or soft rock composed primarily of clay-sized or colloidal particles, having high plasticity and a considerable content of clay minerals. (Bates and Jackson, 1984)"

assemblage is clay-silica-K feldspar-zeolite which suggested to them hydrothermal alteration at low pressures and temperatures. The clays are in the main Fe-chlorites and smectites, in most cases depleted in Al and enriched in Fe and Mg relative to their source rocks. The alteration of impact glass at most sites was found to be complete, but the alteration of crystalline melt rock was limited to a few percent of the rock volume. The impact breccia appeared to be altered to only a slight extent compared with the alteration of glass. If significant quantities of ground ice and/or water are present at the site of a Martian impact crater, they therefore concluded that impact-induced hydro-thermal alteration would be common in Martian impact ejecta. Given widespread impact cratering on Mars, many of the clays found in the soils may be derived from diagenesis of ejecta, especially glass.

The Spherules – The Real Story

OK, now that we know why people care about postimpact diagenesis of impact products and how they go about looking for them, we need to know what it is they are looking for, specifically and why should we care in the context of the Chicxulub impact and K/T boundary layer. The following is from Kring and Boynton (1991) with some additional material from other noted sources.

Kring and Boynton (1991), Bohor and Glass (1995) and other works have conducted extensive studies on the alteration of Haitian K/T impact spherules and microspherules. In particular, Kring and Boynton (1991) note that the alteration of these spherules clearly took place after they were deposited (i.e. diagenesis). The original morphologies of the spherules were preserved as they were altered, indicating that smectite precipitated at approximately the same rate that the glass dissolved. However, not all the spherules from the K/T boundary layer were altered to smectite. Those in Italy were altered to glaucony. The things that control what sort of clay is the final product of diagenesis include: redox state, acidity of the sediment-water interface, nature of the diagenetic water and original composition of the glasses. Glaucony apparently appears in very

reducing environments, and pyrite is a further indication of reducing conditions. These products have been seen in the Italian site, but not the Haitian site.

The rate of the dissolution of glass increases with decreasing silicon content. Therefore, the less SI rich Haitian glass is expected to be more alteration-prone than that of the more SI rich tectite glass. In marine environments (Haiti) the glasses with more Ca, Na, and K dissolve faster than those with lower concentrations. The rates for glass to dissolve around about 2×10^{-3} to 5.4×10^{-1} microns per year. Even at the very lowest dissolution rate, all the glass spherules less than ~14 cm in the K/T boundary layer would have dissolved in 65 Ma. The presence of much smaller glass spherules (1 to 10 mm) in the K/T boundary sediments of Haiti therefore indicates that glass was not dissolving continuously over the entire interval that it was buried.

Izett (1991) found very high concentrations of glass in the K/T boundary layer in Haiti. They found large numbers of spherules with glassy cores, and were able to demonstrate that the cores were glass when emplaced. This reinforced the idea that these spherules are partly to completely altered impact products. The heterogeneity of the relic glass in the sediments was probably caused by some sort of weathering rather than marine diagenesis, further elucidating the history of the materials.

The melts from the original Chicxulub impact have been suggested to be dacitic to basaltic in composition. However, basaltic glasses have not been seen in the Haitian samples. These basaltic glasses would have altered faster than the more SI rich glasses, as previously mentioned. It is also possible that the lack of these type of glassy spherules in the Haiti samples is not due to alteration, but rather to such melts quenching to a fine-grained crystalline assemblage, or partially crystallize to clinopyroxene or olivine.

"*Kaolinite* – A common clay mineral $\text{Al}_2\text{Si}_2\text{O}_5(\text{OH})_4$, high-alumina. that does not appreciably expand under varying water content and does not exchange iron or magnesium. *Smectite* – A group of expanding-lattice clay minerals of the general formula $\text{R}_{0.33}\text{Al}_2\text{Si}_4\text{O}_{10}(\text{OH})_2 \cdot n\text{H}_2\text{O}$, where R includes one or more of the cations Na^+ , K^+ , Mg^{+2} , Ca^{+2} and possibly others. These minerals are subject to swelling on wetting due to the introduction of interlayer water. The smectite minerals are the chief constituents of bentonite; montmorillonite is now considered a mineral of the smectite group. *Goyazite* – Clay mineral with the formula $\text{SrAl}_3(\text{PO}_4)_2(\text{OH})_5 \cdot (\text{H}_2\text{O})$, a hydrous aluminum phosphate. (Bates and Jackson, 1984; Izett, 1990)"

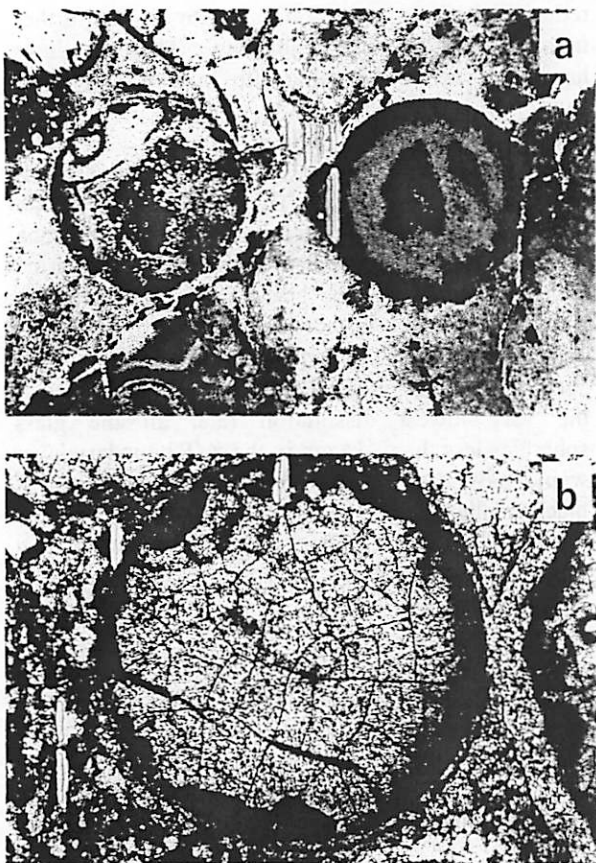


Figure 1 – Photomicrographs of altered impact spherules and microspherules in thin section. (a) Two altered spherules. The color of the clay in the one on the right varies from orange (medium gray in photo) to dark brown (dark gray to black); it also has a small hollow core. Apparent diameters are 0.95 mm (left) and 1.01 mm (right). (b) Another altered spherule in which the clay has a uniform habit. Apparent diameter is 1.19 mm. (from Kring and Boynton (1991).

References and Related Sources

Allen, C. C.; Keil, K.; Gooding, J. L. (1982) Hydrothermally altered impact melt rock and breccia - Contributions to the soil of Mars, International Colloquium on Mars, 3rd, Journal of Geophysical Research, vol. 87, Nov. 30, 1982, p. 10083-10101.

Bates and Jackson, eds. (1984) Dictionary of Geological Terms, 3rd Edition. American Geological Institute. Doubleday.

Bohor, B. F.; Glass, B. P. (1995) Origin and diagenesis of K/T impact spherules -- From Haiti to Wyoming and beyond, *Meteoritics*, vol. 30, p. 182.

Crossey L. J. and P. McCarville (1993) Post-Impact Alteration of the Manson Impact Structure, 24th Annual Lunar and Planetary Science Conference.

Davis, G. (1984) Structural Geology of Rocks and Regions. John Wiley and Sons, New York.

Gostin, Victor A.; Zbik, Marek (1999) Petrology and microstructure of distal impact ejecta from the Flinders Ranges, Australia, *Meteoritics & Planetary Science*, vol. 34, no. 4, pp. 587-592.

Izett, G.A. (1990) The Cretaceous/Tertiary boundary interval, Raton Basin, Colorado and New Mexico, and its content of shock-metamorphosed minerals; Evidence relevant to the K/T boundary impact-extinction theory. *GSA Special Paper 249*.

Kring, D.A. (1993) The Chicxulub Impact Event and Possible Causes of K/T Boundary Extinctions, Proc. of the 1st Annual Symp. of Fossils in AZ, Boaz and Dornan, eds., Mesa SW Muse. SW Paleont. Soc., Mesa, AZ, 66-79.

Kring, D.A. and W.V. Boynton (1991) Altered spherules of impact melt and associated relic glass for the K/T boundary sediments in Haiti, *GCA*, 55, 1737-1742.

Nations, J. and J. Eaton, eds. (1991) Stratigraphy, depositional environments, and sedimentary tectonics of the western margin, Cretaceous Western Interior Seaway. *GSA Special Paper 260*.

Newsom, Horton E.; Sowards, Terry; Keil, Klaus; Graup, (1986) Guenther Fluidization and hydrothermal alteration of the suevite deposit at the Ries Crater, West Germany, and implications for Mars, *Journal of Geophysical Research*, vol. 91, Nov. 30, 1986, p. E239-E251. Research supported by the Barringer Crater Co.

Pollastro and Pillmore, 1987, *J. Sed. Petrol.* 54, 456-466.

Pollastro and Bohor, 1993, *Clays and Clay Minerals* 41, 7-25.

"Glass – A state of matter intermediate between the close-packed, highly ordered array of a crystal, and the poorly packed, highly disordered array of a gas. Most glasses are supercooled liquids, i.e. metastable, but there is no break in the change in properties between the metastable and stable states. The distinction between glass and liquid is on the basis of viscosity. (Bates and Jackson, 1984)"

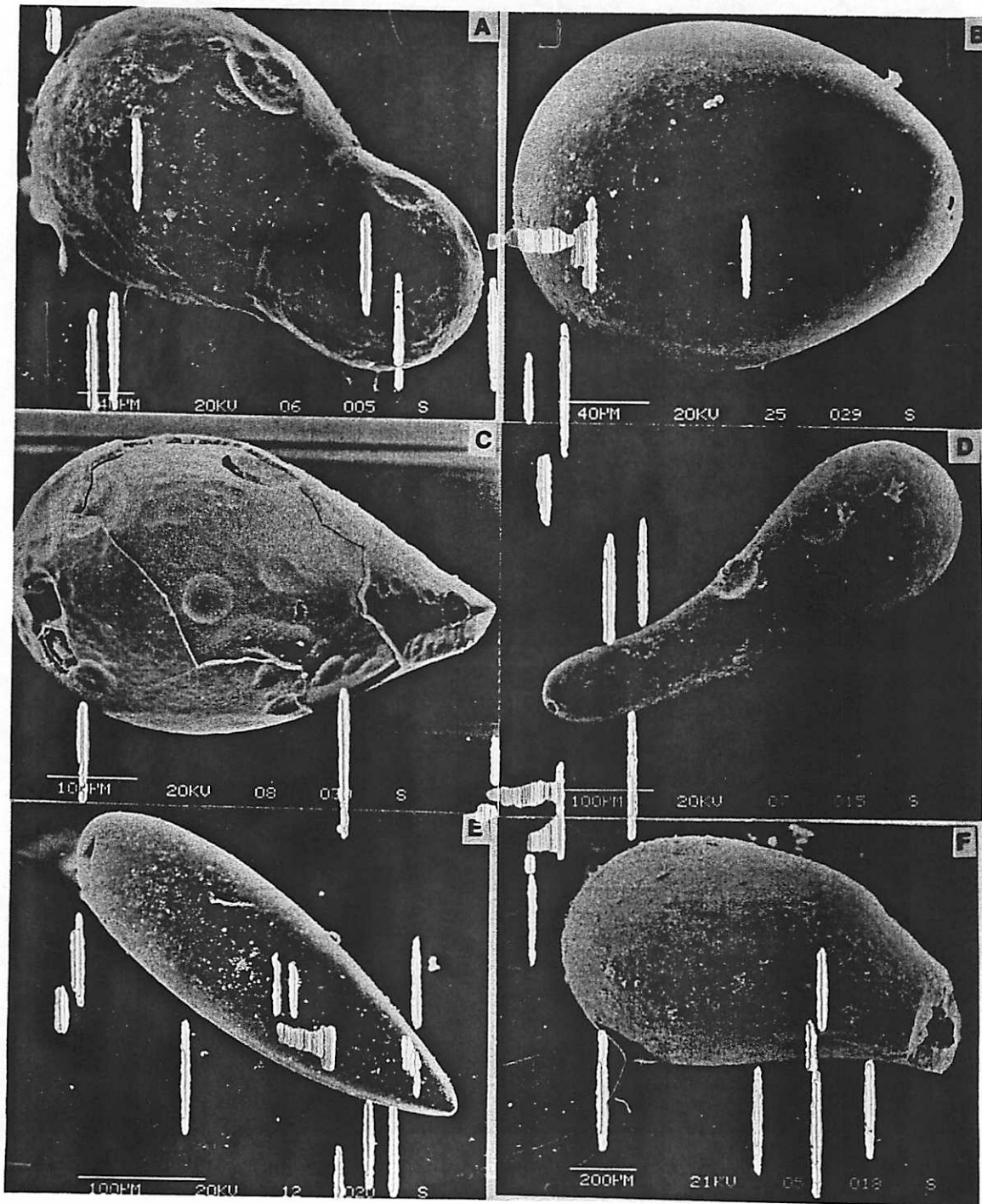


Figure 2 – Rare types of goyazite objects loosely referred to as “spherules” in the K/T boundary claystone bed at the Dogie Creek, Wyoming site. (Izett, 1990)

"Squeeze Job - The forcing of cement slurry into a borehole, in order to re-cement a channeled area behind the casing or to close off perforations. (Bates and Jackson, 1984)"

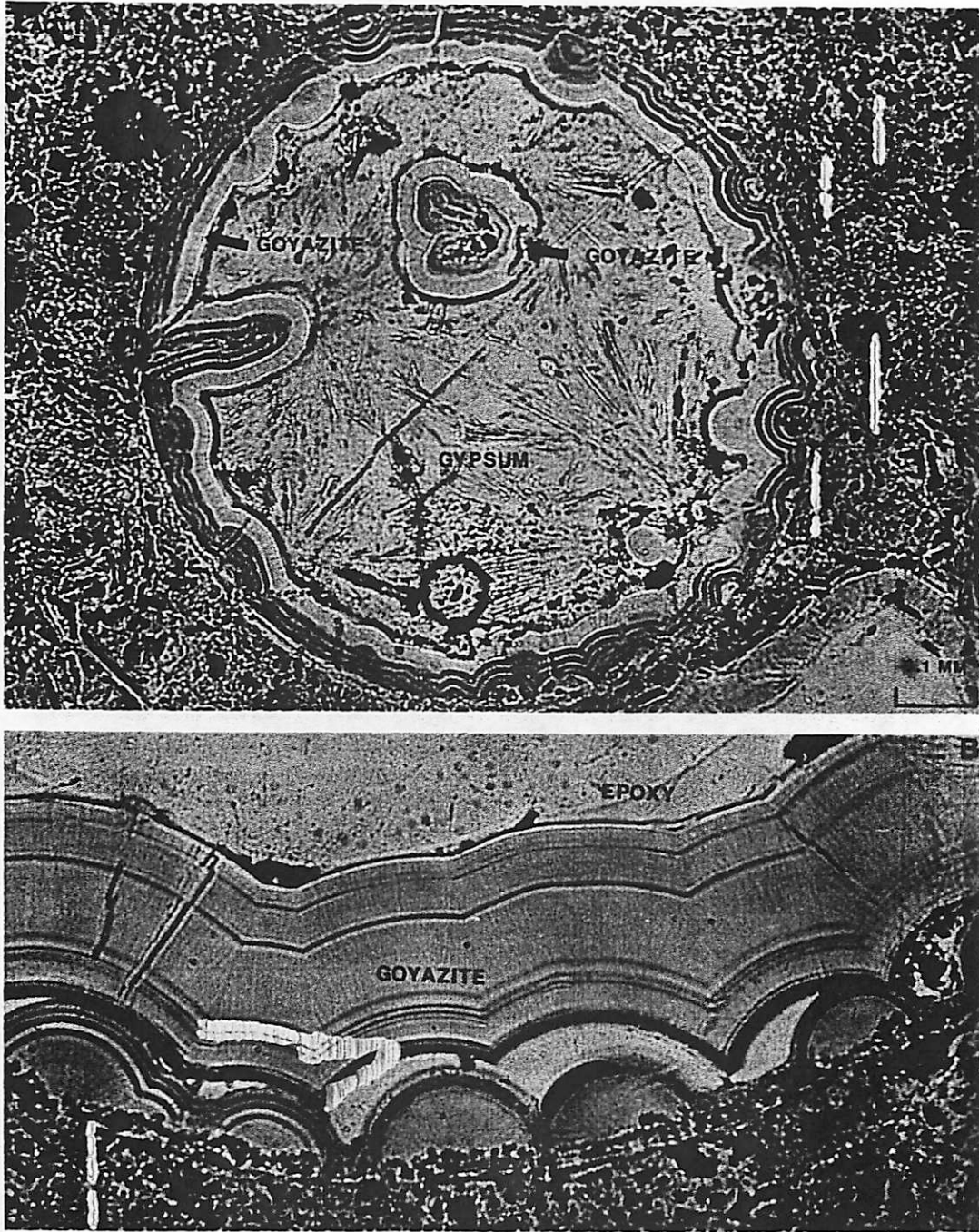


Figure 3 - Photomicrographs of thin sections containing goyazite spherules from the Dogie Creek, Wyoming, K/T boundary locality. (A) Shell of spherule composed of microlaminated goyazite. Center of spherule filled with gypsum. Goyazite inclusion (?) in upper part of spherule. (B) details of the structure of the shell of a goyazite spherule. Goyazite filled a spherical cavity in the kaolinitic claystone of the K/T boundary claystone. (Izett, 1990)

Impact Ejecta and Volcanic Ash Layers, what's the difference?

Ross A. Beyer

Here on earth, we generally don't worry too much about confusing an impact ejecta layer with a volcanic ash layer, but maybe we should. In the broadest sense let's group ejecta/ash layers into two groups based on their deposition thickness: thin and thick. I'll talk about these two categories and compare and contrast impact ejecta and volcanic ash layers in this context.

Thin Layers

Both large impacts and large volcanoes can spew out material that can cover large portions of a planet. If a planet does not have an atmosphere then the impact or the volcano must be large enough to ballistically deliver particles to the far side of the planet. This, of course, requires a large amount of energy, and you might end up ejecting those particles from the gravity well entirely. However, if there is an atmosphere then much smaller impacts or eruptions can reach around the globe. A large enough impact or a strong enough volcano will eject particulate material high into the atmosphere where it will remain for long periods. While its there, the atmospheric currents will distribute it, until it rains down out of the atmosphere and is deposited evenly over the surface of the planet. These layers will be very thin and composed of very small particles.

Odds are good that you are not going to be able to detect a layer like this from orbit via remote sensing. So you'll probably only really deal with these thin layers up close and personal in an outcrop. While the origin of these two materials is rather different, their emplacement mechanism as described above is very similar, and so the layers produced by both origins will be quite similar.

So let's say you come across one of these layers. It covers a large areal extent (possibly global), it consists of very fine-grained material, and the odds are good you won't be able to tell from just looking at it whether this stuff came from a volcano or a colossal impact. Taking a sample back to the lab and analyzing its chemistry is probably your next step. On chemical grounds, you should be able to distinguish between a composition that reflects meteoritic origins rather than planetary upper crust origins. This is not always so clean-cut, so you may want to see Barb Cohen's handout in this volume about KT boundary layer chemistry. Finally, if you think that it's an impact crater, it's going to be pretty big, and you should be able to find one that's about the right size, at about the right time in your stratigraphic sequence. However, that may be more difficult on Mars where there are lots of big craters than it might be on the Earth.

Thick Layers

Both impacts and volcanoes can also create thick layers of material that range from meters to kilometers in thickness, but are proximal to the crater or the vent. Large impacts are going to spew out a lot of material as they excavate out their craters, and the bulk of this material is going to land nearby in a possibly thick stack. Similarly,

volcanoes are known to do the same thing. Volcanic ashes generally rush outwards from the vent in a base surge of dense material that has lots of momentum and turbulence. These ash layers can be quite thick and cover lots of real estate.

If you're staring at one of these thick layers on the ground, then you should be able to tell if it's a volcanic ash layer or part of an impact ejecta sheet mostly from just looking at it. Both will have clasts in them, but volcanic ash or tuff has a rather distinctive look that should be easy to identify. Again if there is some ambiguity, a sample can be taken back to the lab and analyzed for its chemistry.

However, what if you are seeing thick layers in an image of the Martian surface? Are these layers volcanic, or are they the overlapping ejecta blankets of multiple large impacts? Unfortunately, that is an open question.

The layers that we do see in MOC images are tens of meters in thickness, and seem contiguous for great distances (many kilometers). In this case, the application of Occam's Razor seems to indicate that these vast layers are volcanic in origin. There are lots of volcanoes on Mars, and volcanic activity can easily be responsible for multiple episodes that cover vast areas of the surface of the planet. However, Mars also has a rich history of bombardment, it could be possible that over the millennia a sequence of impact ejecta layers has been built up. This may seem a little implausible because one might expect that to generate layers at the small size range (tens of meters) that is observed, the impacts would not be large enough to distribute that material over the great distances that these layers appear to traverse. Additionally, one might expect that if laid out on an originally horizontal surface the bottom of an ejecta layer would be horizontal, but the upper surface would grade upwards towards the impact crater. The layers we see seem to be relatively horizontal, but one could argue that we do not have enough quantitative data to say anything about this other than to eyeball it.

The differences between impact ejecta and volcanic ash layers can be subtle, but should be resolvable. Making that distinction without the benefit of doing fieldwork on the rock, however, can be quite difficult.

K-T Boundary Sites in North America *And a smorgasbord of other crap I found*

Fred Ciesla

With the Chicxulub crater being located in Mexico, it is logical to expect to find many areas where we can see the ejecta of the crater in the neighborhood of the crater that is North America. Due to weathering, sedimentation, and other processes this isn't the easiest thing to do. Even though many studies of the K-T boundary layer are done in deep sea drilling projects, there are places, like the Raton Basin, where you can see the layer on ground.

Impacts excavate craters by producing ejecta and impact melt. There is an equation relating the amount of impact melt produced to the complex crater diameter:

$$\delta = 0.14 R_C^{0.74} \left(\frac{r}{R_C} \right)^{-3.0 \pm 0.5}$$

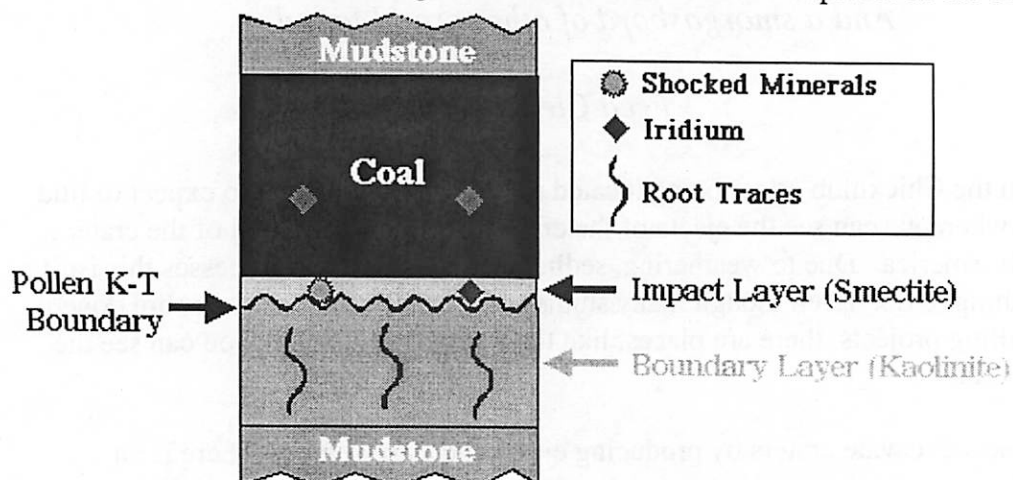
where r is the distance from the crater, and R_C is the crater diameter. This implies that we expect to see the thickest amount of melt closer to the crater. If we look at places where melt was measured, we see this distribution:

<u>LOCATION</u>	<u>THICKNESS</u>
Beloc, Haiti	0.465 m
Raton Basin, CO	0.013-0.028 m
Dogie Creek, WY	0-0.033 m
Teapot Dome, WY	0-0.026 m
Hell Creek, MT	0.01-0.02 m

Other evidence of the impact is found across North America (and the world) as well. Specifically, what had first played a role in the impact hypothesis for extinctifying the dinosaurs ("extinctify" isn't officially a word, but thank Jason for it anyway) was the detection of iridium anomalies in the K-T boundary clays. This iridium anomaly and clay can be detected in many parts of the US. For instance, there is a site in Montana called Iridium Hill, which shows the K-T boundary very well (for a virtual field trip of this place, visit http://www.athro.com/geo/trp/ktm/ktintro_fc.html). In fact, there are many places along the Rocky Mountain region of the US that provide good places to view the K-T boundary. The layering that we will see in the Raton Basin is typical of this area and looks as below. This can be seen in areas of New Mexico, Colorado, Wyoming, and Montana.

The Brazos River area in Texas gives other evidence of a giant impact having taking place at the K-T boundary. There an iridium anomaly and fossil boundary is apparent, but the sandstone around it imply a 50-100 meter tsunami took place at the

time, which would match up well with the impact taking place in water. Other signs of such waves are also visible along the Gulf of Mexico and other places in the Caribbean.



The first recognizable ejecta layer north of the Gulf of Mexico was found as a 6 centimeter spherule layer immediately above the K-T boundary. Along the Bass River in New Jersey. Its deposition supports the supports the southeast low angle impact hypothesis of Schultz and D'Hondt (1996). For more information, check out the website for the project at: <http://www-rci.rutgers.edu/~geolweb/rkogeology.html>.

However, further north in Saskatchewan, in the Rock Creek area, shocked zircon grains were found in the K-T boundary clays. Uranium-lead dating was done on these grains and matched up well with grains found in Raton Basin, the Beloc formation and Chicxulub Crater. Plotted on a Concordia diagram, these grains give ages of roughly 550 ± 10 Ma and 60 ± 10 Ma. The first age represents the time of formation of the target rocks of the impact, and the second age represents the date of resetting of the ages, that is the time of the impact. This gave the among the strongest support to Chicxulub being the impact site for the K-T boundary extinctions.

There is a HUGE amount of literature out there describing what has been learned from studying each different K-T boundary site. And there have been tons of studies of sites not in North America (Italy, India, and New Zealand often came up in researching this project). For a good bibliography on K-T boundary studies look at:

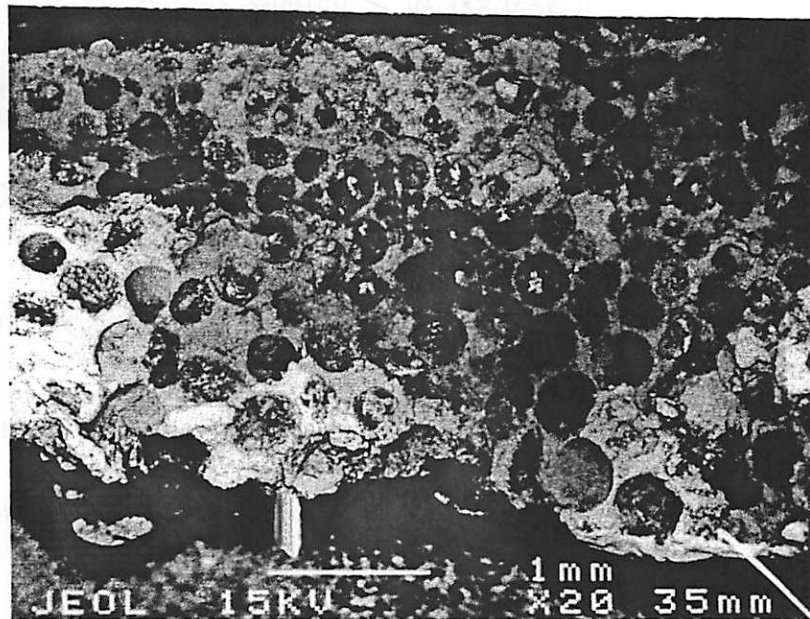
http://www.scn.org/~bh162/extinction_refs.html

How are Marine Sequences Different?

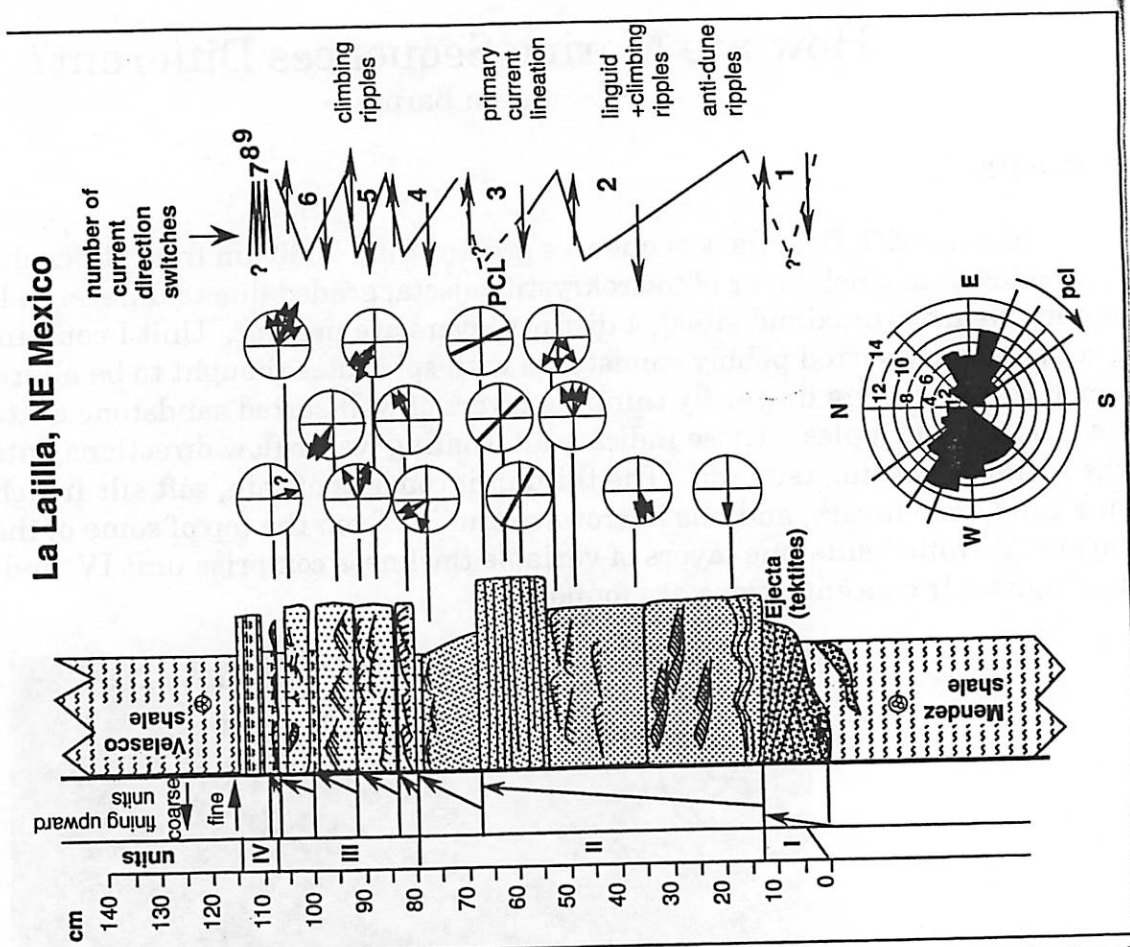
Jason Barnes

Summary:

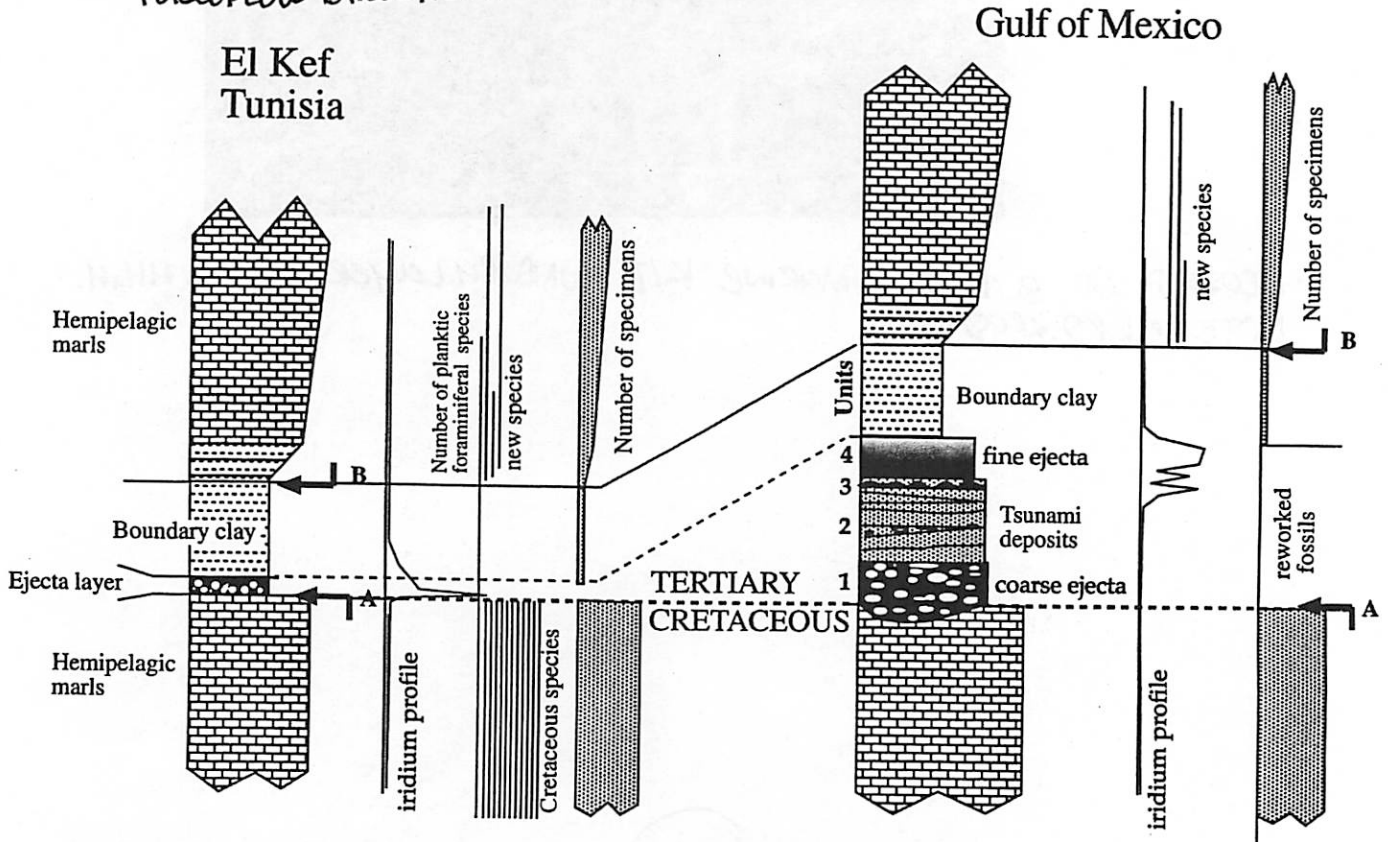
Marine K/T Boundary sequences greater than 7000 km from Chicxulub (distal sites) have a few mm thick layer of microkrystite ejecta, graded due to differential settling in water. Nearby (proximal sites), 4 distinct layers are present. Unit I contains coarse-grained, poorly sorted pebbly sandstones with spherules thought to be altered tektites. On top of this are many upwardly thinning layers of well-sorted sandstone containing parallel lineations and ripples. These indicate alternating water-flow directions, interpreted to be the result of passing tsunamis. The third unit consists of thin, soft silt Ir-rich layers and fine sandstone layers, and has burrows extending from the top of some of the sandstone layers. Lithified siltstone layers of variable thickness comprise unit IV, and it is here that the highest Ir concentrations are found.



CLOSEUP OF A DISTAL MARINE K/T BOUNDARY LAYER, ~3mm HIGH.
NOTE MICRO KRYSITES.



UNITS I-IV OF THE PROXIMAL SEQUENCE FROM LA LAJILLA INDICATING PALEOFLOW DIRECTION.



COMPARISON OF DISTAL AND PROXIMAL MARINE KIT BOUNDARY SEQUENCES

(53)

The Chicxulub Crater

Adina Alpert

Location:

On the northern edge of the Yucatan Peninsula in Mexico, centered on the Mayan fishing village of Chicxulub (Fig. 1).



FIG. 1 – Location of the Chicxulub crater. The red circle is 180 km in diameter on its outside edge, denoting one of the possible crater diameters that is being debated.

Recent History:

- 1980 – Alvarez et al. proposed the “Asteroid Impact Hypothesis” for the mass extinction at the K/T boundary, but noted that there is no known crater that accounts for the impact.
- 1981 – Penfield and Camargo announced that they had found a large, buried impact crater on the Yucatan Peninsula (based on gravity and magnetic field data).
- 1990-1991 – Research suggested that the crater could be the site of the K/T impact (e.g. Hildebrand, Boynton, Penfield, etc.)
- 1996 – Seismic reflection survey (BIRPS) (see Fig. 5)
- Current – Drilling project

Lithology:

The asteroid/comet impacted into 3-5 km of carbonate and evaporite sediments, overlying a granitic or gneissic basement. It is now buried by a ~1 km thick sequence of carbonate sediments. The only surface expression of the impact structure is a cenote ring (see below).

Morphology:

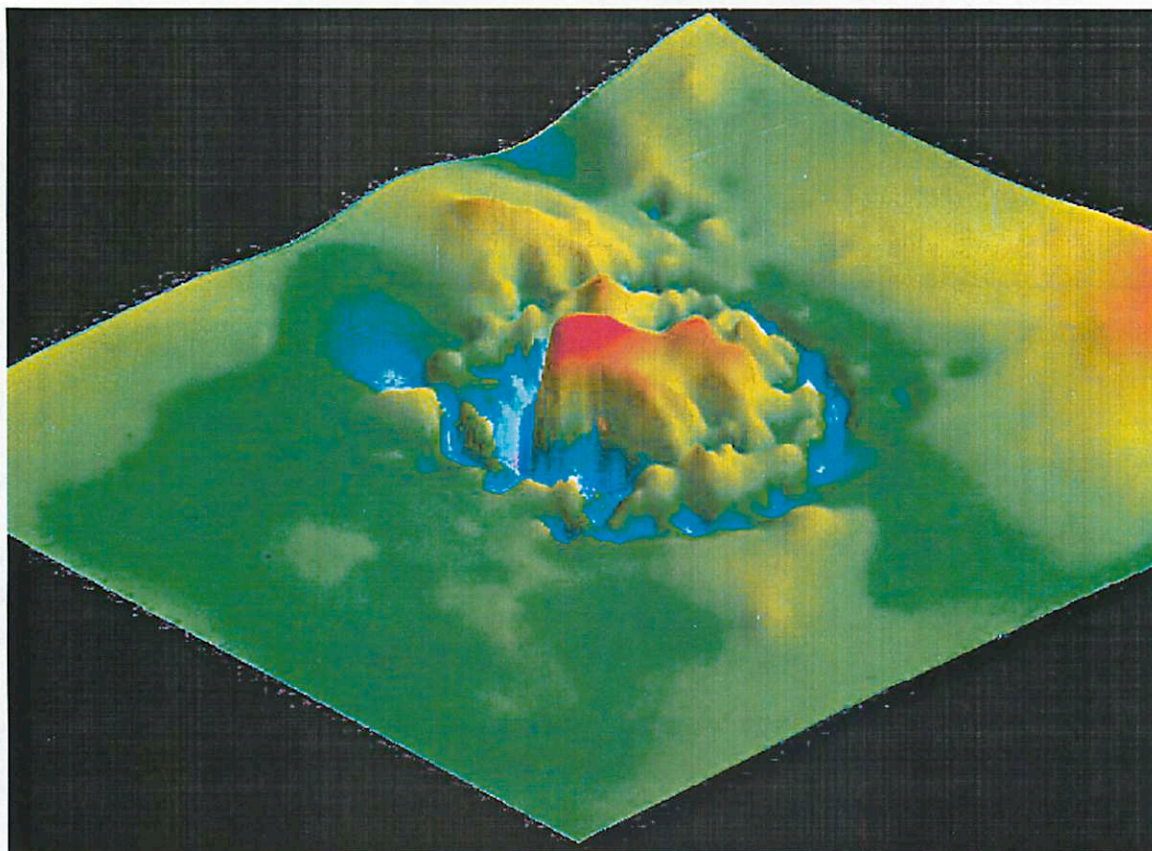


FIG. 2 – Magnetic field data over the Chicxulub crater, indicating its structure.

• *Complex craters and multiring basins*

COMPLEX CRATERS are formed during the collapse phase when the material of a transient crater slumps inwards, increasing the final crater diameter and decreasing its depth. The slumping results in TERRACED WALLS, and in larger craters, flat floors. CENTRAL PEAKS are formed in complex craters when a wave of acoustically fluidized material in the transient crater propagates inward, and the material freezes in place as the energy of acoustic fluidization dissipates. If the energy has not dissipated by the time the central peak begins to collapse, the wave of material will propagate outwards again and it will freeze in a ring structure called a PEAK RING.

MULTIRING BASINS form from larger impact events and differ from complex peak-ring craters in that at least one ring forms *outside* the original crater rim, and the rings tend to be asymmetric. The classification of the Chicxulub impact structure as a peak-ring crater or a multiring basin is still under debate, though most evidence points to it being a multiring basin.

• *Ring locations*

The diameter of the “main rim” is still being debated. The two proposed diameters are 180 km, from Bouguer gravity anomaly and short wavelength magnetic anomaly data (Penfield and Camargo-Zanoguera 1981, 1991; Hildebrand *et al.* 1991), and 295 km, from other gravity data (Sharpton *et al.* 1993). Ejecta thickness distributions around North America indicate a crater diameter of no larger than 180 km (Kring 1995). Recent seismic data also indicates the main ring is about 180 km (Snyder *et al.* 1999). The ring of CENOTES (sinkholes associated with increased groundwater flow) may be a result of the presence of the main ring nearby, and has a diameter of about 160 km expressed only on the non-oceanic half of the impact structure.

Due to the controversy over the rim diameter, there are several interpretations for the locations of other impact features. One plausible geometry is outlined here and shown in Figs. 3 and 4, from Snyder *et al.*'s 1999 paper, based upon seismic reflection data of the structures in the Cretaceous strata. If this interpretation is correct, then Chicxulub would be classified as a multiring basin.

Feature	Diameter (km)	Label in Fig. 4
Peak ring	80 ± 4	I
Outer edge of collapsed terraces	130 ± 5	II
Cenotes	160	-
Restored “rim”	176 to 195	III
“Ring fracture”	250 ± 10	IV

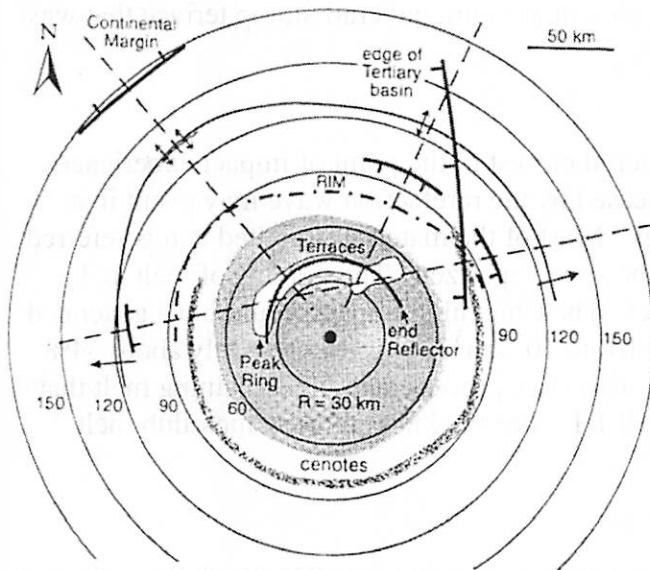


Fig. 3 - Tectonic map showing major subsurface structures associated with the Chicxulub impact by our interpretation of the new seismic reflection data. The straight dashed lines are the BIRPS profiles. Most of the ringed zones of deformation show slight asymmetry. The lightly shaded ellipse in the center indicates where the reconstructed prominent anhydrite strata was presumed destroyed by the impact. The grey line coincident with the peak ring (dark shading) marks the innermost edge of the prominent reflector horizon today in its collapsed position. The patterned band onshore marks the ring of cenotes [e.g., Pope *et al.*, 1996]. Arrows indicate fold vergence; ticked lines indicate normal faults (ticks on down thrown side). Circles labelled R=30 km, 60 etc. give reference distance to the crater center (black dot at 21.29° N, 89.52° W). Most of the observed asymmetry drawn onto this map is consistent, using analogies with lunar craters, with an oblique impact arriving from the SSE.

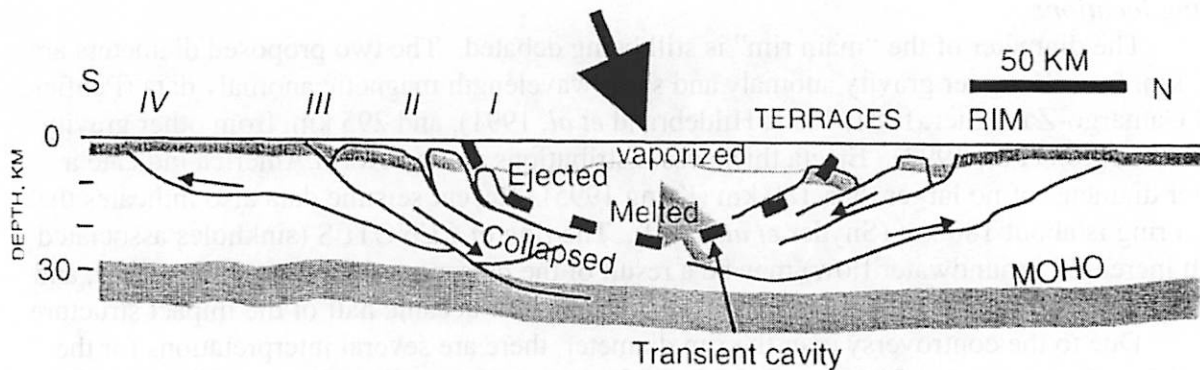


Fig. 4 — Cartoon summary cross section of the Chicxulub impact based on the new seismic reflection data. The four major ringed zones of deformation are indicated: I, the peak ring; II, the outer margin of collapsed terrace blocks; III, the restored crater rim area; and IV, the thrust faults and shears of the ring fracture. Other labels on the cross section indicate the fate of rock originally in the position indicated [from Melosh, 1989]. An oblique impact is indicated by the large arrowhead; the resulting thrusting, collapse along normal faults, terrace formation and flow within the lower crust is therefore drawn as asymmetrical. The N-S designation is arbitrary.

- *Faults and underlying beds*

The seismic profiles taken by the 1996 BIRPS survey indicate inward-dipping faults within the Cretaceous sediments that correspond to the ring features (Fig. 4).

Looking closely at the Cretaceous strata, the observed deformation intensity decreases progressively inward toward the crater center from the crater rim, and beyond a diameter of ~300 km, the crust is presumed to have minimal deformation. The strata just inward of the “main rim” indicate a block of intact crust underlain by an inward dipping reflection that reaches the lower crust and possibly the Moho. This block may represent a traditional crater slump terrace that was downdropped into the crater.

- *Melt sheet*

During an impact, some of the target material closest to the point of impact experiences extremely high shock pressures, which when released by the rarefaction wave may result in a phase change due to the increased internal energy. Most of the material is melted and is referred to as IMPACT MELT and a small fraction may become vaporized. The volume of melt and vapor scales with the kinetic energy of the impact. The Chicxulub impact would have generated a large volume of impact melt, estimated to be $\sim 10^4$ to 10^5 km³ (Kring 1995). Only about 24% of the melt generated is ejected during the excavation flow process, and the remaining melt that is left in the crater forms the IMPACT MELT SHEET. The thickness of the Chicxulub melt sheet is approximated to be ~4.2 to 7.2 km.

- *An oblique impact?*

The asymmetry of the Chicxulub structure suggests that the impactor struck the surface at an oblique angle. There are two popular directions of impact being debated in the literature: the impactor struck from the SSE or the WSW. The SSE hypothesis is supported by the reconstruction of strata to their pre-impact positions (Snyder *et al.* 1999). The WSW hypothesis is based upon the central peak offset (Schultz and D’Hondt 1996), but such offsets have been shown to be statistically uncorrelated with impact direction (Ekholm 1999).

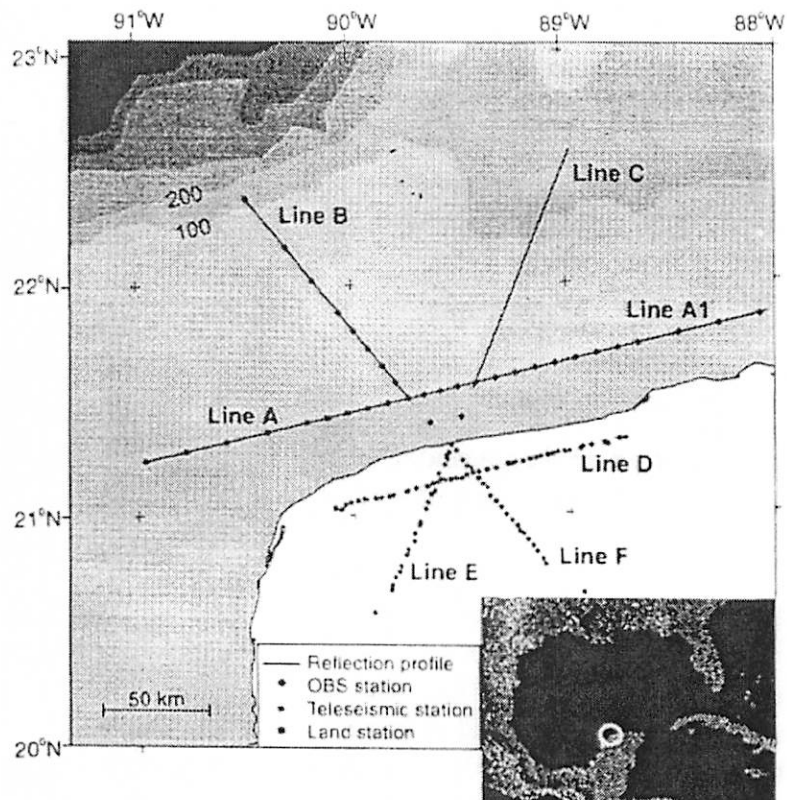


Fig. 5 — Location map showing the Yucatan Peninsula of Mexico, the seismic reflection profile survey lines of the 1996 BIRPS experiment, and locations of stationary seismometers, onshore and on the seafloor, that recorded the survey shots in order to provide velocity estimates. Contours offshore are bathymetry at intervals of 100 m.

Further Reading

- Alvarez *et al.* 1980. *Science*, **208**, 1095-2208.
 Ekholm, A. G. 1999. *LPS XXX*, #1706.
 Hildebrand, A. R. and W. V. Boynton 1990. *Science*, **248**, 843-847.
 Kring, D. A. 1995. *J. Geophys. Res.*, **100**, 16979-16986.
 Melosh, H. J. 1989. *Impact cratering: A geologic process*. Oxford Univ. Press, London.
 Penfield, G. T. and Z. A. Camargo 1981. *A. Mtg. Soc. Expor. Geophys. Abstr.*, **51**, 37.
 Schultz, P. H. and S. D'Hondt 1996. *Geology*, **24**, 963-967.
 Sharpton, V. L. *et al.* 1993. *Science*, **261**, 1564-1567.
 Snyder, D. B. *et al.* 1999. *J. Geophys. Res.*, **104**, 10743-10755.

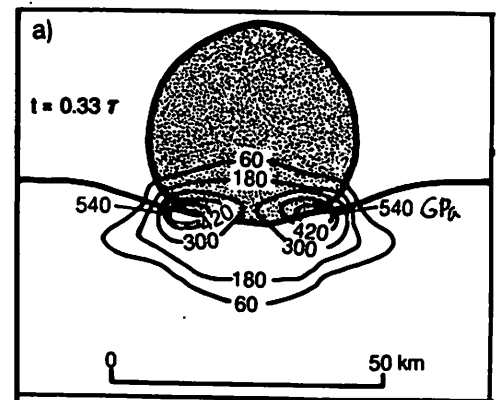
Impact Ejecta Mechanisms & How Do We Know That Chicxulub is the Source of the K/T Boundary Debris?

Andreas G. Ekholm
May 12, 2000

IMPACT EJECTA MECHANISMS

Jetting

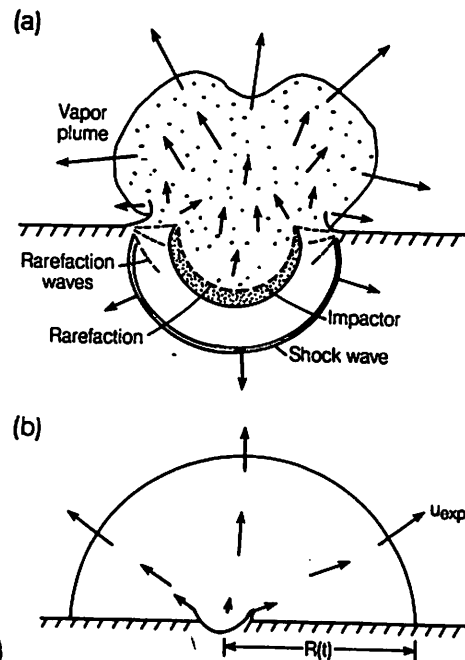
As the impactor makes contact with the target surface, a torus of ultra-high (a few Mbar) pressure develops around the edge of the contact surface. An incandescent mix of melted and vaporized projectile and target material squirts out at several times the impact velocity. This is known as *jetting*. Jetting is not quantitatively important in near-vertical impacts, but may be significant in oblique impacts. It lasts until the projectile has plunged halfway into the target.



The Vapor Plume

When the rarefaction wave reaches the rear of the projectile and releases it from high pressure, vaporized projectile and target material expands out of the crater at speeds comparable to the impact velocity (the impact velocity must exceed 10 km/s for significant amounts of vaporization to occur). This so-called *vapor plume* forms just after the first ejecta has been thrown out from the target surface adjacent to the impact, but it quickly outruns the ejecta curtain.

Fig. 5.6 Expansion of vapor produced during the early stages of an impact. Part (a) shows the initial stages of the expansion where the vapor flow pattern may be complex as a result of the timing of release of various portions of the projectile and target from high pressure. Pressure release first occurs near the rim of the growing crater so that initial vapor expansion occurs there. The remainder of the projectile and target beneath it begins expanding later, producing a dominantly upward flow in the center of the crater, although small inward velocity components may occur at this stage. Part (b) illustrates the flow somewhat later, when the expanding vapor plume is nearly hemispherical and is moving so rapidly that its front outdistances the solid ejecta curtain. The expansion velocity in the vapor plume increases nearly linearly with distance from the crater's center to a maximum u_{exp} at the plume's edge.



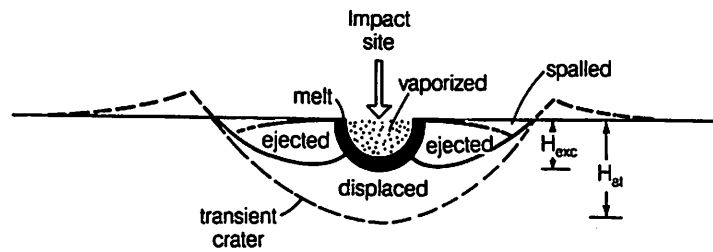


Fig. 5.13 Provenance of material expelled from the crater. Vaporized material expands outward in the vapor plume. Of the remaining material some is ejected and some is displaced out of the crater and deforms the adjacent rocks, uplifting the surface near the rim and downwarping rocks beneath the crater. The ejected material is excavated from a maximum depth H_{exc} that is only about one-third of the transient crater depth or one-tenth of the transient crater diameter. The dashed lines show the profile of the transient crater.

Some ejecta can become entrained in the expanding gas cloud and accelerated to very high velocities. Entrained droplets of impact melt that solidifies in flight form small glassy spherules known as tektites.

The hot gas cools as it expands and eventually condenses into solid particles that slowly settle out of the atmosphere. If the impact is large enough, the vapor plume will "blow out" of the top of the atmosphere and its contents will be spread globally. This is how the global K/T boundary layer was emplaced.

Spallation

Because the target surface outside the crater is a free surface, the pressure on it must be zero. This results in a steep pressure gradient close to the surface as the shock wave from the impact passes by below. This pressure gradient accelerates material from the near-surface zone to velocities up to half the impact velocity, without exposing it to very high pressures. This process is called *spallation*.

The unshocked or very slightly shocked material ejected in this fashion represents a small fraction of the total ejecta, but is believed to be responsible for secondary crater formation.

Spallation occurs just after the shock wave arrives, and so spalled material is ejected earlier than any other solid ejecta. It is preceded only by jetted material and perhaps the vapor plume.

The Excavation Flow

The ejection velocity of a piece of material in the crater depends inversely on the sub-surface distance it travels before reaching the surface (see figure). The reasons for this are friction, gravity, and Bernoulli's law (the cross section of the flow increases as it moves outwards, so its velocity must decrease to maintain the same flow rate).

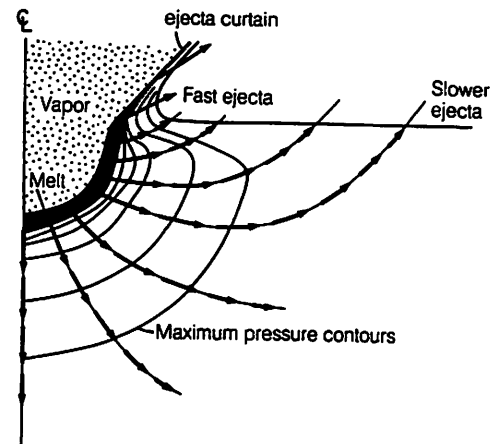


Fig. 5.9 Geometry of the excavation flow field. The arrows illustrate the upward and outward excavation flow left behind by the rapidly expanding shock wave, which has moved beyond the boundaries of this illustration. The velocity vectors are connected by streamlines that define the boundaries of streamtubes. In a steady flow, material within each streamtube stays within that tube as it expands. Also shown are contours of peak shock pressure. It is clear that streamlines cut across pressure contours, so that material ejected from a given streamtube contains a mixture of shock levels. Even the lowest velocity ejecta will contain some highly shocked impact melt. When a material following a streamline crosses the initial surface it is ejected ballistically and forms part of the ejecta curtain. Ejecta from near the impact site travels at high speed, whereas ejecta emerging at larger distances travels at slower velocities.

The ejection velocity thus declines with distance from the impact—where it drops to zero the transient crater rim forms. The slowest material is deposited on the rim, while faster material is deposited at progressively greater distances from the crater, forming an *ejecta blanket*.

Material is not excavated from the entire depth of the final crater; the deepest ejecta comes from 1/3–1/2 the depth of the transient crater below the pre-impact surface.

The Ejecta Curtain

The debris ejected from an impact crater travels together in the form of an *ejecta curtain*. Each fragment follows a ballistic trajectory, but the times and velocities of ejection are organized so that most of the debris lies on the surface of an expanding inverted cone that makes an angle of about 45° with the target surface.

The Ejecta Blanket

The so-called continuous ejecta blanket, which completely covers the pre-existing surface, generally stretches to about one crater radius from the crater rim. The thickness of the ejecta blanket declines roughly as the inverse cube of the distance from the crater center. According to this relationship, there should be 1–10 cm of Chicxulub ejecta at Raton (~2,300 km from the crater), and this matches very well with the actual thickness of 1.3 cm.

Distal ejecta contains a higher proportion of shocked or melted material than less distal ejecta. The size of the ejecta fragments also declines with distance from the crater.

Ballistic Sedimentation

At distances from the crater where the ejecta velocity is large enough as it hits the surface, surface material is eroded and mixed with the debris. The combined mass then continues to flow outward along the surface for some distance in a manner similar to that of a large dry-rock avalanche. The term *ballistic sedimentation* has been coined to describe this process. Depositional features such as dunes, ridges, and radial troughs indicative of high-speed flow are characteristic of ballistic sedimentation.

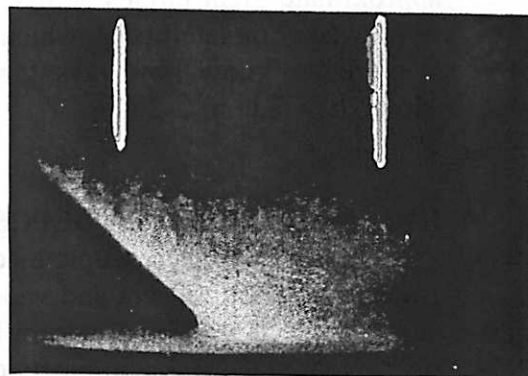
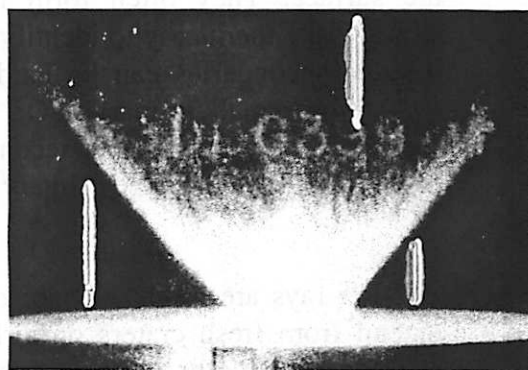
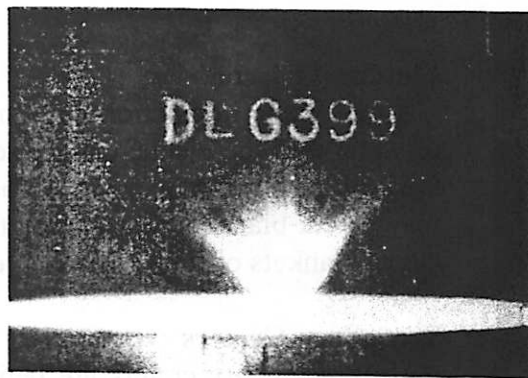


Fig. 5.10 The ejecta curtain produced in a small-scale experiment forms an inverted cone that expands with time. Photo courtesy of P. H. Schultz.

Fluidized Ejecta

Atmospheric interaction with the ejecta curtain, or the inclusion of significant amounts of water into the ejecta, can cause it to behave in a fluid-like manner and flow out along the surface instead of traveling ballistically. Martian craters larger than about 5 km display ejecta blankets that appear to have been emplaced in this fashion. The continuous ejecta blankets of these craters stretch about twice as far as those of "normal" craters.

Secondary Craters

Most secondary craters are believed to be formed by spallation fragments impacting the surface. They often form in clusters, which make them easy to identify. However, isolated secondaries can be hard to distinguish from small primaries. On the Moon, the diameter of the largest secondary crater is about 4% of that of the primary crater.

Rays

Crater rays are bright albedo features that extend from fresh craters on airless bodies as roughly radially oriented filaments and diffuse patches, often forming streaks that approximate great circles across the surface of the planet or satellite on which they form. We do not know how rays form. On the Moon they fade in 1–2 Gy.



A fluidized ejecta blanket

CHICXULUB EJECTA DEPOSITS

There are two macroscopic ejecta layers in North America (ballistic ejecta and vapor plume material) and a single layer in the eastern hemisphere (vapor plume material). Ballistic ejecta deposits have been identified in at least five locations (in Haiti, north-eastern Mexico, at the crater, and in central and northern Belize).

The maximum ejecta thickness is ~500 m at the crater rim.

The presence of a thick ejecta layer (16 m) at Albion Island in northern Belize, 360 km from the crater center, indicates that the continuous ejecta blanket extends at least four crater radii from the crater center, much farther than expected (2–3 crater radii). The ejecta is also an order of magnitude thicker than expected at that distance.

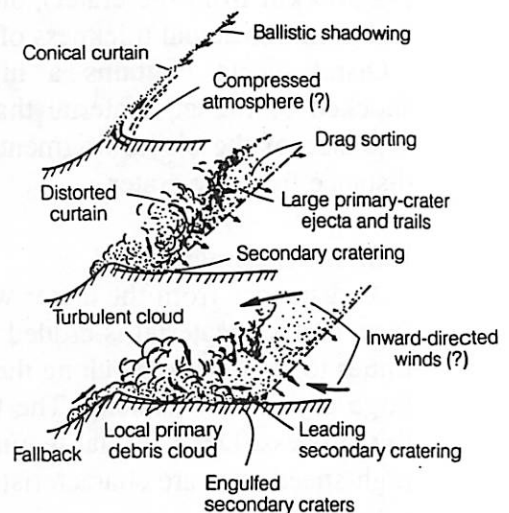


Fig. 6.8 The effect of Mars' atmosphere on impact crater ejecta. Atmospheric drag winnows fine ejecta from the expanding curtain. The resulting turbulent dust cloud over the crater falls back producing density currents (base surges) whose deposits might explain some features of Martian fluidized ejecta blankets, according to the hypotheses of P. H. Schultz and D. E. Gault. Larger ejecta fragments are not deflected and produce secondary craters. Winds driven by the expanding ejecta curtain may modify the deposition of ejecta. After Schultz and Gault (1979).

The Albion Island ejecta seems to be composed of multiple debris flows, both turbulent and laminar, and there are two separate populations of clasts: one with 2–8 m diameter clasts, and one containing clasts less than 25 cm in diameter.

All of this indicates that the Chicxulub ejecta was deposited in a fluidized manner, probably because of atmospheric interaction with the ejecta curtain.

HOW DO WE KNOW THAT CHICXULUB IS THE SOURCE OF THE K/T BOUNDARY DEBRIS?

How Do We Know That Chicxulub is an Impact Crater?

- From shock metamorphosed mineral grains (mainly quartz) found at Chicxulub.
- From correlating circular magnetic, gravimetric, and hydrogeologic (sink holes) anomalies.

How Do We Know That the Discovered Ejecta Deposits Originated at Chicxulub?

- From the unique chemistry of the Chicxulub impact melt and its similarity to glassy K/T ejecta in Haiti and target rock at Chicxulub (the 35-km Manson crater in Iowa was excluded as a candidate crater based on this).
- From the ejecta thicknesses at various locations relative to the size and location of Chicxulub (e.g. 16 m in northern Belize and 50 cm in Haiti)
- From the amount and size of shocked minerals in the ejecta deposits (e.g. the Haiti K/T site contains ten times as much shocked quartz as U.S. and Canadian sites, and the grains are larger).
- From impact-generated tsunami wave deposits and slumps in the Gulf of Mexico.
- From matching radiometric ages (65 Ma) of the Chicxulub impact melt and Haiti K/T tektites.

REFERENCES

- Blum, J. D. et al., 1993, Isotopic comparison of K/T boundary impact glass with melt rock from the Chicxulub and Manson impact structures, *Nature* **364**, 325–327.
- Hildebrand, A. R., and J. A. Stansberry, 1992, K/T boundary ejecta distribution predicts size and location of Chicxulub crater, *Lunar Planet. Sci. Conf.* **23**, 537–538.
- Hildebrand, A. R., and W. V. Boynton, 1990, Locating the Cretaceous/Tertiary boundary impact crater(s), *Eos* (Transactions, American Geophysical Union) **71**, 1424–1425.
- Hildebrand, A. R. et al., 1991, Chicxulub crater: A possible Cretaceous/Tertiary boundary impact crater on the Yucatan Peninsula, Mexico, *Geology* **19**, 867–871.
- Melosh, H. J., 1989, *Impact cratering—A geologic process*, Oxford University Press, New York.
- Pope, K. O., and A. C. Ocampo, 1999, The Chicxulub continuous ejecta blanket and its implications for fluidized ejecta blankets on Mars, *Lunar Planet. Sci. Conf.* **30**, #1380.
- Pope, K. O., and A. C. Ocampo, 2000, Chicxulub high-altitude ballistic ejecta from central Belize, *Lunar Planet. Sci. Conf.* **31**, #1419.
- Pope, K. O. et al., 1993, Surficial geology of the Chicxulub impact crater, Yucatan, Mexico, *Earth, Moon, and Planets* **63**, 93–104.

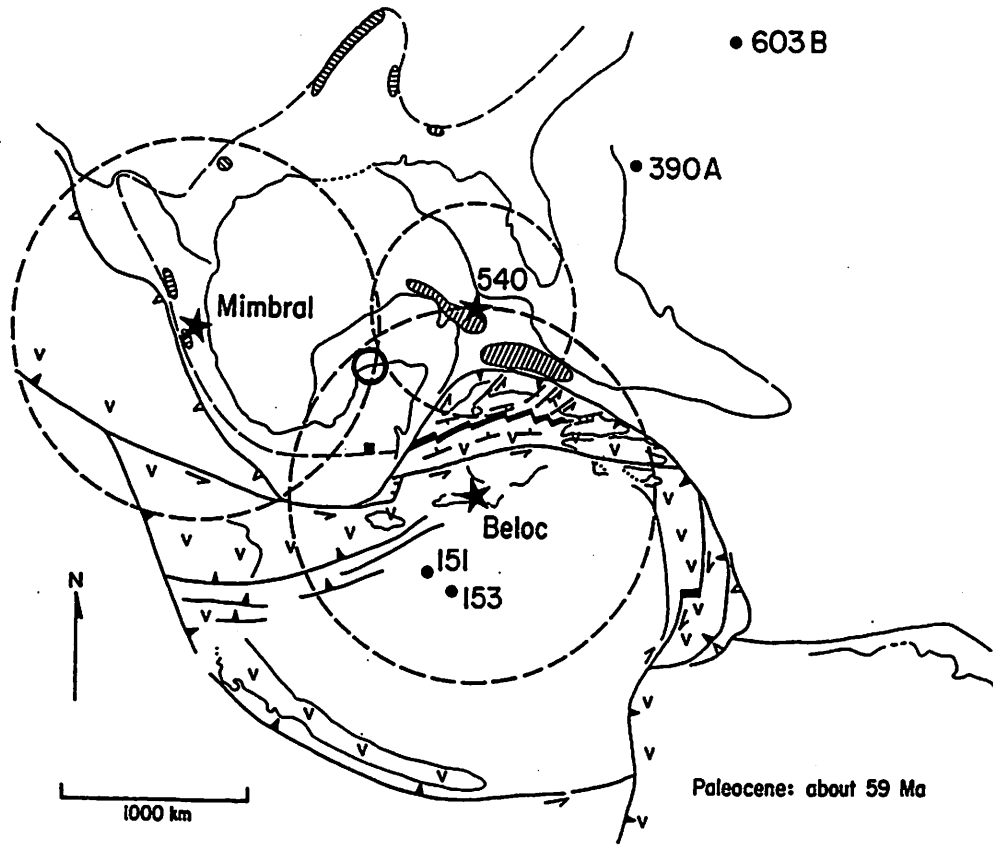


Figure 1: Plate reconstruction from (1) showing calculated distances to 180 km crater for 3 proximal K/T ejecta localities (stars). Circle is Chicxulub crater.

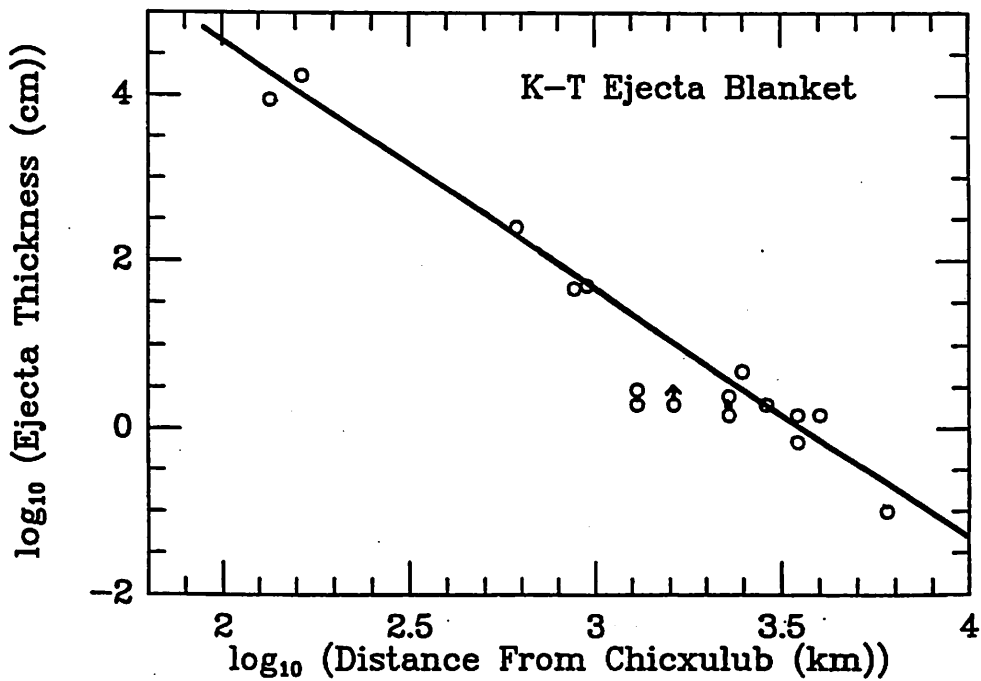


Figure 2: K/T ejecta thickness (observed and predicted) vs. distance.

The K/T Impactor: Asteroid or Comet?

Dave O'Brien

Introduction

In 1980, it was proposed by Alvarez *et. al.* that the iridium enrichment in sediments from the Cretaceous-Tertiary (K/T) boundary were due to the impact of a large asteroid or comet, a position which is held by most researchers today. While this spawned a large amount of research into the nature of the sediment layers, the impact itself, and the resultant mechanisms for causing the mass extinction associated with the K/T boundary, it still remains unclear whether the impactor involved was an asteroid or a comet. The following summary presents three lines of evidence that can be used to try to answer this question, and a brief analysis of why none of them give a conclusive answer.

Line 1: Enhanced extraterrestrial matter in layers preceding and succeeding the K/T boundary layer.

In 1994, Wickramasinghe and Wallis (henceforth referred to as W&W for obvious reasons) proposed that the K/T impactor was a comet. The main evidence for this hypothesis is that the layers immediately bordering (+/- 50,000 yr) the main boundary sediments are enriched in extraterrestrial amino acids.

The scenario that they propose is one of an earth-crossing Jupiter-family comet which is fragmented due to a close encounter with Jupiter approximately 60,000 yr Before the K/T impact event. The smaller fragments of this comet, when within several AU of the sun, would disintegrate further leading to increased dust levels in the inner solar system which would have a lifetime of around 100,000 yr. Such dust can settle non-destructively into the earth's atmosphere and diffuse to the ground, leading to an enrichment of extraterrestrial amino acids in the sediments deposited around that time. Also during this time, a large fragment of the original comet (~10 km) impacts the earth, causing the observed impact structure and the main K/T boundary layer due to the ejecta from the crater. The combined effect of the increase in accreted dust blocking solar radiation, leading to a potential drop of 4-11 degrees Celsius, and the catastrophic effects of the impact itself, lead to the K/T mass extinction. The geological result of this scenario is the observed K/T boundary layer surrounded by layers of approximately +/-50,000 yr which are enriched in extraterrestrial amino acids.

I haven't found any major objections to this theory, but there probably are some.

Line 2: Discovery of a possible meteorite fragment in K/T/ sediments.

An opposing line of evidence to the last scenario is the discovery of a possible meteorite fragment from K/T boundary sediments in the northern Pacific Ocean (Kyte 1998). The

fragment in question is approximately 2.5 mm in diameter, and is interpreted to be a heavily weathered fragment of a CO, CR, or CV carbonaceous chondrite.

Chixilub impact simulations indicate that at least 10% of the material in an impacting asteroid would be unmelted, so it would be possible for fragments of it to survive in boundary layer sediments. Ir, Fe, and Cr abundances in the sample fragment remain close to chondritic, while Ni and Co are depleted by 70 and 40%, respectively. This depletion pattern is somewhat similar to a heavily weathered CK chondrite found in Australia which Kyte uses for comparison. Among the inconsistencies, however, is a 1,000X enrichment of Au over chondritic values. This would require all of the Au deposited in ejecta over an area of 30 cm² to diffuse into the meteorite fragment, which is highly unlikely.

The main problem with Kyte's hypothesis is that the fragment is not conclusively proven to be a meteorite, or even necessarily extraterrestrial at all. As carbonaceous material is hypothesized to make up the rocky portion of comets, a comet cannot be ruled out as the source of this fragment if it is, in fact, extraterrestrial. If it's not extraterrestrial, then it's just some weird rock that nobody can explain yet.

Line 3: Impact and ejecta modeling.

Theoretical modeling of the distribution of ejecta from cometary and asteroidal impactors of various velocities, compared with the actual distribution, can give at least a probabilistic assessment of whether the impactor was a comet or an asteroid (Vickery and Melosh 1990).

Vickery and Melosh take into account the observed distribution of ejecta and attempt to correlate it with the expected distribution of ejecta from cometary and asteroidal impacts at a range of sizes, velocities, and probabilities expected for them. The ejecta distribution calculations explicitly take into account the effect of the atmosphere on the ejecta plume, which is important in determining how ejecta will be distributed. They conclude that the impactor is most likely an asteroid, and less likely a short period comet. A long period comet is deemed extremely unlikely.

However, Dave Kring (personal communication) believes that their results can be interpreted to show that a short period comet is the most likely impactor. I haven't looked into it too deeply, so I'll leave it at that.

Conclusion

Basically, there are several different lines of evidence, including some I probably missed, that give conflicting or uncertain answers to the question of whether or not the K/T impactor was a comet or an asteroid. As nobody seems to be sure, I won't claim to be either.

References

Alvarez, L. W., W. Alvarez, F. Asaro, H. V. Michel. Extraterrestrial cause for the Cretaceous-Tertiary extinction. *Science* **208**:1095-1108 (1980).

Kyte, F. T. A meteorite from the Cretaceous/Tertiary boundary. *Nature* **396**:237-239 (1998).

Vickery, A. M. and H. J. Melosh. Atmospheric erosion and impactor retention in large impacts, with applications to mass extinctions. Geological Society of America Special Paper 247 pp. 289-300 (1990).

Wickramasinghe, N. C. and M. K. Wallis. The cometary hypothesis of the K/T mass extinction. *Mon. Not. R. Astron. Soc.* **270**: 420-426 (1994).

Global Wildfires Resulting from the K/T Impactor

Jonathan Fortney
Spring 2000 594A Fieldtrip

A global charcoal and soot layer, which coincides with the famous Iridium layer, is present at the Cretaceous/Tertiary (K/T) boundary. At this point in our understanding, it seems clear that this layer is due to burned biomass caused by major wildfires. Soot is present even in the lowermost regions of the boundary clay, implying fires raged even while ejecta was raining down on the planet. These fires had astounding environmental impacts, both during the burning and for decades thereafter.

Evidence: In at least a dozen (possibly more?) sites around the world, 1 to 3 order of magnitude increases in carbon and soot have been measured in the K/T boundary clay. [1] Soot is defined as the elemental carbon component of smoke, is a component of the total carbon. Figure 1 (2nd page) contains the abundance profiles at the Woodside Creek, New Zealand site. Table 1 lists increases in enrichments of Ir, C, and soot at the K/T boundary.

As can be seen in Table 2, the percentage of C^{13} appears fairly constant at each site and is quite close to the value found in charcoal from forest fires. [1] Additionally, the boundary clay is enriched at much as 1000-fold in various polynuclear aromatic hydrocarbons (PAHs) which are a diagnostic of wood fires. These two lines of evidence lead to the conclusion that the layer is due to burned biomass, rather than fossil carbon

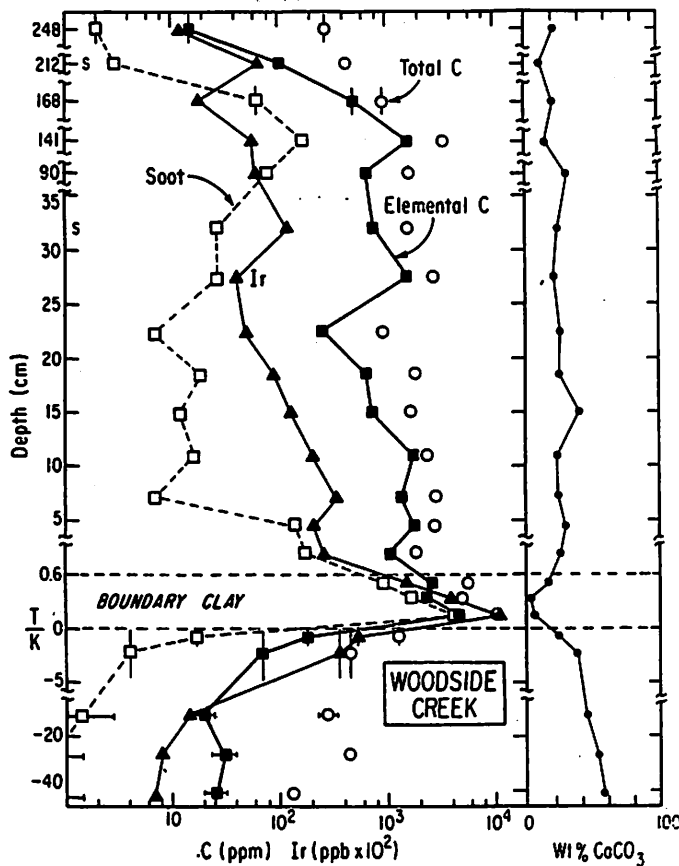


Figure 1. Abundance profiles across the K/T boundary at Woodside Creek. Note expanded scales from -5 to +5 and especially 0 to 0.6 cm. Ir, soot, and elemental C all rise at the boundary by two to three orders of magnitude, and then slowly revert to Cretaceous levels. Soot appears in the basal 0.3 cm of the boundary clay, showing that the fires were in progress before the primary fallout had settled (from Wolbach and others, 1988a).

TABLE 1. IRIIDIUM, CARBON, AND SOOT ENRICHMENTS AT THE K/T BOUNDARY

Site		Increase at K/T Boundary Over Cretaceous Values		
		IR	C	Soot
Woodside Creek	NZ	1400	210	3600
Chancet Rocks	NZ	290	≥790*	≥660*
Stevns Klint	DK	2000	1200†	340†
Agost	E	—	37	—
Sumbar	SU	55	10	≥610

*As the Cretaceous values were smaller than their errors, we used 2σ upper limits.

†Cretaceous marl from Nye Kløv, 190 km away, reanalyzed by Wolbach and others (1988a, 1990). The residue of 77 ppm C remaining after 60 hr oxidation with Cr₂O₇ = disappeared after 132 hr, and thus must have been resistant kerogen rather than elemental C, which has t_{1/2} ~ 600 hr.

Some of the elemental C and soot values cited by Wolbach and others (1988a) for Stevns Klint or Nye Kløv are in error, as the soot values were based on the mass of the 0.08 - 3µm size fraction rather than on planimetric measurement of particles with soot morphology. The correct values, in ppm, are (soot in parentheses): Cretaceous ≤2(≤2), boundary clay 2500 (520), Tertiary ≤430(0.6).

TABLE 2. CARBON AND IRIIDIUM AT THE K/T BOUNDARY

Site		Carbon		Soot (%)	δ ¹³ C _{PDB} (‰)	Iridium Abund. (ng/cm ²)	Ref.†	
		Abund.*	(mg/cm ₂)				C	Ir
Woodside Creek	NZ	4.8	±0.5	69	-25.23	91	1	1
Chancet Rocks	NZ	35 ^a	+5/-20	68	-25.42	32 ^a	1	1
Stevns Klint	KD	11 ^b	+11/-1	21	-25.81	250 ^b	2	5
Caravaca	E	10 ^{bceh}	+10/-1	14	-25.00	38 ^b	2	6
Gubbio	I	13 ^{bceh}	+13/-1	17	-25.48	15 ^b	2	7
Agost	E	3.6 ^g	+3.8/-0	-2	-26.04	≤24.5	2	8
Raton	USA	4.0 ^{ag}	+6.5	-1	-26.70	7.2	2	9
El Kef	TN	15 ^{begh}	+15	19	-26.57 ⁱ	49 ^b	2	10
Flaxbourne River	NZ	≤1.3 ^d	+0/-0.6	55	(-26.08) ^d	134	3	11
Elendgraben	A	>0.8 ^f	+8/-0	12	(-23.37)	125	2	12
Sumbar	SU	13 ^g	±3	15	-25.96	580	4	13
		Mean 11 ± 3		Mean -25.80 ± 0.58				

79

Effects: The ~global fires produced $\sim 7 \times 10^{13}$ kg (That is 7×10^{16} g if for some reason you like c.g.s.) of soot. [1,2] This would aggravate environmental stresses that could have already been happening. *Darkness and cold* would last longer because soot absorbs sunlight more effectively than rock dust. *Poisons* such as NO and NO₂ would be liberated and would be accompanied by CO and several organic pyrotoxins such as dioxins and PAHs. Many of these organic pyrotoxins are also *mutagens*. The CO₂ added to the atmosphere would add around 5-10 °C in temperature increase to accompany the ~ 8 °C increase due to water—both due to the *greenhouse effect*. This CO₂ greenhouse component could last decades however, rather than months. [1] Liberation of $\sim 10^{12}$ kg of Cl and $\sim 10^{10}$ kg of Br into the atmosphere, which, together with NO, could have destroyed all of the Earth's ozone layer. [3]

Mechanism: Ejecta from the impact crater would travel at extremely high speed. Some (small) amount could even travel in excess of the escape velocity of Earth. The component of ejecta that does not escape Earth's gravity will rain back down in and through the atmosphere at several kilometers per second. The heating and radiating of this ejecta would create a thermal radiation increase at the Earth's surface on the order of 10 kW/m^2 . This is *significantly* greater than the solar constant, which as every undergraduate knows, is 1.37 kW/m^2 . This is somewhere near the lower level of power/area needed for the spontaneous combustion of wood. [4] Certain areas of the planet surely had thermal radiation fluxes in excess of the average value quoted above, so this mechanism is indeed believed to have led to widespread fires across the globe.

References:

1. Wolbach, W.S., et al, 1990, Global Catastrophes in Earth History, Geological Society of America Special Paper 247: Geological Society of America, p. 391-400.
2. Kring, D. A, *Impact Events and Their Effect on the Origin, Evolution, and Distribution of Life*, Submitted to GSA Today, 6 May 2000.
3. Kring, D.A., *Ozone-depleting Chlorine and Bromine Produced by the Chicxulub Impact Event*, Meteoritics & Planetary Science, vol. 34, Supplement, p.A67.
4. Melosh, H. J., et al, 1990, *Ignition of global wildfires at the Cretaceous/Tertiary boundary*, Nature 343, p. 251-254

Bonus Coverage:

TABLE 3. ENVIRONMENTAL STRESSES CAUSED BY K/T IMPACT

Stress	Time Scale	Reference
Darkness	Months	a, b
Cold	Months	a, b, c
Winds (500 km/h)	Hours	d
Tsunamis	Hours	d, e
H ₂ O-Greenhouse	Months	d
CO ₂ -Greenhouse	Decades	f, g
Fires	Months	h, i
Pyrotoxins	Years	h, i, j, k
Acid rain	Years	l
Destruction of ozone layer	Decades	l, m
Impact-triggered volcanism	Millennia?	n
Mutagens	Millennia	j

a = Alvarez and others (1980)	h = Wolbach and others (1985)
b = Toon and others (1982)	i = Wolbach and others (1988a)
c = Thompson (1988)	j = Gilmour and Guenther (1988)
d = Emiliani and others (1981)	k = Venkatesan and Dahl (1989)
e = Bourgeois and others (1988)	l = Lewis and others (1982)
f = Wolbach and others (1986)	m = Prinn and Fegley (1987)
g = Crutzen (1987)	n = Rampino and Stothers (1988)

Tertiary Volcanism in the Raton Basin

Celinda Kelsey
Spring 2000 Field Trip

Where?

Figure 1 on the next page shows the location of Tertiary and later volcanoes around Raton, New Mexico. The volcanic units have been outlined. Asterisks and stars indicate source vents of the flows. This map is based on a geological map of New Mexico produced by the New Mexico Bureau of Mines and Mineral Resources [1].

What?

The units marked Tb on Figure 1 are mid-Tertiary andesite and basaltic andesite flows, breccia and tuffs. The units marked QTb are early quaternary basalt and basaltic andesite flows. In various places they are referred to as the Clayton basalts or Raton-Clayton volcanic field. (Note the town of Clayton on the far eastern side of Figure 1.) Clayton basalts are described as being vesicular porphyritic olivine basalts. The flows are interpreted as being overlapping and interfingering, indicating that several vents were active at the same time, on a geologic timescale. [2]

Isotopic studies of the Clayton basalts indicate that they are the result of lithospheric mantle melt material mixing with the lower crust. These studies also suggest that the crust beneath this region is depleted in Rb, U, and Th. [3]

Why?

Tertiary Volcanism in the southern Rocky Mountains was controlled by regional tectonics [4]. Indeed, many of the younger basalt flows are associated with high angle normal faults [5]. While some authors propose other explanations, many agree that the inception of extension along the Rio Grande rift began a series of magmatism. This magmatism generally trended from calc-alkalic, to basalt and rhyolite flows [6]. This trend is demonstrated in the Raton basin. The volcanics in this region are also reported as increasing in alkalinity with distance from the Rio Grande rift [3].

[1] Dane and Bachman, Geologic map of New Mexico. (1965). [2] USGS, Clifton House Quadrangle, Colfax County, New Mexico, geologic map. (1994) [3] Housh, Eos. 73: 14, supplement, p.338 (1992). [4] Lipman, GSA. 19; 5, p.315 (1987). [5] Lipman, GSA. 15; 5, p.288 (1983). [6] Gordon GSA. 15; 5, p.288 (1983).

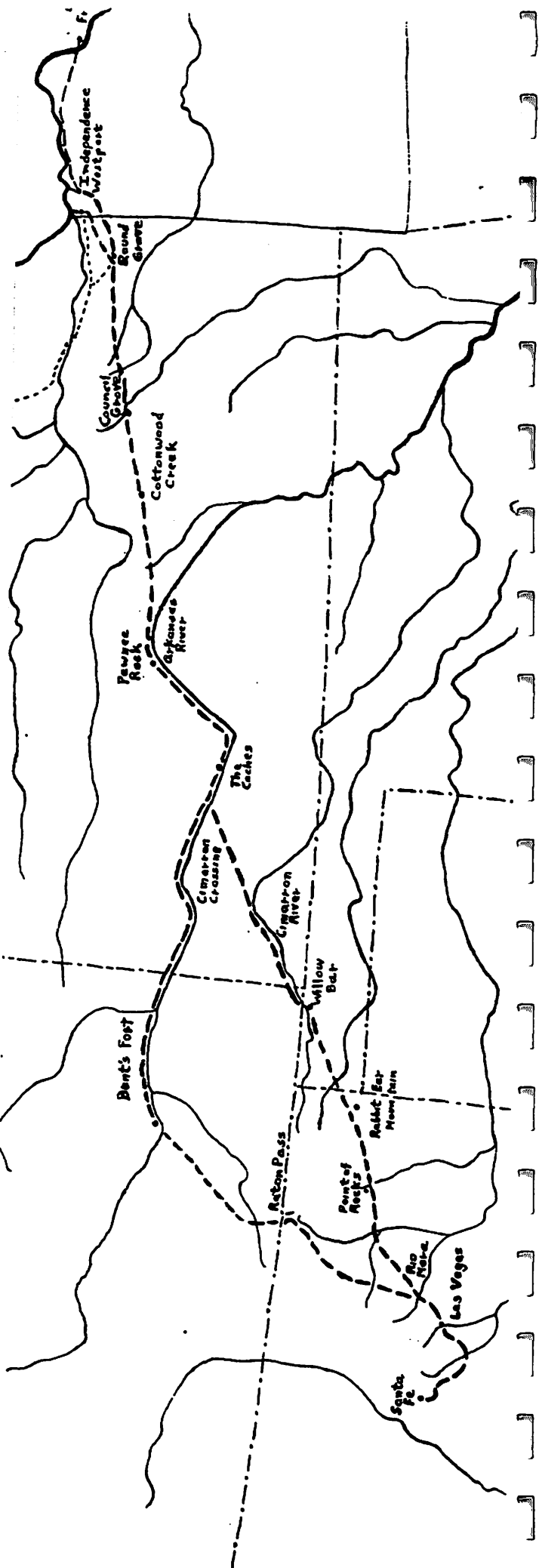
History of the Raton Pass and the Cimarron Trail

A part of the Santa Fe Trail

The Spanish first colonized the southwestern part of the United States. Alvar Nunez Cabeza de Vaca stumbled through New Mexico on his way back Mexico. After losing his ships and being stranded in Texas, he and his men were trying to march back to civilization. Upon his return tails of a Pueblo people with streets made of silver and doors of turquoise inspired further investigation of the New Mexico area by Francisco Vasquez de Coronado. He explored all the territory from the Grand Canyon eastward to the Texas panhandle. In 1609 Juan de Onate led a large colonizing party into New Mexico and founded Santa Fe.

Although a handful of American and French trappers visited Santa Fe, few other non-Mexicans probed the Southwest. In 1803 the United States purchased the Louisiana Territory and gained the lands all the way to the Rocky Mountains. United States' interest in the west immediately grew. While Louis and Clark explored the north, several smaller, less successful explorations were carried out in the south. William Dunbar and George Hunter explored Arkansas in 1805. A year later Thomas Freeman led a group up the Red River until it met Spanish soldiers and turned back. Zebulon Pike though avoided the Spaniards and ventured up the Arkansas River and into the "Mexican Mountains" in search of the Red River's headwaters. The Lieutenants expedition met with problems. The cold Colorado winter was hard on his men and supplies ran short. He managed to straggle across the Rockies and was placed under arrest by the Spaniards. He and his men were marched to Santa Fe and then farther south into Chihuahua City before being allowed to return. Although a failure the Pike Expedition opened the entire Southwest to the United States. After being arrested Pike was able to provide accurate reports on the New Mexican settlements.

In 1822 trade with Santa Fe was established by William Becknell. Often called the "founder of the Santa Fe Trail and the father of the Santa Fe Trail," Captain Becknell organized the first trade caravan to reach Santa Fe. The Mexican government had won its independence from Spain



shortly before Becknell's expedition. With the Spanish gone the Mexicans in Santa Fe were now anxious to trade for goods with the Americans.

Captain Becknell's first route to Santa Fe traveled along the Arkansas River to the edge of the Rocky Mountains. Heading south through the Raton pass they could follow the edge of the Sangre de Cristos toward Santa Fe. On his second trip to Santa Fe Becknell founded the "Dry Cimarron Trail." This trail more directly headed for Santa Fe by cutting across the arid plains of Texas and New Mexico. The first use of the Cimarron Trail almost cost Becknell his life. Unable to procure water along the way they nearly died. A lone buffalo, gorged with water, saved their lives.

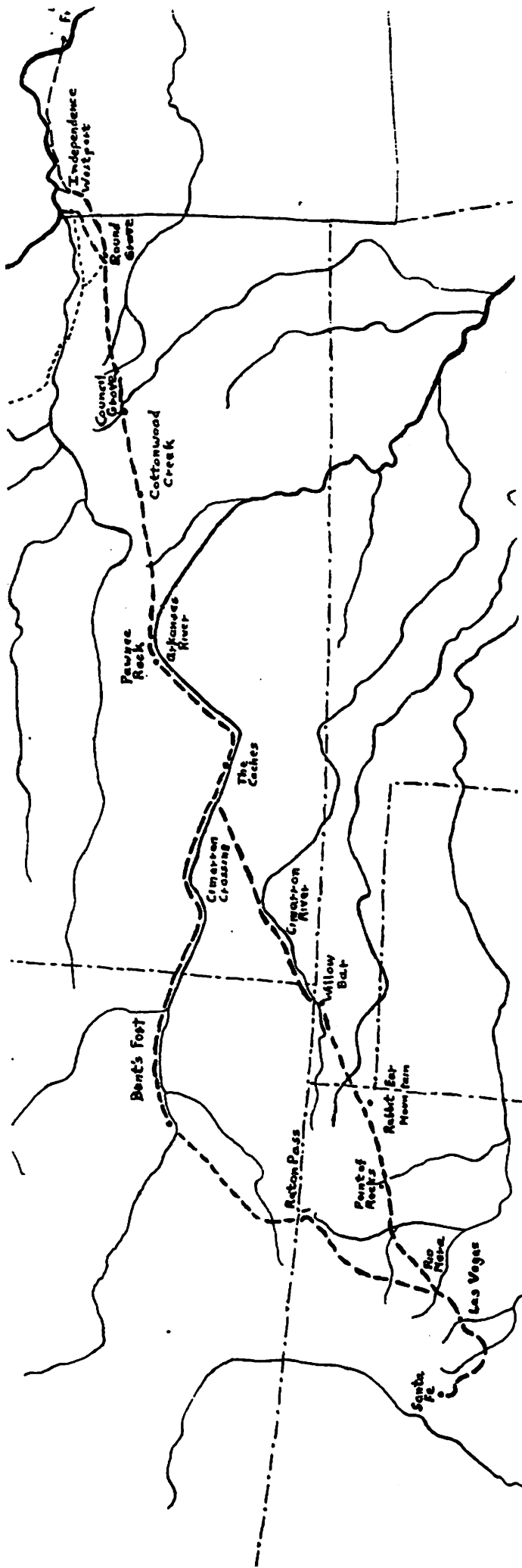
The two trails provided a choice in the trip to Santa Fe. The trail through the Raton pass was longer. However then mountains provided plenty of water and protection from Indian attacks. The rocky mountainous route though was hard on the wagons. The Cimarron Trail was faster and easier for wagons. Water though was hard to find along its path. Comanche Indians also frequented the area. The first trail remained the favorite among traders.

Today I-25 follows the Santa Fe trail between Santa Fe and the Raton Pass skirting along the foot of the Sangre de Cristos mountains. US-64 parallels some of the Cimarron Trail.

Books Used:
Roadside Geology of New Mexico

Out in God's Country:
A history of Colfax County, New Mexico

Lost Trails of the Cimarron

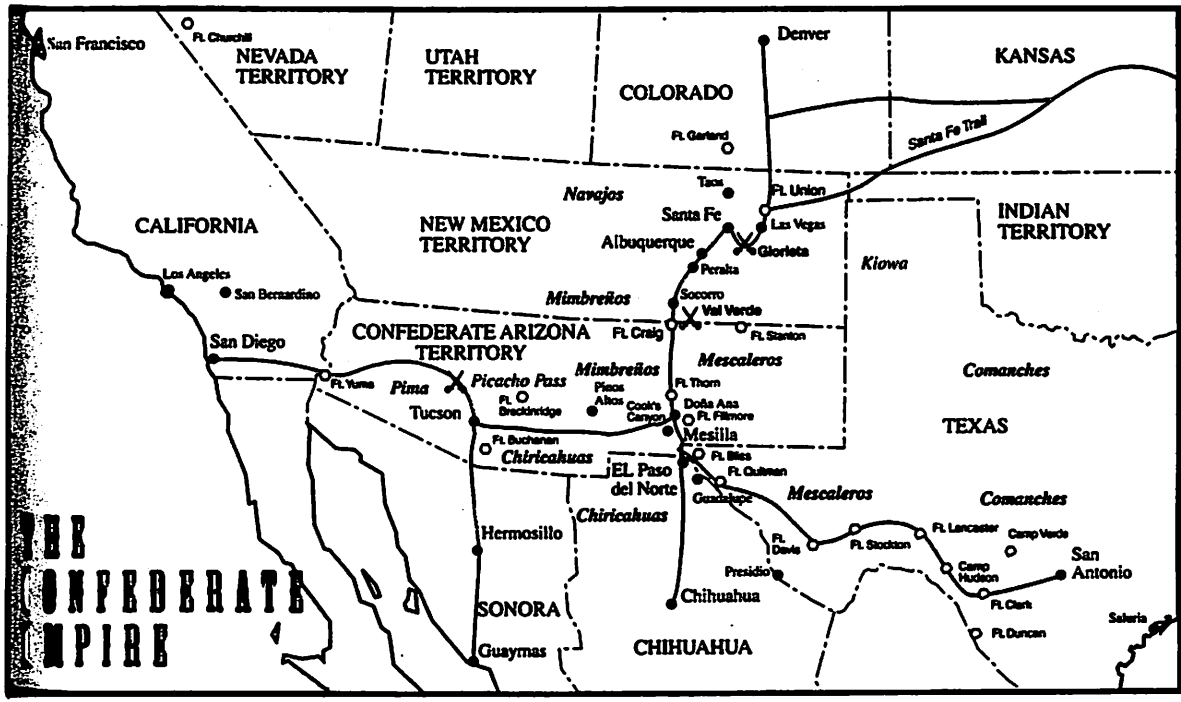
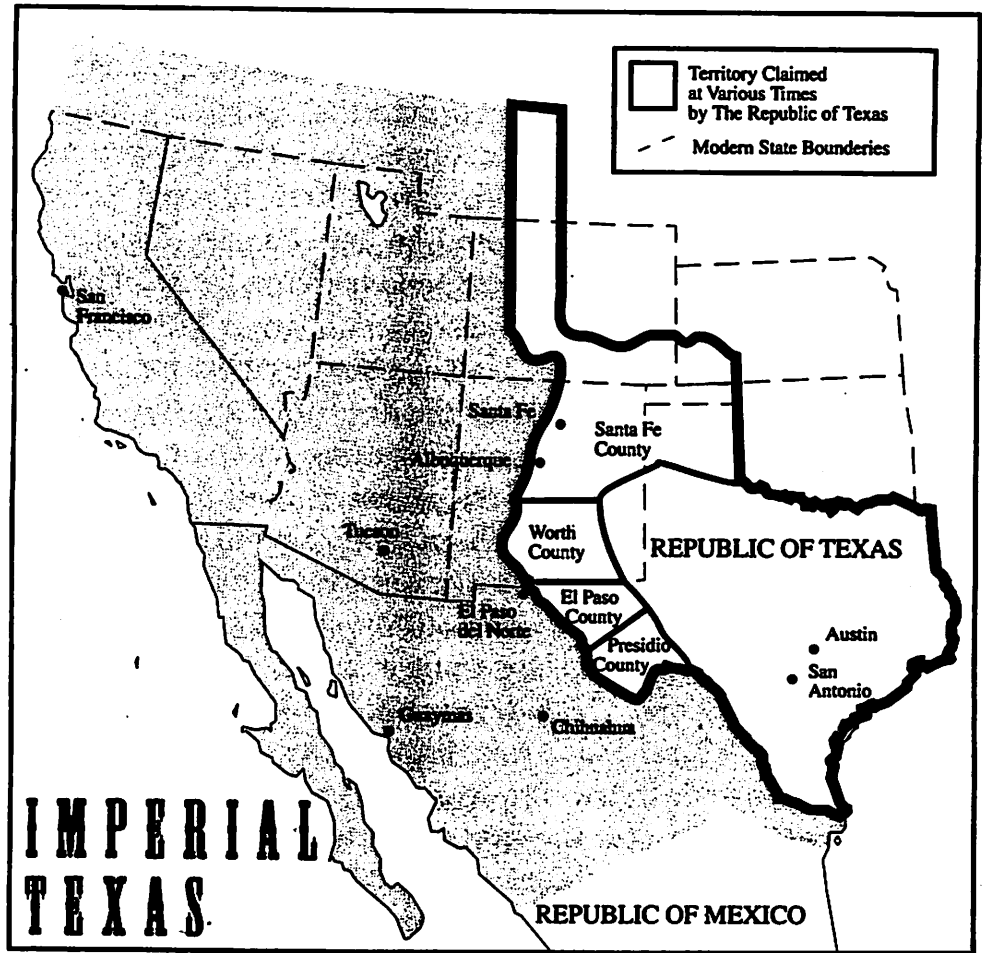


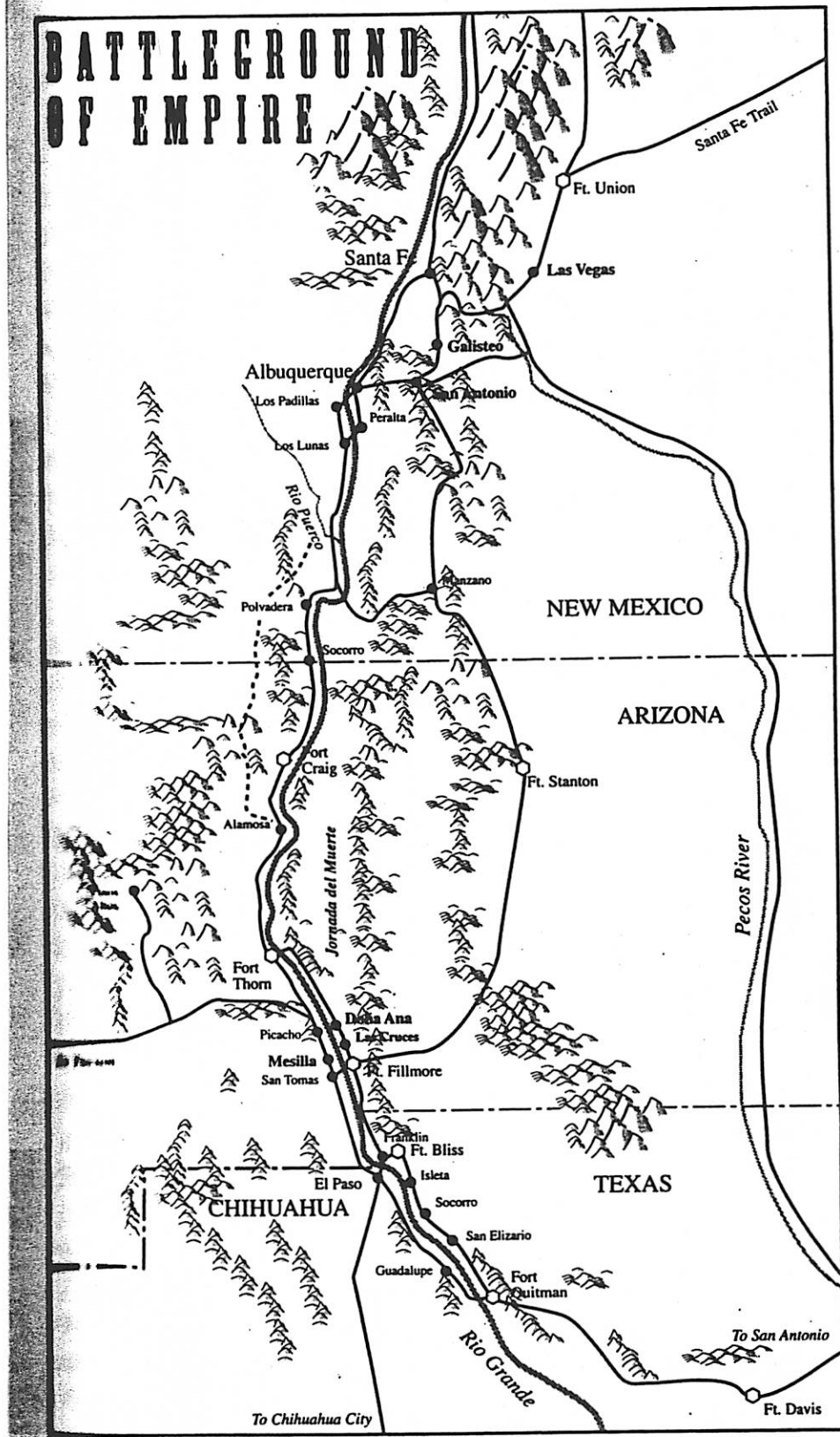
The Civil War in New Mexico (and Arizona!)

with your Yankee Abolitionist host, Andy Rivkin

- 1857- President Buchanan recommends Congress form Arizona Territory. He does so again in 1858, but both times is ignored.
- 5 April 1860- "Arizona" secedes from New Mexico, forms separate territory, sends delegates to Congress hoping for recognition
- 1 Feb 1861- Texas secedes from the Union
- Feb 1861- War with the Apaches (led by legendary chief Cochise) breaks out throughout Arizona/New Mexico
- 16 March 1861- "Arizona Territory" votes to support Confederacy
- 24 April 1861- The Confederate flag appears in Denver. It is quickly torn down.
- 11 June 1861- Union general Canby placed in charge of New Mexico
- 8 July 1861- Confederate general Sibley ordered to invade New Mexico
- 23 July 1861- Confederate Col. Baylor and the 2nd Texas Regiment enter New Mexico Territory (or Arizona Territory, depending on who you ask) near El Paso.
- 25 July 1861- Mesilla captured by Confederates. Baylor proclaims Confederate Territory of Arizona, with Mesilla as capital and himself as governor.
- 27 July 1861- Confederates capture retreating Union forces north of Fort Fillmore
- August 1861- A convention in Tucson elects Granville Oury as delegate to the Confederate Congress.
- December 1861- Arizona Territory bill reintroduced to Congress.
- 4 December 1861- The New Mexico territorial assembly outlawed slavery in the territory
- 20 December 1861- Sibley releases proclamation of impending Confederate "liberation" of New Mexico. 1500 Union regulars and 4000 New Mexican militiamen were waiting.
- late 1861-early 1862- 2350 men of "California Column" concentrate at Fort Yuma, commanded by General Carleton.
- January 18 1862- Confederate Territory of Arizona "officially" created with Jefferson Davis' signature. Boundaries: 34th parallel in north, Texas in east, California in west, Mexico and Texas in south.
- February 1862- Sibley enters New Mexico with 2500 men
- 21 Feb 1862- Battle at Valverde, NM. In aftermath, Confederates bypass Fort Craig, Union troops stay in fort.
- 22 February 1862- First Colorado Volunteer Regiment leaves Denver
- 28 Feb 1862- Confederates occupy Tucson, Union spy John Jones arrives
- 2 Mar 1862- Albuquerque evacuated by Union

- 4 Mar 1862- Santa Fe abandoned by Union, Las Vegas NM made provisional capital.
- 6 March 1862- A Union squad is sent to search for Jones, who's later than expected; Confederate troops arrive at Pima Indian villages
- 8 March 1862-Colorado Volunteers meet a courier from Fort Union at Raton Pass, desperately requesting their aid. Though they'd marched 92 miles in 36 hours through several inches of snow, they pledge to do their best.
- 9 March 1862- Union squad captured at Pima villages
- 10 March 1862- Confederates enter Santa Fe. However, short of supplies, the Confederates must capture Ft. Union NE of Santa Fe to keep their army "in being". Colorado Volunteers reach Ft. Union, after a march of over 400 miles in 13 days. Colorado Col. Slough takes command of combined units.
- mid-March 1862- Jones reaches Ft. Yuma
- 22 March 1862- Colorado Volunteers, New Mexican Volunteers, U. S. Regular troops and others leave Ft. Union heading toward Santa Fe.
- 26 Mar 1862- Battle at Apache Canyon, NM
- 28 Mar 1862- Battle at Glorieta Pass, NM. Though the Confederates hold the battlefield, a Union force under Major Chivington destroys the Confederate supply wagons. This, for the Confederates, is bad.
- 29 Mar 1862- Skirmish at Stanwix Station, AZ (near exit 78 on I-8)
- 5 April 1862- Confederates evacuate Santa Fe.
- 12 April 1862- Confederates evacuate Albuquerque
- 15 April 1862- Battle of Picacho Pass, AZ; Battle of Peralta, NM.
- 5 May 1862- Confederates Battle Apaches at Dragoon Springs, AZ
- 14 May 1862- Confederates abandon Tucson
- 20 May 1862- Tucson reoccupied by Union troops. Fort Lowell established.
- 8 June 1862- General Carleton proclaims creation of "Provisional Federal Territory of Arizona"
- 4 July 1862- The vanguard of the California Column reaches the Rio Grande
- 8 July 1862- The remnants of the "Confederate Army of New Mexico", 400 men, retreated to Fort Bliss, Texas.
- 15 July 1862- En route to New Mexico, elements of the California Column battle Apaches in Apache Pass
- 27 July 1862- Fort Bowie established in Apache Pass
- 9 August 1862- California Column enters Las Cruces, NM
- 17 August 1862- Union forces enter El Paso
- 20 February 1863- Arizona Territory created, with borders we know today, except for southern Nevada!





Maps from "Blood and Treasure", by Donald S. Frazier
 Texas ABM Press, College Station TX 1995

89